Genome-Driven Targeted Cancer Therapy

by

Shayesteh Roshdi Ferdosi

A Dissertation Presented in Partial Fulfillment
of the Requirements for the Degree
Doctor of Philosophy

Approved October 2017 by the
Graduate Supervisory Committee:

Karen Anderson, Co-Chair
Joshua LaBaer, Co-Chair
Neel Woodbury
Chad Borges

ARIZONA STATE UNIVERSITY

December 2017

ABSTRACT

Cancer is a heterogeneous disease with discrete oncogenic mechanisms. P53 mutation is the most common oncogenic mutation in many cancers including breast cancer. This dissertation focuses on fundamental genetic alterations enforced by p53 mutation as an indirect target. p53 mutation upregulates the mevalonate pathway genes altering cholesterol biosynthesis and prenylation. Prenylation, a lipid modification, is required for small GTPases signaling cascades. Project 1 demonstrates that prenylation inhibition can specifically target cells harboring p53 mutation resulting in reduced tumor proliferation and migration. Mutating p53 is associated with Ras and RhoA activation and statin prevents this activity by inhibiting prenylation. Ras-related pathway genes were selected from the transcriptomic analysis for evaluating correlation to statin sensitivity. A gene signature of seventeen genes and TP53 genotype (referred to as MPR signature) is generated to predict response to statins. MPR signature is validated through two datasets of drug screening in cell lines. As advancements in targeted gene modification are rising, the CRISPR-Cas9 technology has emerged as a new cancer therapeutic strategy. One of the important risk factors in gene therapy is the immune recognition of the exogenous therapeutic tool, resulting in obstruction of treatment and possibly serious health consequences. Project 2 describes a method development that can potentially improve the safety and efficacy of gene-targeting proteins. A cohort of 155 healthy individuals was screened for pre-existing B cell and T cell immune response to the *S. pyogenes* Cas9 protein. We detected antibodies against Cas9 in more than 10% of the healthy population and identified two immunodominant T cell epitopes of this protein. A de-immunized Cas9 that maintains the wild-type functionality was engineered by mutating the identified T cell

epitopes. The gene signature and method described here have the potential to improve strategies for genome-driven tumor targeting.

DEDICATION

To Nasrin, my source of courage and inspiration

and

Ricardo, for the unconditional love and support all the way

and

My never forgotten dad and mamani

ACKNOWLEDGMENTS

I would like to thank my advisor Dr. Anderson for the great opportunities she provided me. Her passion and dedication to science were reflected on to me. I acknowledge my co-advisor Dr. LaBaer for his sharp intellectual critics and his strong science leadership of CPD and the Biodesign Institute. My committee members, Dr. Woodbury for being an extraordinary person and a true example of collaborative attitude, and Dr. Borges for his kind and encouraging mentorship.

I have a special thank for professor Gould for his tremendous support early on in the Chemistry Ph.D. program. I am thankful for teaching with Dr.Bhushan all these years and getting to know many students. I had an amazing opportunity to collaborate with Dr. Kiani and Dr. Jin Park to expand my research perspectives. I was fortunate to work for Dr. Matt Greving who taught me to “not give up!”.

I am so grateful to start this journey with two of the bests, Sri Krishna and Diego Chowell. I learned so much from them and they always believed in me. I also thank Radwa Ewaisha who offered me a whole new chapter in friendship and collaboration that paved my way to the end. I was blessed to work with very good friends, Eva Amouzougan, Emma Chen, Peaches Ulrich. I had a great mentoring experience with highly talented undergrads, Valerie Loo, Harneet Grewal and Tincy Simon that their efforts made my research a possibility. Special thanks to Dr. Milad Mesgar for igniting my interest to science.

I could not have succeeded without the support of Seron Eaton, Dr. Shanshan Yang, Anasuya Paul, Dr. Jordon Yaron, Marika Hopper, Dr. Ben Katchman, and I owe to

the designer and investor of the Biodesign building because it is truly a place suitable for science discovery and collaboration.

Thanks to my beloved sister, Shadi, for fulfilling my Ph.D. life all these years. I am deeply thankful to Narges Masoumi and Rouzbeh Valamanesh for being alongside with me in every step like a family. Lastly, I want to thank my family for their support and encouragement.

TABLE OF CONTENTS

Page

LIST OF FIGURHES……..viii

LIST OF TABLES…….x

LIST OF ABBREVIATIONS…….xi

CHAPTER

INTRODUCTION.....1

1.1. Cancer Cell Metabolism 2

1.2. p53 and Cell Metabolism.....3

1.3. Ras Small GTPases.....5

1.4. Prenylation 6

1.5. Prenylation Inhibition.....8

1.6. Therapeutic Methods for p53 Deficiency in Tumor 10

1.7. Thesis Contributions 11

PRENYLATION INHIBITION OF MUTANT P53 CELLS 12

2.1. Abstract.....13

2.2. Background.....14

2.3. Material and Methods.....15

2.4. Results.....21

2.5. Discussion.....52

GENE THERAPY USING CRISPR-CAS9 SYSTEM.....52

3.1. Introduction and Background.....55

3.2. Materials and Methods.....57

CHAPTER Page

3.3. Results....62

3.4. Discussion....77

REFERENCES....81

APPENDIX

A LIST OF ENRICHED PATHWAYS IN MP53 MCF10AS ……..……..…89

LIST OF FIGURES

Figure Page

1. Graphical Overview of p53 and Fatty Acid Metabolism …. 5

2. Schematic Representation of the Prenylation Pathway.....8

3. Mutant p53 Expression Level in the Generated MCF10A 22

4. Simvastatin Proliferation Inhibition of mp53 MCF10As. 24

5. Dose-Response to Simvastatin in mp53 MCF10A. 25

6. Correlation of Proliferation Inhibition With Apoptosis Induction in mp53 MCF10A.....26

7. Rescue Experiment for Simvastatin Treatment of mp53 MCF10As…. 27

8. Migration Inhibition Assay of Mutant and Wild-Type p53 MCF10A… 28

9. Migration Inhibition by Prenylation Inhibitors for mp53 MCF10As. 29

10. Multi-Dimensional Scaling Plot.. 30

11. Biological Function Analysis of $p53^{R273H}$.MCF10A. 32

12. Pathway Analysis for Statin-Treated $p53^{R273H}$.MCF10A.. 35

13. HMGCR Expression Is Upregulated After Cholesterol Pathway Inhibition.. 36

14. Cholesterol Deprivation Resulted in Significant Upregulation of LDLR Expression in mp53 Cells. 37

15. Relative Expression of Res-Related Genes in mp53 MC10FAs.....38

16. Relative Gene Expression Post-Statin in Mutant and Wild-Type p53 Cells. 40

17. Ras and RhoA Activation in mp53 MCF10As……. 41

18. Schematic Diagram of Ras Activation.....42

19. Ras Translocation With SV Treatment……. ..…. 43

20. p53 Mutation Is Not a Good Predictor of GI_{50}. 45

Figure Page

21. Ras-Related Gene Signature of SV Sensitivity. 46

22. Prediction of Simvastatin Response in Breast Cancer Cell Lines.. 47

23. Breast Cancer Cell Line Sensitivity to Simvastatin....48

24. Prediction of Prenylation Inhibitors to Breast Cancer Cell Lines. 49

25. Differentially Expressed Genes Post-Statin in Two Groups of MPR+ and MPR-Patients. 50

26. MPR Signature for Prediction of Atorvastatin Response in Patients 51

27. Serum Antibody Detection Against S.pyogenes and Cas9. 63

28. Improved Epitope Prediction Model With Applying Immunogenicity Score....67

29. IFNγ ELISpot Assay Screening for T cell Reactivity.....68

30. Reactivity of Healthy Donor T Cells With the HLA Types Shown to Epitopes Across the Different Domains of the Cas9 Protein. 69

31. ELISpot Assay for Screening Healthy Donors' PBMCs to Cas9 Epitopes.....70

32. Decreasing T Cell Response to Epitope 85 and 94 by Mutating the Epitope.. 71

33. Comparable Functionality of Mutated Cas9 and Wild-Type Cas9. 73

34. Mutated Cas9 Proteins Recognize and Bind to Their Target DNAs. 74

35. T Cell Activation With Cas9 Epitope and Mutated Epitope.....75

36. Epitope Specific CD8 T Cell Response to Epitope 85.....76

37. SpCas9 Protein Domains and Epitope 85 and 94 Locations on the Protein.....79

LIST OF TABLES

Table Page

1. The Half Maximal Inhibitory Concentration of Prenylation Inhibitors for mp53 MCF10As. 23

2. Pathway Analysis for $p53^{R273H}$.MCF10A.. 33

3. Binding and Processing Scores for Cas9 Epitopes..…..64

4. Predicted Cas9 Immunogenic T Cell Epitopes.....65

LIST OF ABBREVIATIONS

CoA	coenzyme A
EV	empty vector
FASN	fatty acid synthase
FTI	farnesyl transferase inhibitor
FTase	farnesyl transferase
GGTI	geranylgeranyl transferase inhibitor
GTP	guanosine triphosphate
GDP	guanosine diphosphate
GI_{50}	growth inhibition at half of maximal concentration
HDR	homology-directed repair
HMGCoA	3-hydroxy-3-methyl-glutaryl-coenzyme A
hr	hour
ICMT	isoprenylcysteine carboxyl methyltransferase
IP	immunoprecipitation
LDLR	low density lipoprotein receptor
mp53	mutant p53
NHEJ	non-homologous end-joining
OE	overexpressed wild-type p53
PBMC	peripheral blood mononuclear cell
PI	prenylation inhibitor
SREBP	sterol regulatory element-binding protein

SV	simvastatin
RCE1	Ras Converting CAAX Endopeptidase 1
rt	room temperature
WT	wild-type
wtp53	wild-type p53
SD	Standard Deviation

CHAPTER 1

INTRODUCTION

Discovery of gene mutations necessary for cancer initiation and progression have shown that tumors can demand a required mutation using the power of selection. One of the genes commonly mutated across all cancers is TP53, known as “the guardian of the genome”, leading to genome instability and facilitating more mutations generation (Bieging, Mello, & Attardi, 2014). With some exceptions, proteins recruited by a tumor cell also play critical roles in normal cell and are difficult to target. More and more evidence is being collected with the message that metabolic alteration is inherent to oncogenic activation (Hao et al., 2016; Jones & Thompson, 2009; Lee et al., 2014; Levine & Puzio-Kuter, 2010). Although direct targeting the oncogenes is challenging and most likely replaceable by other oncogenes, synthetic lethal targeting is often the way to target tumor cells (Luo et al., 2009; Mendes-Pereira et al., 2009; Scholl et al., 2009). Synthetic lethality is when targeting two oncogenes separately is not applicable but targeting simultaneously is significantly effective. Metabolic changes enforced by certain oncogenes can be detected for synthetic lethality and be targeted for prominent results.

This chapter describes a background on the metabolic requirements of cancer and the current understanding of the cancer mechanisms of controlling metabolism. First, some of the fundamental knowledge in the field is reviewed and then p53 tumor suppressor and its critical role in regulation of metabolism is explained. To further discuss the Ras and Rho collaboration with p53, this chapter explains the importance of small GTPases and the lipid modification necessary for their function. At the end of this chapter, current drugs and the clinical relevance is discussed.

1.1. CANCER CELL METABOLISM

It has been about a century since metabolic alteration in tumors has been detected and described by Otto Warburg (Koppenol, Bounds, & Dang, 2011). He showed tumor tissues prefer glycolysis over the more efficient ATP production pathway, oxidative phosphorylation, even at the presence of extra oxygen. Today, aerobic glycolysis is accepted as a hallmark of cancer and glucose uptake is routinely used by fluorodeoxyglucose positron emission tomography (FDG-PET) in clinical diagnostic settings (Pavlova & Thompson, 2016). Metabolic alterations by tumors are applied to 1- elevate the metabolite influx (Lieberman et al., 2011; Thompson, 2011), 2- consume the nutrients in tumor preference metabolic pathway (Commisso et al., 2013; Conrad & Sato, 2012). For instance, traced glucose uptake shows more involvement of carbon from glycolysis into lipid construction of macromolecules. Lipid biosynthesis genes are shown to be upregulated in TP53 mutant cancer cells that will affect fluidity and lipid saturation of plasma membrane (Rysman et al., 2010). 3- affecting tumor environment (Chen et al., 2007; Chowdhury, Gemin, & Singh, 2005; Comerford et al., 2014; Oldham, Clish, Yang, & Loscalzo, 2015). It is fascinating to know that influx seems to be strictly controlled by extra matrix stimuli (Grassian, Coloff, & Brugge, 2011). In the absence of growth factors or when extracellular matrix is detached, cells did not uptake more glucose and nitrogen even with extra nutrients available in the media (Lindsten et al., 2003).

Unleashed proliferation and invasion of cancer cells requires high import of nutrient supply including glucose, glutamine, lipids and fatty acids for cell building block construction. Cholesterol inhibition by statins blockade of hydroxymethylglutaryl coenzyme A reductase (HMGCR), the rate-limiting step of cholesterol biosynthesis,

retained the normal acinar morphology of breast cancer cells (W. A. Freed-Pastor et al., 2012). Fatty acid enzymes are also reported to be upregulated in multiple cancers. Fatty acid metabolism starts with carboxylation of cytosolic acetyl-CoA carboxylase (AAC) to generate malonyl-CoA for further production of long chain fatty acids by fatty acid synthase (FASN) (Nomura et al., 2010). Additionally, evidence suggests that cancer cells need more glycolysis to escape apoptosis (Hanahan & Weinberg, 2000). In brief, we know net influx of carbon, nitrogen and sulfur is increased, but exact metabolites and pathways that serve tumor demands are still under investigation.

1.2. P53 AND CELL METABOLISM

p53 is an important tumor-suppressor protein and loss of function of wild type p53 is a common event in all human cancers. It is interesting that 75% of p53 mutations are single missense mutations that not only lose wild type function but also participate in activities that have not been seen in wild-type (P. a J. Muller & Vousden, 2013). The majority of these single mutations occur in DNA binding domain that shows the importance of p53 as a transcription factor. Yet there are structural mutations that cause conformational changes and therefore different function (W. A. Freed-Pastor & Prives, 2012). We can divide mutant p53 function into four main groups; 1- binding to DNA to change gene expression, 2- binding to transcription factors to promote their function, 3- binding to transcription factors to promote their function, 4- interactions with proteins to alter their function directly. Mutant p53's acquired function is vastly context dependent and we encounter functions that are inhibitory to another one.

Studies of p53 has made it clear that its anticancer activity is far beyond just a tumor-suppressor and its connections between p53 and cell metabolism has been revealed (Vousden & Ryan, 2009). p53 regulates gene expression of cytochrome c oxidase 2 which is crucial in mitochondrial activity. Loss of p53 results in mitochondria malfunction and eventually leads to the Warburg effect. TP53-induced glycolysis and apoptosis regulator (TIGAR) inhibit glycolysis and upregulate glucose-6-phosphate (G6P) for entry into the oxidative arm of the pentose phosphate pathway (PPP) (P. Jiang et al., 2011). Therefore, ribose and NADDPH will be produced for nucleotide biosynthesis in response to DNA damage stress. Mutant p53 but inactivates the rate-limiting PPP enzyme, G6P dehydrogenase to block PPP. Human cell culture deprivation of glucose and fatty acids were an indication of the important role of p53 in distributing the energy source and regulating gene expression in an attempt to provide an alternative source. For example, in case of glucose deprivation, p53 is activated and induces guanidinoacetate N-methyltransferase (GAMT) (Ide et al., 2009) and lipin1 (LPIN1) gene expression leading to increased fatty acid oxidation (FAO) and fatty acid synthesis inhibition (Assaily et al., 2011) (**Figure 1)**. p53 upregulation of FAO inhibits glycolysis and this is one of the tumor-suppressor mechanism of wild type p53. Another important access of p53 to metabolic pathways is through binding ability to PGC-1 α. Peroxisome proliferator-activated receptor gamma coactivator 1α (PGC-1 α) is a central transcriptional coactivator that strongly coordinates lipid metabolic gene expressions (Sen, Satija, & Das, 2011). p53 studies in adipocytes of obese mice suggested p53 involvement in fatty acid synthesis such as FASN (Yahagi et al., 2003). Mutant p53 interaction with SREBP2 is found to upregulate mevalonate pathway gene transcription leading to breast cells acquiring a malignant state

(W. A. Freed-Pastor et al., 2012). Additionally, p53 regulates sphingolipids-mediated cell cycle and apoptosis (Heffernan-Stroud & Obeid, 2011).

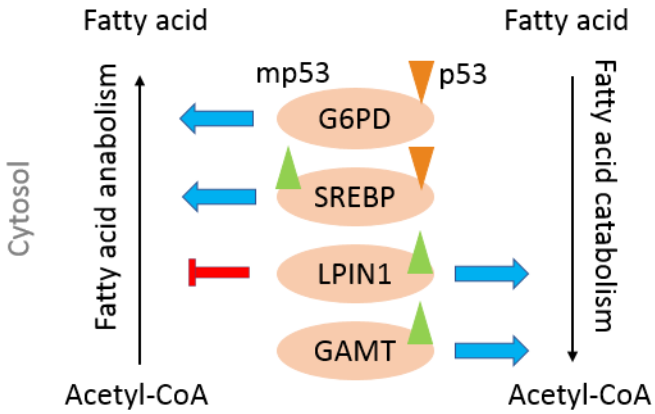


Figure 1. Graphical overview of p53 and fatty acid metabolism. p53 represses G6PD and SREBP and induces LPIN1 and GAMT. Loss of p53 increases anabolism and decreases catabolism. Mutant p53 is shown to upregulate SREBP genes.

1.3. RAS SMALL GTPASES

The Ras oncogene family was the first to be discovered and there has been an intense effort to inhibit them with targeted pharmaceuticals. Ras proteins are the master regulator of cellular signaling and cell cycle, growth, adhesion, migration, and differentiation. Ras is also involved in reprogramming metabolic pathways to support cancer cells' biosynthesis needs. Activated Ras will induce aerobic glycolysis to promote glucose import through SLC2A1 stimulation. Ras activation has been linked to elevating non-hypoxic levels of HIF-1 and MYC activity. SRC phosphorylation is another mechanism of controlling glycolytic enzymes by Ras activation.

Ras superfamily GTPases includes 21 members of the Rho subfamily, such as RhoA, Rac1 and Cdc42, and 18 members of Ras subfamily, such as H-Ras, N-Ras and K-Ras. Rho subfamily is known to control actin cytoskeleton, and the Ras subfamily is known to control cell growth and is frequently mutated in cancer (Coleman, Marshall, & Olson, 2004). Ras/Rho proteins are active when GTP-bound and deactivated when GDP-bound and a large group of proteins are involved to turn this switch on and off. RasGTP and RhoGTP are in a conformational state capable of interacting with other effector proteins for initiating downstream signaling cascades. This tight regulation is achieved by guanine nucleotide exchange factors (GEFs) facilitating GDP dissociation and GTP binding and GTPase-activating proteins (GAPs) that accelerates Ras/Rho GTP hydrolysis to GDP. Rho GDP-dissociation inhibitors (RHOGDIs) regulate Rho proteins by preventing nucleotide exchange and membrane association. Although Ras mutation raised considerable concern in clinical oncology, Ras oncogenic signaling can be induced by Ras deregulation and this has shown to be associated with hyperproliferation (Eckert et al., 2004). RhoA GTPase is a well-known intercellular regulator in gene expression, cell cycle, vesicle trafficking, cell polarity and migration. RhoAGTPase does not get mutated very often but cancer progression has been correlated with RhoAGTPase tissue expression to the extent that it is suggested as a quantitative marker for staging and prognosis (Sahai & Marshall, 2002).

1.4. PRENYLATION

Small GTPases undergo a lipid post-translational modification called prenylation to be transferred to the membrane for activation and initiating signaling cascades. Signaling

activities of cellular proteins such as Ras, Rac1, and Rab are tightly controlled by immobilizing them to a wide variety of subcellular membrane locations. The biological function of prenylation is also coming from their role in facilitating protein-protein interaction. Prenylation, a side product of cholesterol biosynthesis pathway, is a covalent addition of a carbon chain to the carboxyl terminus of proteins contain CAAX sequence. Subsequently, the Rce1 endopeptidase cleaves off the three terminal amino acids and the prenylated Cys residue is methylated by the isoprenylcysteine carboxyl methyltransferase (ICMT). Farnesylation (15 carbon chain) and Geranylgeranylation (20 carbon chain) both referred as prenylation are the products of a 5-carbon building block, isopentenylpyrophosphate, from isoprenoid pathway. Genomic and structural and functional analysis predicts expression of over two hundred proteins with CAAX sequence that undergo prenylation. In conditions where X is a methionine, serine, glutamine or cysteine, protein will be farnesylated and where X is a leucine or isoleucine, geranylgeranylation is preferred. Prenylation is required for normal cellular function and RasGTPases transformation. Ras tends to get farnesylated while Rho is commonly geranylgeranylated. Different proteins have different preferences of prenylation, some prefer farnesylation, some geranylgeranylation and some can be prenylated either way. For example, HRas and NRas are farnesylated whereas KRas can be geranylgeranylated if farnesylation is blocked. This phenomenon, known as cross-prenylation, is implicated as a cause of resistance to FTIs. ICMT and RCE1 are able to modify both farnesylated and geranylgeranylated proteins but the fact that they are both membrane anchored limits their use due to restricted solubility while retaining function (

Figure 2).

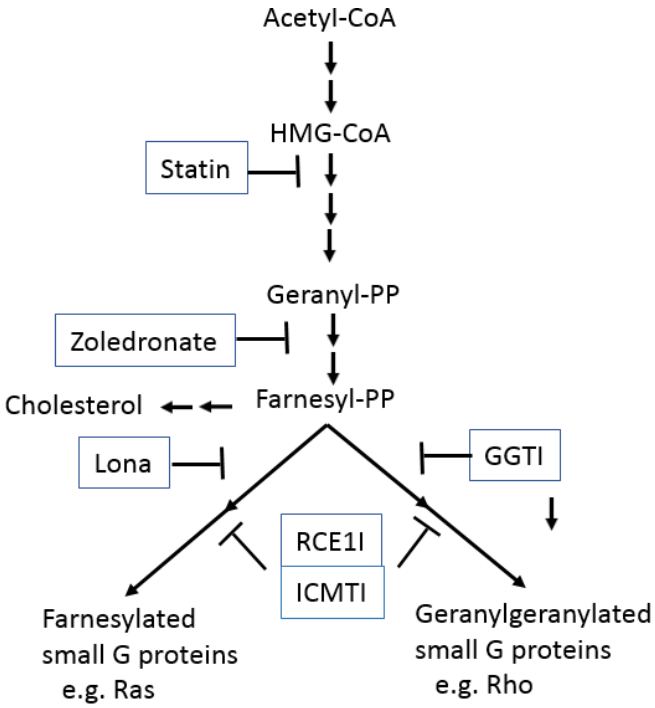


Figure 2. Schematic representation of the prenylation pathway. Compounds used as inhibitors of the prenylation are indicated along the pathway. Lona, Lonafarnib; ICMTI, ICMT inhibitor; RCE1I, RCE1 inhibitor.

1.5. PRENYLATION INHIBITION

Inhibiting HMG-CoA reductase by statins or any of these modifying enzymes, farnesyl-transferase (FTase) and geranylgeranyl-transferase (GGTase), RCE1 and ICMT have been suggested as a cancer therapeutic agent (Walker & Olson, 2005). Statin is a class of drugs prescribed for cardiovascular diseases that dramatically reduced the cerebrovascular events and mortality. Clinical and epidemiology data for over 20 years has suggested a benefit of statin use for cancers patients. Statins are divided into two groups of hydrophilic statins (such as pravastatin, rosuvastatin, and fluvastatin) and

lipophilic statins (such as atorvastatin, lovastatin, and simvastatin). Statins are considered to be safe drugs with few side effects. Researchers have shown the anti-proliferative and anti-migrative effect of statins, particularly for lipophilic statins, in vitro followed by mice studies in different types of cancer including breast, prostate, gliomas. Epidemiology data supports that statin response varies between patients and depends largely on tumor type.

Zoledronic acid, Nitrogen-contacting Bisphosphonates, bind to farnesyltransferase enzyme and therefore inhibits prenylation. It is the most potent osteoporosis drug being used for the clinical adjuvant setting with over 30% breast cancer risk reduction (Drake, Clarke, & Khosla, 2008). Another class of drugs targeting prenylation is FTase inhibitors that have been the subject of intense drug development attempt a decade ago in the hope of targeting KRAS. FTIs are small molecules that compete with, CAAX motif or FPP to bind the FTase. More than 75 clinical trials for FTase inhibitors (FTIs) have been started and among those Lonafarnib and Tipifarnib progressed to phase III (Tsimberidou, Chandhasin, & Kurzrock, 2010). Clinical studies demonstrate very low toxicity for Farnesyltransferase inhibitors. An alternative prenylation of Ras is geranylgeranylation that is shown to be necessary for transformation. Geranylgeranyl transferase inhibitors (GGTIs) are developed for Ras targeting. Researchers have reported successful results in vitro and in animal models (Kazi et al., 2009; Sun, Ohkanda, Coppola, Yin, Kothare, Busciglio, & Hamilton, 2003; Zimonjic et al., 2013). Selective GGTIs have demonstrated to impede transformation and tumor development in vivo (Peterson, Kelly, Weinbaum, & Casey, 2006; Sun, Ohkanda, Coppola, Yin, Kothare, Busciglio, Hamilton, et al., 2003; Vogt, Sun, Qian, Hamilton, & Sebti, 1997). GGTIs increase apoptosis and cell cycle arrest in G1 which is not observed for FTIs (Drake et al., 2008; Sun et al., 1999). There are ongoing clinical trials for different GGTIs for example GGTI-2148 for breast cancer and

myeloma that is going to start for phase I/II. RCE1 and ICMT inhibitors are another group of drugs for targeting Ras oncogenic signaling by prenylation inhibition. It has been shown that knocking down RCE1 protease or methyltransferase leads to RAS mislocalization (Bergo et al., 2000; Kim et al., 1999). It is striking that ICMT gene disruption completely shut down the KRAS-mediated transformation of fibroblasts and BRAF oncogenic transformation (Bergo et al., 2004). Unfortunately RCE1 and ICMT inhibitors are not meeting the required safety profile yet to enter the clinical setting (Winter-Vann & Casey, 2005).

1.6. THERAPEUTIC METHODS FOR P53 DEFICIENCY IN TUMOR

p53 function is so critical for cancer prevention that p53 loss of function is the most common cancer cells event. There is no doubt that developing therapies for preserving p53 function will do a great service to cancer field. Inhibition of p53-MDM2 interaction is one of the strategies that has been applied to prevent inhibitory effect of MDM2. Nutlin3 is a potent drug that competes with MDM2's binding domain enhancing wild-type p53 dependent apoptosis in cancer cells (Grasberger et al., 2005; Issaeva et al., 2004; Vassilev, 2004). Targeting mutant p53 is another important option that has made considerable progress. PRIMA-1 is a good example that specifically targets growth of mutant p53 and has made it to phase I clinical trial (Bykov et al., 2002). 17AAG is an HSP90 inhibitor that disrupt HSP90-mp53 complex hence sends mp53 off to degradation (Li et al., 2011). Lastly, p53 vaccines have been designed stimulating an immune response to p53. Wild-type p53 has a short half-life in comparison with mutant p53 in

cancer cells. Studies have shown p53 antibodies in cancer patients' sera suggesting that p53 antigen could be used for immunotherapy (Katchman et al., 2016). One of the methods that is extensively developing is gene therapy for delivering wild type p53 to cancer cells. Adenoviral delivery of p53 increases apoptosis and prevent tumor progression in different in vitro and in vivo studies of neck cancer (Clayman et al., 1995), lung cancer (Zhang et al., 1994), prostate cancer (C. Yang, Passaniti, Cirielli, Capogrossi, & Cirielli, 1995). The same method of gene therapy can be used to directly deliver other p53 family proteins such as p63 and p73 that can do p53 function (Bisso, Collavin, & Del Sal, 2011; Jost, Marin, & Kaelin, 1997). Genetic editing advancements by discovery of CRISPR-Cas9 technology has opened new avenues to the field of gene therapy. CRISPR-Ca9 system raises the hope to correct genetic diseases including Li-Fraumeni syndrome which is caused by TP53 loss of function and over 80% TP53 missense mutation. In addition, this dissertation introduces a modulated Cas9 for a more efficient and immune silent CRISPR-Cas9 gene therapy.

1.7. THESIS CONTRIBUTIONS

This dissertation addresses a number of fundamental gaps in understanding the mechanism of p53 mutation gain of function in cancer. The mevalonate pathway regulation in mutant p53 tumors with the focus on signaling events. The primary contributions of this dissertation to the field of cancer biology are:

1. Detailing the impact of p53 mutations dependence on proliferation and migration.

2. Demonstrating that the oncogenic mutant p53/Ras/RhoA pathway is activated by p53.

1. Systematic analysis of the correlation of prenylation inhibition, including FTI, GTI, and statins, with 4 different TP53 mutations in breast cancer cell lines.
2. Discovery of an inhibitory mechanism of statin on mutant p53 proliferation and migration.
3. Biochemical analysis, including co-IP and immunofluorescence, to demonstrate that simvastatin functions in the context of mutant p53 to block Ras- induced-RhoA activation.
4. Identifying a gene signature, termed MPR (mutant p53-Ras) that combines expression of 17 genes within the Ras pathway with TP53 mutation status to predict anti-tumor response to statin inhibition.
5. Prediction of the frequency of potential “statin-sensitive” breast cancers within the TCGA cohort.

In addition to clarifying the role of Ras and RhoA activation in mutant p53 cells, this dissertation also describes the development of a method to improve gene therapy with CRISPR-Cas9 system relevant to targeting p53 loss of function:

1. Identification of pre-existing T cell and B cell immune response to Cas9 protein in human.
2. Identification of the two immunodominant T cell epitopes of Cas9 protein.

CHAPTER 2

PRENYLATION INHIBITION IN MUTANT P53 CELLS

2.1. ABSTRACT

TP53 driver mutations are independent biomarkers of poor prognosis in adenocarcinomas. Despite the difficulty in developing direct inhibitors of mutant p53 (mp53), identification of pathways that confer synthetic lethality with mp53 may reveal therapeutic strategies. In this study, we highlight the downstream effect of the mevalonate pathway on prenylation, that is necessary for mp53-induced activation of proliferation and migration. We show that inhibiting prenylation in vitro by statins blocks farnesylation and geranylgeranylation of Ras and Rho induced by mp53. Select TP53 mutations increase the sensitivity to prenylation inhibitors in stably transduced MCF10A cell lines. Transcriptome analysis of MCF10A cells expressing mutant and wild-type p53 demonstrates that the Ras/Rho small GTPases are upregulated in cells expressing mp53, and the FoxO signaling apoptotic pathway is induced post-statin treatment ($p<0.024$, Fold enrichment$\simeq$1.84). We defined a mp53/Ras (MPR) gene expression signature (composed of 16 genes and TP53 mutation status) to predict response to statins. This gene signature was validated in two cell line datasets, 17 breast cancer cell lines (89% accuracy), and the NCI-60 cell line panel (100% accuracy). In summary, we have identified Ras and RhoA as key downstream mediators of p53 mutation, and have used these data to build and validate a predictive classifier of prenylation inhibition.

2.2. BACKGROUND

TP53 is the most common driver mutation in human cancers, but targeted inhibitors have been elusive (W. A. Freed-Pastor & Prives, 2012; P. a J. Muller & Vousden, 2013). In addition to genetic instability due to loss of wild type p53, there is a wide spectrum of neomorphic functions of mutant p53 that alter downstream pathways to enhance tumor progression, survival, and migration. Synthetic lethal targeting of these perturbed cellular pathways that mediate mutant p53 gain of function results in reducing p53 mutation oncogenesis (Khoo, Hoe, Verma, & Lane, 2014; P. A. J. Muller & Vousden, 2014; Parrales & Iwakuma, 2015; Wade, Li, & Wahl, 2013; Yu, Narayanan, Vazquez, & Carpizo, 2014). The mevalonate pathway is one of the pathways upregulated in mutant p53 breast cancer cell lines and inhibiting this pathway by statins has resulted in inhibition of malignant phenotypes (Clendening et al., 2010; W. A. Freed-Pastor et al., 2012; W. Freed-Pastor & Prives, 2016). One product of the mevalonate pathway is protein prenylation, which is necessary for Ras and Rho translocation to the cell membrane for activation and initiation of downstream signaling (Berndt, Hamilton, & Sebti, 2011; M. Wang & Casey, 2016).

It is not surprising that cooperation between two cancer drivers, mutant p53 and Ras signaling pathway, expedites transformation. Mutations in TP53 usually occur in the absence of Ras mutation, but Ras overexpression can trigger similar oncogenic signaling mechanisms as mutations in Ras, and is associated with uncontrolled proliferation (Eckert et al., 2004). Loss of p53 increases Ras activity and aberrant Ras activation, result in p53-mediated apoptosis (Ma, Magut, Chen, & Chen, 2002; Xia & Land, 2007). However, Ras has a complex dynamic interaction with RhoA, leading to RhoGTPase-mediated downstream signaling. RhoGTPases are reported to be upregulated in the presence of

p53 mutation promoting YAP/TAZ activation that can be controlled by inhibiting the mevalonate pathway (Sorrentino et al., 2014). RhoGTPases are both upstream and downstream activators of PI3K leading to cell polarization and recruitment of PI3K to the plasma membrane for cell migration (Fritsch et al., 2013; H. W. Yang et al., 2012). Activation of Rac1 and Cdc42 and mitogenic kinase signaling is required for Ras-induced transformation (Khosravi-far et al., 1995). The mechanisms of how the Ras and Rho signaling pathways integrate to contribute to oncogenesis in mutant p53 tumors is under active investigation (Lawson et al., 2016).

Farnesylation and geranylgeranylation are the products of a 5-carbon building block, isopentenylpyrophosphate, derived from the mevalonate pathway and both are required for normal cellular function and RasGTPase-mediated cellular transformation (Berndt et al., 2011; M. Wang & Casey, 2016). Inhibition of HMG-CoA reductase, the rate-limiting step of the mevalonate pathway, by statins, or inhibition of any of the prenylation enzymes, such as farnesyl-transferase (FTase), geranylgeranyl-transferase (GGTase), Ras Converting CAAX Endopeptidase 1 (RCE1), or isoprenylcysteine carboxyl methyltransferase (ICMT) are under investigation as cancer therapeutics (Walker & Olson, 2005). The anticancer effect of statins, especially hydrophobic statins such as simvastatin, has been observed in multiple clinical studies (Coxon, Oades, Kirby, & Colston, 2004; Xie, Li, Gong, Zhang, & Ma, 2015). The use of cholesterol-lowering medication during adjuvant endocrine therapy is associated with lower breast cancer recurrence in hormone receptor–positive early-stage breast cancer in a retrospective study (Borgquist et al., 2017). Statin use has also been associated both with lower cancer incidence and improved recurrence-free and overall survival, leading to ongoing clinical trials (Bjarnadottir et al., 2013; Brewer

et al., 2013; Nielsen, Nordestgaard, & Bojesen, 2012; “Postdiagnosis Statin Use and Mortality in Danish Patients With Prostate Cancer.,” n.d.).

Here, we hypothesized that the neomorphic activity of mutant p53 functions, in part, by increased prenylation of Ras and RhoA, both of which can be blocked by inhibitors of the mevalonate pathway. Using a panel of MCF10A cell lines engineered to express different mutant p53 proteins as well as breast cancer cell lines, we demonstrate that the activation of Ras and RhoA signaling can be readily blocked by inhibitors of the mevalonate pathway, including by statins. We developed a combined genomic and transcriptomic signature to predict response to prenylation inhibitors, such as statins. This study highlights the importance of prenylation inhibition in the setting of tumors harboring somatic mutations in *TP53*.

2.3. MATERIAL AND METHODS

2.3.1. Cell lines and culture conditions

All human breast cancer cell lines were obtained from American Type Culture Collection (ATCC, Manassas, VA) and maintained at 37°C and 5% CO2. For MDA-MB-231, MCF-7, and MDA-MB468, DMEM and for HCC70, SKBR3 and TD47, RPMI supplemented with 10% fetal bovine serum (FBS) was used. MCF10A cells were maintained in DMEM/F12 supplemented with 5% horse serum, 10 µg/ml insulin, 0.5 µg/ml hydrocortisone and 20 ng/ml epidermal growth factor (EGF). All cell culture chemicals were obtained from Invitrogen (Carlsbad, CA). Mycoplasma contamination was monitored periodically.

2.3.1. Chemicals, antibodies, and reagents

The anti-GAPDH mAb was obtained from Sigma (St. Louis, MO). Raf-1 antibody (#20446) was obtained from Santa Cruz Biotechnology (Dallas, TX) and Ras antibody (#MA1-012X) from Thermo Fisher Scientific was used for imaging. Anti-RhoA mAb (#ARH03), anti-Pan Ras mAb (#AESA02) from Cytoskeleton (Denver, CO) were used for RhoAGTP and RasGTP pull-down assays. Simvastatin (#6196), cholesterol (#C8667), farnesyl pyrophosphate (FPP) (#F6892), geranylgeranyl pyrophosphate (GGPP) (#76532), geranylgeranyltransferase inhibitor (GGTI-2133) (#G5294) and zoledronic acid monohydrate (#SML0223) were obtained from Sigma. Purified (>99%) simvastatin was dissolved into refrigerated and light-protected DMSO stock solutions and stored at -20 °C in 10 mM aliquots. Lonafarnib (Toronto Research Chemicals, ON, Canada), isoprenylcysteine carboxyl methyltransferase (ICMT) inhibitor (EMD Millipore, Temecula, CA) and farnesyl protein transferase inhibitor (EMD Millipore) were stored at -80°C in 5mM aliquots according to the manufacturer's instructions.

2.3.3 Cell proliferation and apoptosis assays

To quantitate in vitro cell proliferation, 2×10^5 cells/mL of cells were seeded in a 96-well plate in triplicate and treated for 24 hours with 0- 20 µM doses of drug, and cell viability was determined at 48-96 hrs using the CellTiter-Glo® luminescent cell viability assay (Promega, Fitchburg, WI). Apoptosis was measured by Caspase-Glo® 3/7 Assay (Promega). Dose response curves were produced to determine the specific IC_{50} values.

2.3.4. Immunoblot analysis

Briefly, 2-5×10^6 cells were harvested by manual dissociation with ice-cold PBS, and resuspended in 300µl RIPA buffer (Invitrogen) containing a cocktail of protease inhibitors (Roche Diagnostics, Indianapolis, IN). Total protein concentration was measured by Pierce BCA assay from Thermo Fisher Scientific. Equal amounts of protein were loaded on a 4-20 % SDS–poly-acrylamide gel and transferred to a polyvinylidene fluoride membrane. The membrane was incubated with 5% nonfat dry milk in PBST for 1 hr at rt. Primary Ab was added as recommended dilutions and bound Ab detected with ECL substrate (BioRad, Hercules, CA).

2.3.5. Immunoprecipitation

Ras and RhoA activity was measured using a Ras pull-down activation assay (Cytoskeleton). Ten million cells were lysed with the provided lysis buffer and equal amounts of cell extracts were incubated with GST-tagged Raf1-RBD (Ras binding domain) or Rhotekin-RBD (Rho binding domain) for an hour. Raf1-RBD/Ras-GTP or RhoAGTP was successfully pulled down using glutathione affinity beads that was provided by the company. Immunoblot with provided anti-Ras and anti-RhoA antibodies were used to measure the quantity of the pulled down protein.

2.3.6. Quantitative real time-PCR

Total RNA was isolated using RNeasy Mini Kit (Qiagen, Germantown, MD) according per the manufacturer's instructions. The A260/A280 ratio and RNA concentration were determined using a NanoDrop. The RNA integrity was determined by microfluidic capillary electrophoresis using an Agilent 2100 Bioanalyzer and the RNA 6000 Nano Chip kit (Agilent Technologies, Santa Clara, CA). Primers were designed by Primerquest and obtained from IDT (Integrated DNA Technologies, Coralville, Iowa). Number of genes from RNA-Seq results were validated by quantitative real-time-PCR (qRT-PCR) on Applied Biosystems Vii7 (Life Technologies). cDNA was synthesized using iScript cDNA Synthesis kit (BioRad) with oligo(dT) in a (BioRad T100) thermocycler (5 minutes at 25°C; 30 minutes at 42°C; 5 minutes at 85°C). Expression levels were relative to GAPDH expression using $2^{-\Delta\Delta Ct}$ analysis method. Experiments were done at least twice with three replicates.

2.3.7. RNA-Seq

RNA was used to prepare cDNA using Nugen's Ovation RNA-Seq System via single primer isothermal amplification (Catalogue #7102-A01) and automated on the (Apollo 324 liquid handler from Wafergen). cDNA was quantified on the Nanodrop (Thermo Fisher Scientific) and was sheared to approximately 300 bp fragments using the Covaris M220 ultrasonicator. Libraries were generated using Kapa Biosystem's library preparation kit (KK8201). Fragments are end-repaired and A-tailed, individual indexes and adapters (Bioo, catalogue #520999) are ligated on each separate sample. The adapter ligated molecules were cleaned using AMPure beads (Agencourt Bioscience/Beckman

Coulter, A63883), and amplified with Kapa's HIFI enzyme (KK2502). Each library was then analyzed for fragment size on an Agilent's Tapestation, and quantified by qPCR (KAPA Library Quantification Kit, KK4835) on Thermo Fisher Scientific's Quantstudio 5 before multiplex pooling and sequencing a 1x50 flow cell on the HiSeq2000 platform (Illumina) at the ASU's Genomics Core facility. Sequence reads will be deposited in the NCBI BioSample database. RNA-Seq reads for each sample were quality checked using FastQC v0.10.1 and aligned to the human genome build 38 (GRCh38) primary assembly from Ensembl Database using STAR v2.5.1b. A series of quality control metrics were generated on the STAR outputs. Cufflinks v2.2.1 was used to report FPKM values (Fragments Per Kilobase of transcript per Million mapped reads) and read counts. Differential expression (DE) analysis was performed with EdgeR package from Bioconductor v3.2 in R 3.2.3. Multi-dimensional scaling (MSD) plot was drawn by plotMDS, in which distances correspond to leading log-fold-changes between samples. For each comparison, genes with false discovery rate (FDR) <0.05 were considered significant and log2-fold changes of expression between conditions (logFC) were reported. Pathway enrichment was performed by DAVID 6.7 Functional Annotation Tool (https://david.ncifcrf.gov/). Genes enriched in Go terms, KEGG pathways, Panther pathways and Reactome pathways were reported.

2.3.8. Statistical analysis

Data are presented as mean ± SD. The number of replicates for each experiment is stated in the description. Statistical differences between and among groups were determined by two-tailed t test and one-way ANOVA followed by Tukey's range test, respectively. IC_{50}

value is determined by GraphPad using log(inhibitor) vs. drug response equation with four parameters. The statistical significance of Kaplan–Meier survival plot was determined by log-rank analysis. Statistical analysis was performed by Microsoft Excel 2013 and GraphPad Prism 6.0 and R version 3.4.0, unless mentioned otherwise in the figure legend.

2.3.8. Gene signature analysis

From a list of genes (310 genes) from small GTPase-mediated signal transduction pathways, 46 genes were differentially expressed in at least two mp53.MCF10As cell lines, pre-statin treatment. Hierarchical clustering of the Log2(FPKM) of these 46 genes for mp53 and wtp53.MCF10A is shown in a heatmap (Figure 15). In order to construct a classifier with Ras signature to predict simvastatin response, IC_{50} values =20 was used as cutoff to separate 17 cell lines into two categories: resistance and sensitive during training. A Random Forest classifier is trained on the basal gene expression with two categories as the response variable. Variable importance provided by the Random Forest is then used to select a smaller subset of probes that are highly predictive of SV response (34 probes). Then probes with small variance among all cell lines were filtered out (32 probes). Finally, probes with high Pearson-correlation coefficient between the gene expression level and sensitivity were selected (16 probes). The final mP53-Ras (MPR) gene signature for SV response consists of RNA expression of 16 genes and mutation status of TP53. The statin response classifier was constructed by gradient boosting method. All the analysis was performed in Python Anaconda platform.

2.4. RESULTS

2.4.1. Prenylation inhibitors reverse malignant phenotypes

To study the impact of TP53 mutation on prenylation, non-malignant mammary MCF10A cells were stably transduced to overexpress ten of the most common missense mutations of TP53 (W. A. Freed-Pastor & Prives, 2012) and overexpressed (OE) wild-type p53 was used as a control. These cell lines are referred to here as mp53.MCF10A and wtp53.MCF10A, respectively. The expression of mutant p53 was confirmed by immunoblot in comparison to wtp53.MCF10A (OE), empty vector transduced MCF10a cells (EV.MCF10A), and 5 cancer cell lines with known p53 mutations (**Figure 3**).

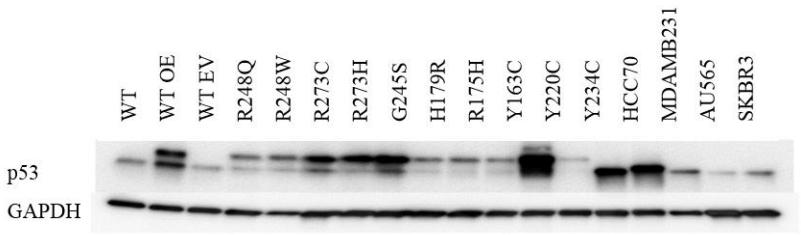


Figure 3. Mutant p53 expression level in the generated MCF10As. Immunoblot representing protein expression of mp53 in comparison to GAPDH as the control. WT OE: wtp53.MCF10A, WT EV: empty vector transduced MCF10a cells.

To investigate the effect of prenylation inhibition on the proliferation of four mutant p53 cells, we selected a panel of prenylation inhibitors, each blocking a different stage of the pathway (**Table 1**). Simvastatin (SV), a competitive inhibitor of HMG-CoA reductase, was used to inhibit upstream mevalonate production. Zoledronate, a bisphosphonate that inhibits farnesylpyrophosphate synthase, blocks both farnesylation and

geranylgeranylation. Lonafarnib selectively inhibits farnesylation, and GGTI-2133 selectively inhibits geranylgeranylation (Berndt et al., 2011; Thurnher, Nussbaumer, & Gruenbacher, 2012). RCE1 is a protease that cleaves three c-terminal residues of both farnesylated and geranylated proteins. NSC1008 was used as a selective RCE1 inhibitor (Mohammed et al., 2016). The final step of prenylation is the methyl esterification of the α carboxyl group of prenylcysteine, and is blocked by ICMT inhibitor II-FTPAT (Bergo et al., 2004).

Table 1. The half maximal inhibitory concentration of prenylation inhibitors for the generated MCF10As.

TP53 status / Drug	IC_{50}(μM)					
	OE	R273H	G245S	R248Q	Y234C	wt/mut
simvastatin	33.19	7.93	8.15	17.81	15.34	2.7
zoledronate	59.09	27.61	25.69	40.45	33.58	1.86
GGTI-2133	1.372	0.46	0.5	0.74	0.88	2.13
lonafarnib	0.48	0.15	0.14	0.2	0.26	2.56
ICMTI	1.01	0.54	0.46	0.68	0.72	1.68
RCEI	44.95	26.84	28.68	36.17	40.65	1.36

As shown in Table **1**, proliferation in all four mp53.MCF10A cell lines is decreased after 48 hours of drug treatment in comparison to the wtp53.MCF10A. To compare the specificity of these drugs to target cells expressing mutant p53, the ratio of the average of the IC_{50} value of the four mp53.MCF10A cell lines over the IC50 value of wild-type is shown as wt-IC_{50} / mut-IC_{50}. Of all inhibitors, simvastatin had the greatest overall

specificity for mutant p53, with an IC_{50} ratio of 2.7. However, there was a range of sensitivity to simvastatin, with R273H and G245S twice as sensitive as R248Q and Y234C.

To further evaluate the impact of p53 mutation on sensitivity to simvastatin, we measured proliferation of 10 mp53.MCF10A cell lines after 60 hours of SV treatment (**Figure 4**). We confirmed that MCF10A cells expressing the p53 mutations R248Q and Y234C were relatively resistant to SV compared to 8 other p53 mutations, which did not correlate with the level of mutant p53 protein expression (**Figure 4**).

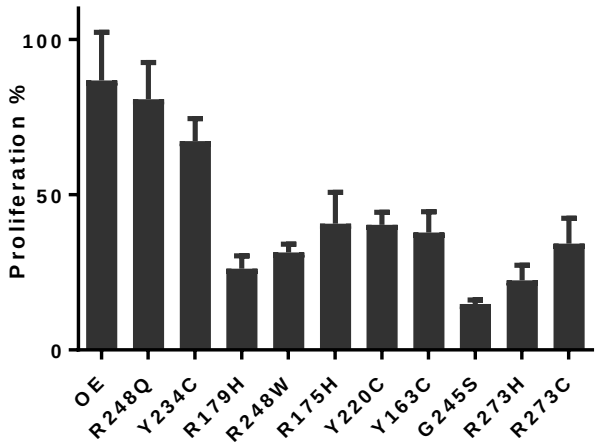
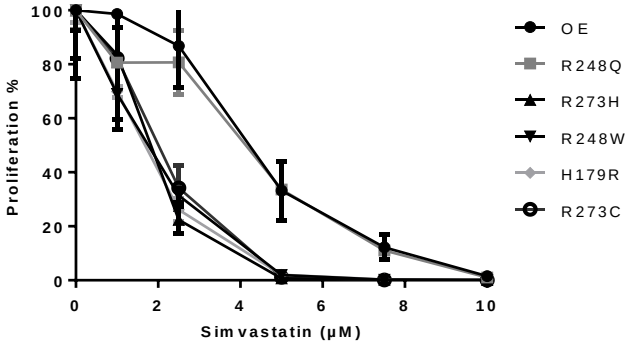


Figure 4. Simvastatin proliferation inhibition of mutant p53 MCF10As. Proliferation percent of mp53 MCF10A cells is reported for 5µM SV-treated cells vs vehicle-treated cells after 60 hrs.

The most sensitive mutation was G245S, which is in the DNA binding domain, but there was no clear correlation between SV sensitivity and presence of mutation in the DNA binding domain or the mutations that alter protein conformation (W. A. Freed-Pastor & Prives, 2012) (**Figure 5**). There are mutations that are in DNA binding domain but shown

to change to conformation therefore grouped as conformational mutation. It is apparent that wild-type over-expressed p53 (OE) as the control is less sensitive to all the mutations

A



B

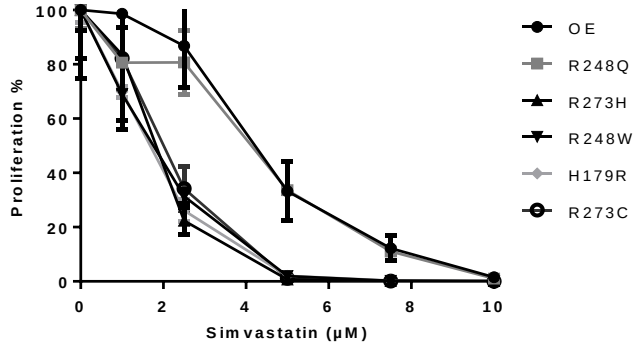


Figure 5. Dose-response to simvastatin in mutant p53 MCF10A. (A) DNA contact mutations of p53. (B) conformational mutations of p53

Inhibition of proliferation by SV is associated with induction of apoptosis in p53 ^{R273H}.MCF10A cells (**Figure 6**). Same doses of concentration are used to compare the both assays. This experiment is designed to test whether the cell viability decreases due to only senescence, or apoptosis as an anticancer activity is involved.

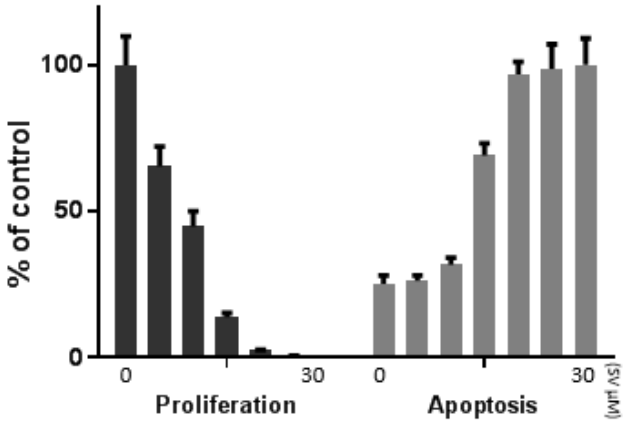


Figure 6. Correlation of proliferation inhibition with apoptosis induction in mutant p53 MCF10A. Proliferation inhibition (CellTiter-Glo assay) and apoptosis induction (Caspase-Glo 3/7 assay) is reported for various SV doses (5, 10, 15, 20, 25, 30) after 48 hrs as a percentage of control.

Unlike the targeted prenylation inhibitors in **Figure 2**, simvastatin has other effects on cholesterol inhibition. To determine whether proliferation inhibition is the direct result of prenylation inhibition, SV-treated (24 hrs, 5μM) wtp53.MCF10A and mp53.MCF10A cell lines were cultured with cholesterol, farnesyl pyrophosphate (FPP), or geranylgeranyl pyrophosphate (GGPP) to rescue inhibition. Both FPP and GGPP, but not cholesterol, efficiently rescued proliferation (**Figure 7**). FPP is the intermediate product necessary for farnesylation. GGPP is the intermediate product in the mevalonate pathway required for geranylgeranylation. The fact that either FPP or GPP are capable of rescuing the cell proliferation means that they can be alternatively used. This effect was no different for R248Q mutation that shows less sensitivity to simvastatin. Same concentration of FPP or GPP was enough independent of how much the proliferation was inhibited.

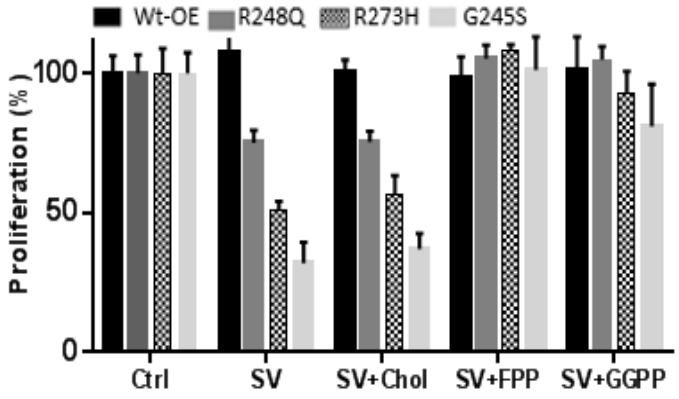
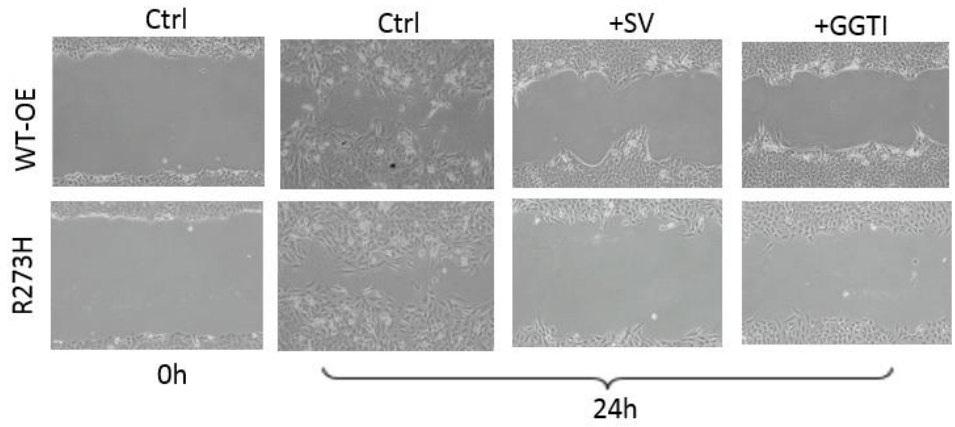


Figure 7. Rescue experiment for simvastatin treatment of mutant p53 MCF10A. GGPP and FPP rescued the viability of SV-sensitive mp53.MCF10As. wtp53.MCF10A and $p53^{R248Q}$, $p53^{G45S}$, and $p53^{R273H}$.MCF10A were treated with 5 µM SV (for 48 h) and vehicle. 5 µM Cholesterol, GGPP, and FPP were added after 24 hrs.

To determine whether prenylation inhibition reverses mutp53-induced cell migration, we preformed wound healing assays with the wtp53.MCF10A and mp53.MCF10A cell lines. Prenylation inhibition reduced migration in all cell lines, but a greater effect was observed in the highly migratory G245S, R273H, and Y234C cell lines (**Figure 9**). The inhibition of migration of $p53^{R273H}$.MCF10A cells after 24 and 48 hours of SV or GGTI-2133 treatment is shown in **Figure 8**.

A



B

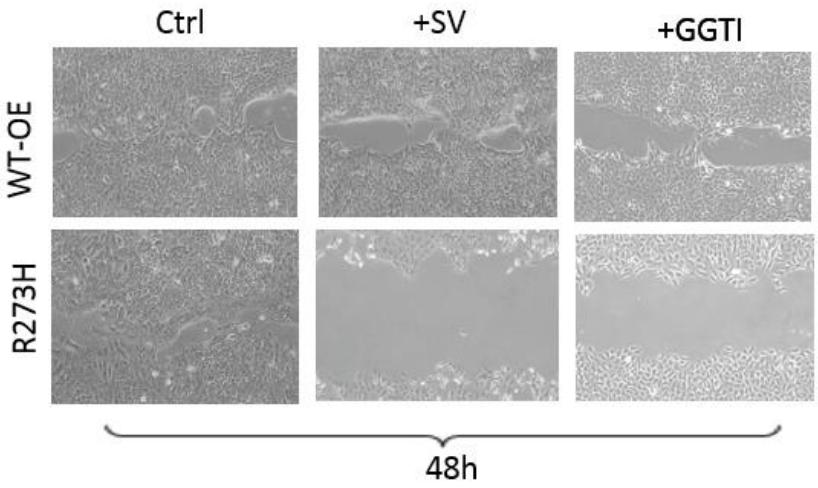


Figure 8. Migration inhibition assay of mutant and wild type p53 MCF10A. Scratch assay for $p53^{R273H}$.MCF10A and WT-OE after 24 and 48 hrs of SV treatment and GGTI-2133 with vehicle-control. Simvastatin=SV, GGPP=Geranylgeranyl pyrophosphate, FPP= farnesyl pyrophosphate

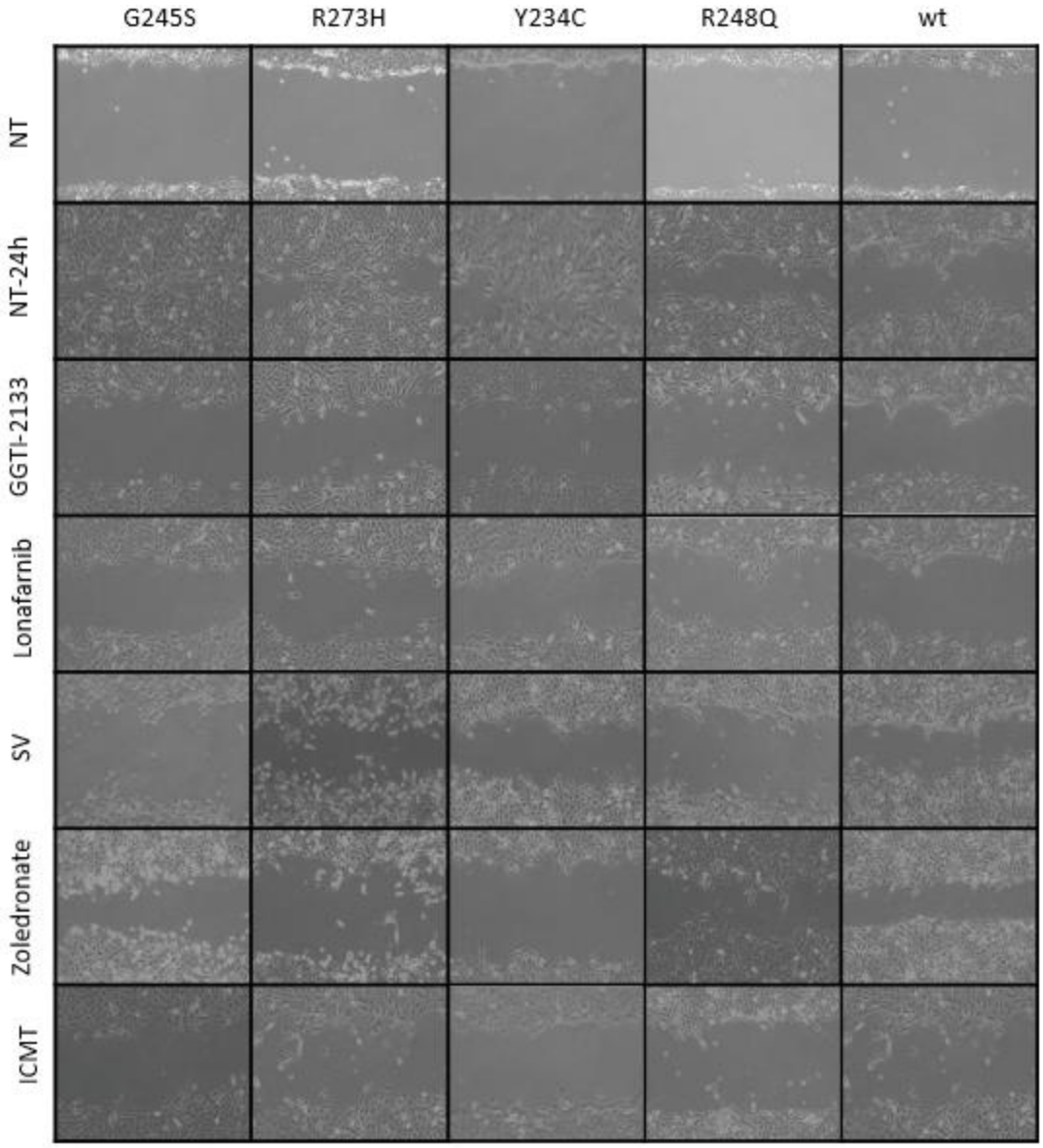


Figure 9. Migration inhibition by prenylation inhibitors for 5 different mp53.MCF10A cell lines is compared to wtp53.MCF10A using a wound healing assay after 24 hrs. Concentrations are 500 nM for GGTI-2133 and Lonafarnib, and ICMTI; 5μM simvastatin; and 25μM zoledronic acid.

2.4.2. mp53 recruits Ras superfamily GTPases for aberrant cell signaling.

To determine the mechanism of SV activity, we performed RNA-Seq analysis of mp53.MCF10A ($p53^{Y220C}$, $p53^{R248Q}$, $p53^{R273H}$, $p53^{G245S}$. MCF10A) and wtp53.MCF10A cells before and after SV treatment. Vehicle treatment (0.1% DMSO) was used for measuring baseline mRNA expression. Since gene expression is an early event we used a low SV concentration (2.5 µM) that preserves morphology and limits senescence. The global gene expression pattern between wild-type and mutant p53 and between SV-treated (red) and vehicle-treated (black) cells is shown by Multi-dimensional scaling (MSD) (**Figure 10**). The MSD plot indicates that each cell line exhibits distinct separation between themselves, and the SV-sensitive cell lines ($p53^{R273H}$and $p53^{G245S}$.MCF10A) have the highest similarity prior to SV treatment.

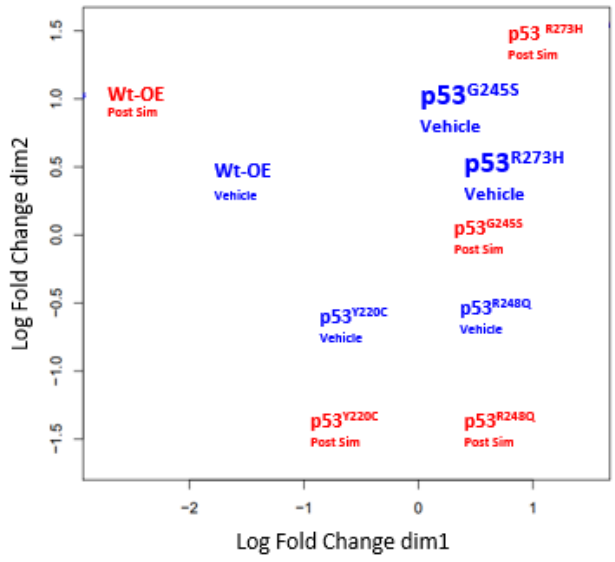


Figure 10. Multi-dimensional scaling plot. Multi-dimensional scaling of logarithm of the gene expression fold change shows the SV sensitive mutant p53s are clustered distinctly**.**

We performed genes enrichment analysis of differentially expressed genes between mp53.MCF10As vs. wtp53.MCF10A using the DAVID pathway analysis tool. it is evident that signal attenuation is an important, common enriched pathway caused by the p53 mutation (**Table 1 and Appendix A**). There is a strong body of knowledge on p53 mutation gain of function on changing the generic transcription (W. A. Freed-Pastor & Prives, 2012) but less attention has been paid to the signaling events. Enriched pathways like ErbB signaling, Ras signaling, RhoGTPase cycle, PI3K and MAPK signaling are closely related to development, proliferation, and migration. To break down the function of the enriched pathways, Cytoscape biological function tool was applied to the most differentially expressed genes in $p53^{R273H}$.MCF10As vs. wild-type ($P<0.05$) (**Figure 11**). The interactome model is presented, comprised of 10 functionally discrete sub-networks or modules including “small GTPase-mediated signal transduction” and “Transmembrane receptor protein tyrosine kinase signaling pathway” (RTK) that are highly interconnected to “Positive regulation of developmental growth”, “Epithelial cell migration”, and “Cellular response to fibroblast growth factor stimulus” (**Figure 11**).

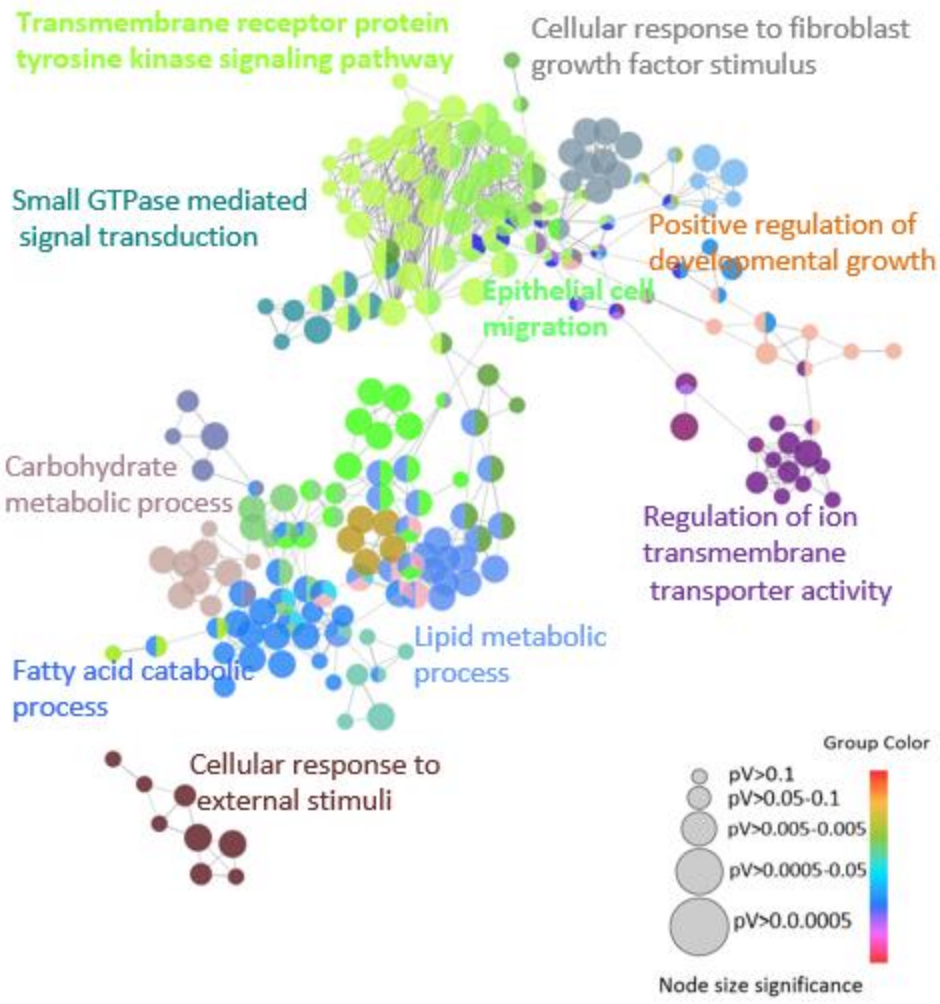


Figure 11. Biological function analysis of mutant p53^{R273H} MCF10A. Global overview of biological functions of enriched pathways in p53^{R273H}.MCF10A vs wtp53.MCF10A using Cytoscape. Pathways within the same biological function are sized and colored the same and corresponding to their p-values.

Next, we applied the DAVID pathway analysis tool to identify the most targeted pathways post-SV treatment in mp53.MCF10As and wtp53.MCF10A

Table 2. Pathway analysis for $p53^{R273H}$.MCF10A. Gene Ontology (GO) enrichment analysis using DAVID for differentially expressed genes in mp53.MCF10A cell lines vs wtp53.MCF10A identifies pathways that are implicated in mutant p53 gain of function in cancer.

Category	Term	P-Value	FE
KEGG	hsa04142: Lysosome	8.15E-05	2.23
KEGG	hsa04010: MAPK signaling pathway	2.08E-04	1.74
REACTOME	hsa983168: Antigen processing: Ubiquitination & Proteasome degradation	5.53E-04	1.66
KEGG	hsa04015: Rap1 signaling pathway	7.73E-04	1.75
REACTOME	R-HSA-5621575: CD209 (DC-SIGN) signaling	0.0010	3.97
KEGG	hsa04012: ErbB signaling pathway	0.0012	2.22
KEGG	hsa04664: Fc epsilon RI signaling pathway	0.0012	2.41
REACTOME	R-HSA-112409: CD209 (DC-SIGN) signaling	0.0014	4.98
KEGG	hsa01100: Metabolic pathways	0.0020	1.23
KEGG	hsa04066: HIF-1 signaling pathway	0.0021	2.07
KEGG	hsa05219: Bladder cancer	0.0023	2.82
KEGG	hsa04668: TNF signaling pathway	0.0025	2.00
KEGG	hsa04722: Neurotrophin signaling pathway	0.0025	1.93
REACTOME	R-HSA-4419969: Depolymerisation of the Nuclear Lamina	0.0033	4.32
REACTOME	R-HSA-2562578: Depolymerisation of the Nuclear Lamina	0.0038	5.05
KEGG	hsa04912: GnRH signaling pathway	0.0049	2.02
KEGG	hsa04070: Phosphatidylinositol signaling system	0.0050	1.97
KEGG	hsa00562: Inositol phosphate metabolism	0.0053	2.17
REACTOME	R-HSA-194840: Rho GTPase cycle	0.0053	1.82
REACTOME	R-HSA-381038: XBP1(S) activates chaperone genes	0.0057	2.31
KEGG	hsa05205: Proteoglycans in cancer	0.0078	1.59
KEGG	hsa04370: VEGF signaling pathway	0.0084	2.21
KEGG	hsa04014: Ras signaling pathway	0.0093	1.54
KEGG	hsa05221: Acute myeloid leukemia	0.011	2.24

KEGG	hsa04510: Focal adhesion	0.012	1.55
KEGG	hsa04962: Vasopressin-regulated water reabsorption	0.013	2.41
REACTOME	R-HSA-204174: Regulation of pyruvate dehydrogenase (PDH) complex	0.013	3.97
KEGG	hsa04064: NF-kappa B signaling pathway	0.016	1.89
REACTOME	R-HSA-6807878: COPI-mediated anterograde transport	0.016	1.79
KEGG	hsa05215: Prostate cancer	0.017	1.86
REACTOME	R-HSA-140534: Ligand-dependent caspase activation	0.017	3.70
KEGG	hsa04925: Aldosterone synthesis and secretion	0.018	1.91
REACTOME	R-HSA-5684264: MAP3K8 (TPL2)-dependent MAPK1/3 activation	0.023	3.47
KEGG	hsa04620: Toll-like receptor signaling pathway	0.023	1.73
REACTOME	R-HSA-200425: Import of palmitoyl-CoA into the mitochondrial matrix	0.024	4.21
KEGG	hsa05200: Pathways in cancer	0.025	1.33
KEGG	hsa04611: Platelet activation	0.025	1.63
REACTOME	R-HSA-1660499: Synthesis of PIPs at the plasma membrane	0.025	2.45
REACTOME	R-HSA-375165: NCAM signaling for neurite out-growth	0.026	2.94
REACTOME	R-HSA-2024096: HS-GAG degradation	0.026	2.94
KEGG	hsa04380: Osteoclast differentiation	0.027	1.62
KEGG	hsa05231: Choline metabolism in cancer	0.029	1.72
REACTOME	R-HSA-937072: TRAF6 mediated induction of TAK1 complex	0.030	3.27
REACTOME	R-HSA-2032785: YAP1- and WWTR1 (TAZ)-stimulated gene expression	0.031	2.55
KEGG	hsa05220: Chronic myeloid leukemia	0.032	1.88
KEGG	hsa00511: Other glycan degradation	0.032	3.22
KEGG	hsa05212: Pancreatic cancer	0.033	1.93
REACTOME	R-HSA-2559585: Oncogene Induced Senescence	0.037	2.47

For $p53^{R273H}$.MCF10A, these pathways are broadly summarized as HMG-CoA reductase related pathways (mevalonate pathway), response to damage, apoptosis, transcription,

and signaling pathways (**Figure 12**). It is critical to seek further biological validations for founded conclusions from gene expression data analysis rather than solely rely on the p-values.

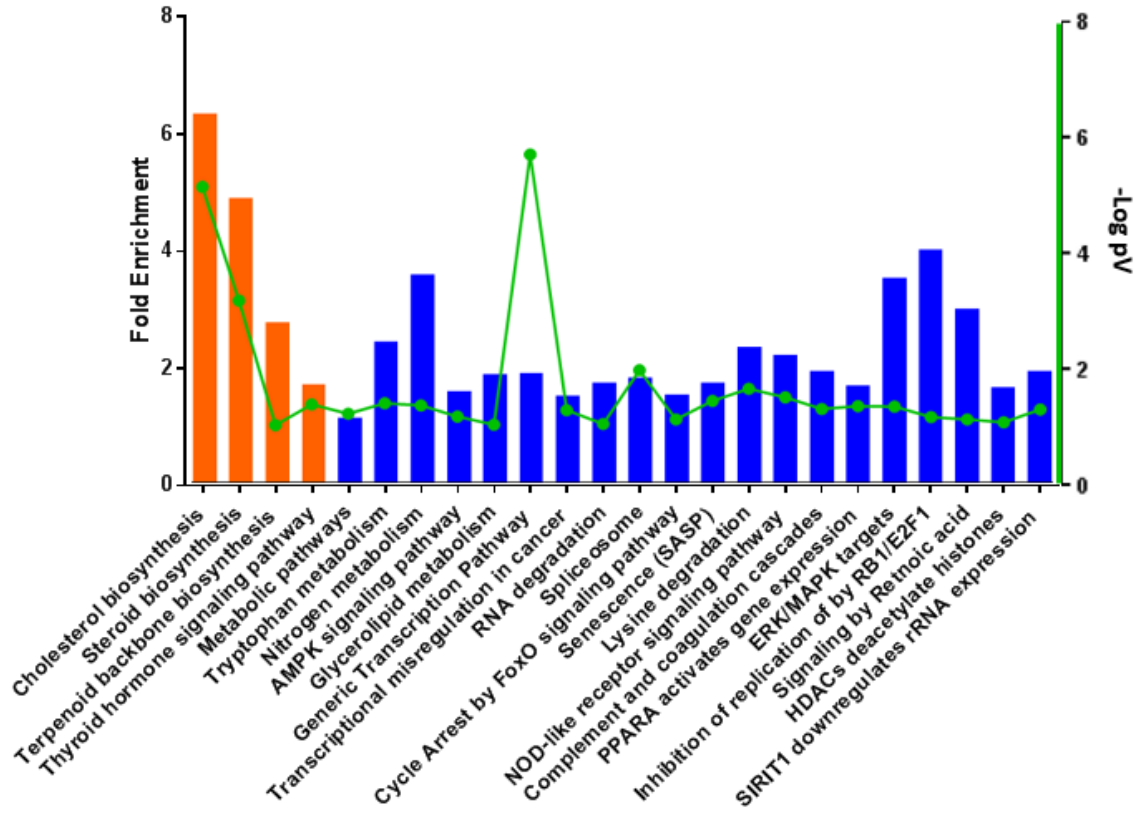


Figure 12. Pathway analysis for statin p53^{R273H}.MCF10A. Enriched pathways in p53^{R273H}.MCF10A SV treated vs vehicle-control. Orange bars are Cholesterol related pathways. DAVID is used for gene enrichment analysis as described in the method section.

First, using quantitative-reverse transcriptase PCR (RT-qPCR), we validated HMGCR expression dose-dependent increase upon SV treatment (**Figure 13**). Inhibiting HMGCR activates the feedback loop to transcribe more enzyme in order to compensate

for the deactivated enzyme. We used 10 and 20 µM to get a clear difference in gene expression. Statin range of concentration that is commonly applied for pre-clinical studies varies between 0-20 µM. The physiological range of statin in patient sera is about 3 µM and definitely not more than 5 µM.

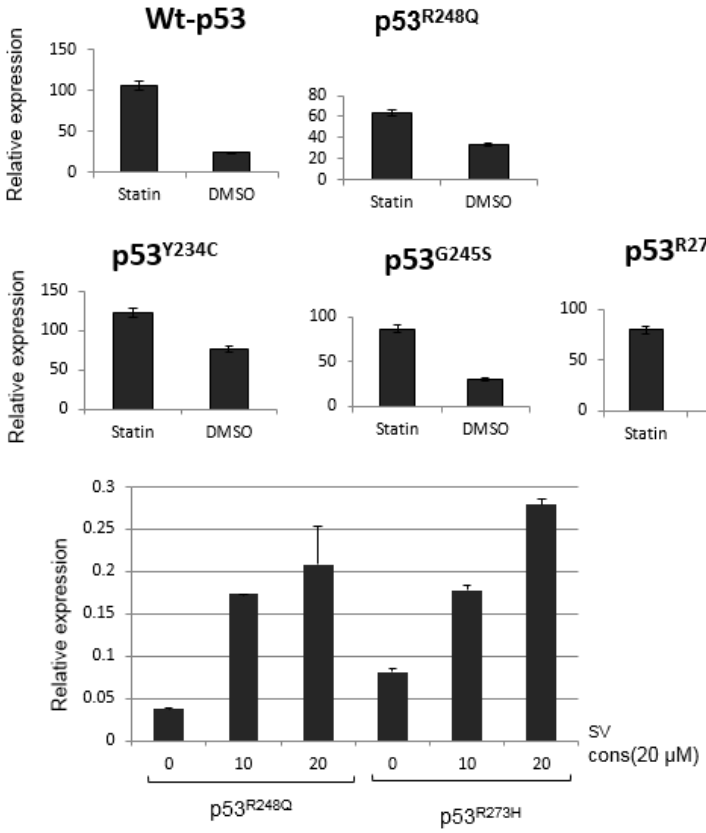


Figure 13. HMGCR expression is upregulated after cholesterol biosynthesis pathway inhibition. In consistent with RNA-Seq results for mp53.MCF10A cell lines, after 2.5 µM SV treatment HMGCR is significantly upregulated as a result of the feedback loop. Dose dependency is demonstrated for $p53^{R248Q}$ and $p53^{R273H}$.MCF10As.

Then assessed the expression of the key transcriptional genes involved in the mevalonate pathway including SREBP2, SREBP1c and LDLR (**Figure 14**). There was a significant upregulation of these genes under cholesterol-deprived conditions. Therefore,

the mevalonate pathway feedback loop is completely functional regardless of TP53 status and there is another underlying mechanism for cell sensitivity to statin treatment. That

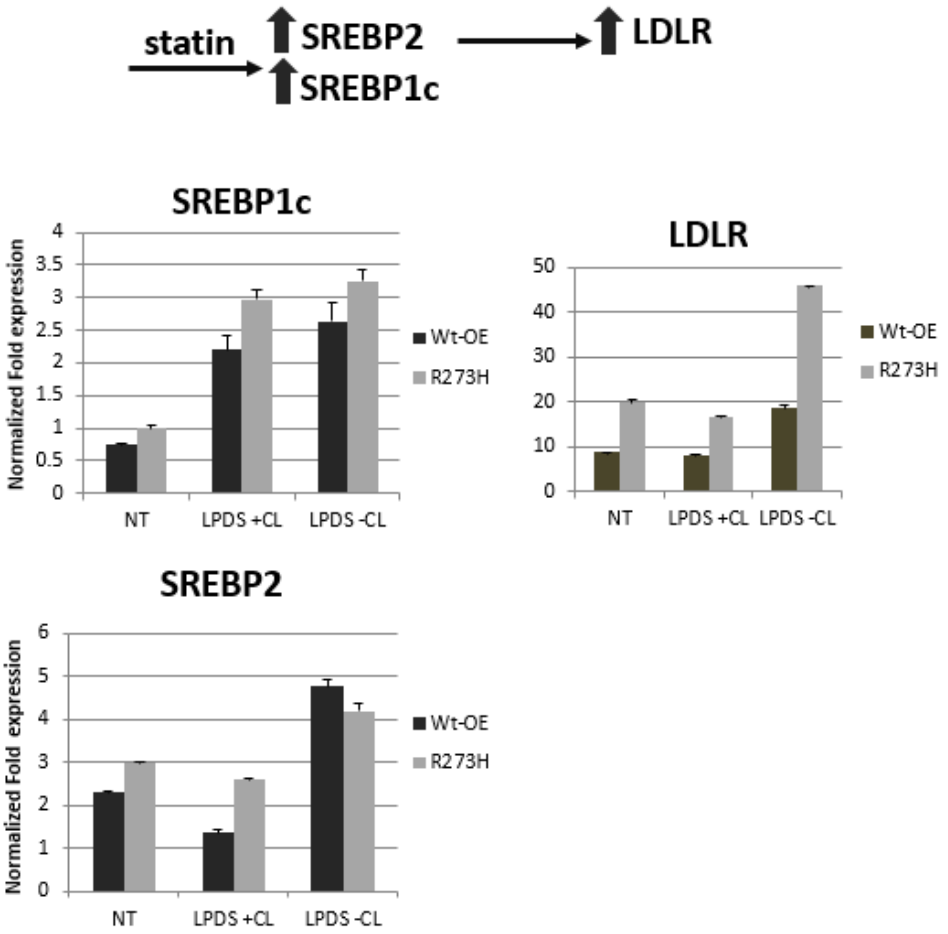


Figure 14. Cholesterol deprivation resulted in significant upregulation of low density lipoprotein receptor (LDLR) expression in mp53.MCF10A cells in compare to the wild-type. Expression of Sterol Regulatory Element Binding Protein 1c and 2 (SREBP1c, SREBP2) and LDLR as genes involved in the cholesterol pathway feed-back loop are measured using RT-qPCR in the following condition. NT cells are in regular standard serum containing media. Cells were incubated in media with Lipoprotein deficient serum for 24 hrs with and without 30µg/ml cholesterol.

motivated us to validate a panel of 17 genes critical in small GTPases and RTK signaling pathway from our RNA-Seq data that had a significant differential expression in mp53 cells vs wtp53 (**Figure 15**). Upregulation of Ras and RhoGTPases and GTPase activators (AGAP4, AGAP6, ARGHGAP28, ACAP3, DLC1, SYDE1, PLEKHG6, RAPGEF), growth factor signaling genes (ERBB2, PTK2 and GRB2,) and downregulation of Rho activation inhibitors (ARGHDIB, ARHGDIA) and anti-proliferation gene (BTG2) in mp53 cells supports our biological function network (**Figure 11**). Significant upregulation of BTG2 post-SV treatment (in a dose-dependent manner) confirms the role of this protein (**Figure 15**). BTG2 downregulation has been reported as a p53 mutation gain of function since it results in unleashed Ras activation in immortalized primary human embryonic lung fibroblasts (WI-38 cells) (Solomon et al., 2012).

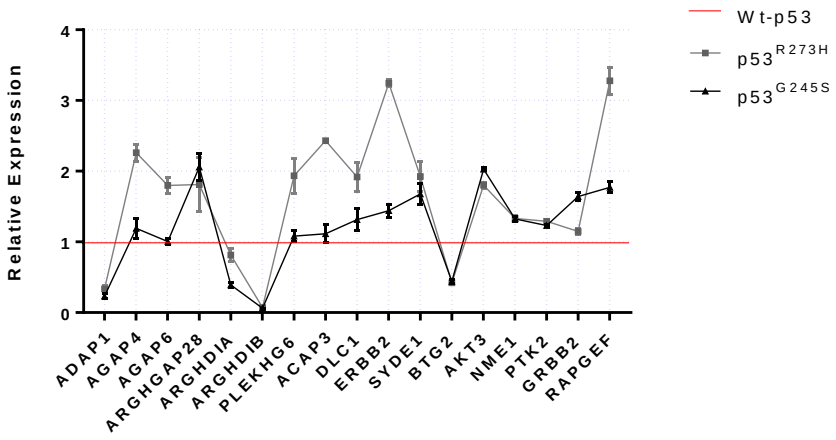


Figure 15. Relative expression of Res-related genes in mutant p53 MC10FAs.
Validation of differentially expressed genes for $p53^{R273H}$.MCF10A and $p53^{G245S}$.MCF10A vs wtp53.MCF10A by RT-qPCR

Another pathway that is enriched after SV treatment in all the mutant and wtp53.MCF10As is FoxO signaling. Forkhead box O (FoxO) transcription factors have

important roles in stress resistance, metabolism, proliferation and apoptosis (Bergo et al., 2004). FoxO proteins can get induced by activation of cell survival pathways PI3K/AKT and Ras/MAPK but also can be activated by stress-activated Jun N-terminal kinase (JNK) and the energy sensing AMP-activated protein kinase (AMPK) upon oxidative and nutrient stress. Reverse-phase protein assay (RPPA) analysis on statin-treated and control breast cancer cells identified FoxO3a protein to be regulated by SV treatment (Wolfe et al., 2015). Consequently, FoxO signaling pathway is in part considered a key pro-apoptotic pathway in response to SV.

In **Figure 13** we observe very similar pattern of gene expression for mutant and wild-type p53. Most of these Ras family related genes expressed more after simvastatin treatment which can be explained by the same logic of increased HMGCR expression after inhibition. Surprisingly, dose dependent expression increase is not linear and that could mean at 20 μM cells are dying and gene expression level is not quite responsive to signaling inhibition anymore.

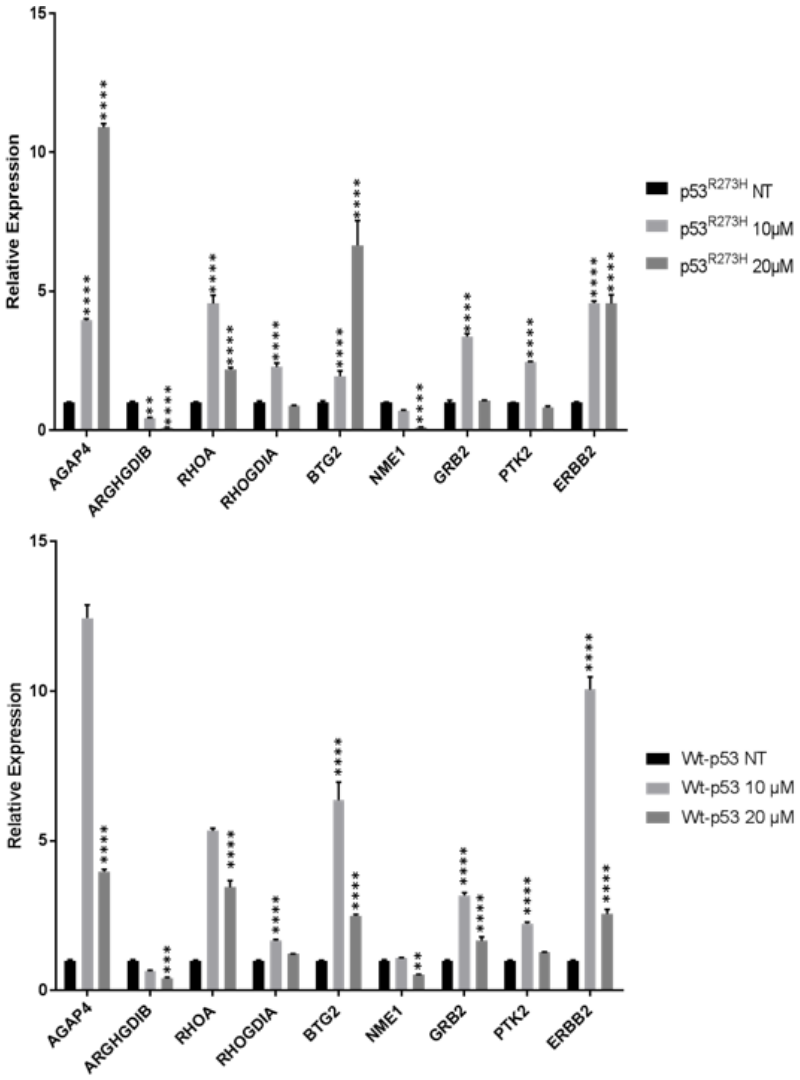


Figure 16. Relative gene expression post-statin in mutant and wild-type p53 cells. Validation of differentially expressed genes for $p53^{R273H}$.MCF10A and $p53^{G245S}$.MCF10A post SV-treated vs vehicle by RT-qPCR. Significantly altered genes are starred. Four stars are $p<0.0005$, Three stars are $p<0.005$, two stars are $p<0.05$.

2.4.3. Prenylation inhibition blocks mp53-induced Ras and RhoA activation.

To explore the mechanistic basis for the increased prenylation dependency in p53 mutant cells, we evaluated the expression of Ras and RhoA because they require prenylation for signal transduction. We performed pull down experiments to probe for

RasGTP in mp53.MCF10A and wtp53.MCF10A cell lines. The Raf1-Ras binding domain was used for RasGTP immunoprecipitation, and the with Rhotekin-Rho binding protein was used for RhoA-GTP immunoprecipitation. Increased levels of RasGTP was observed in all mp53.MCF10A cell lines, while total Ras expression did not change (**Figure 17**).

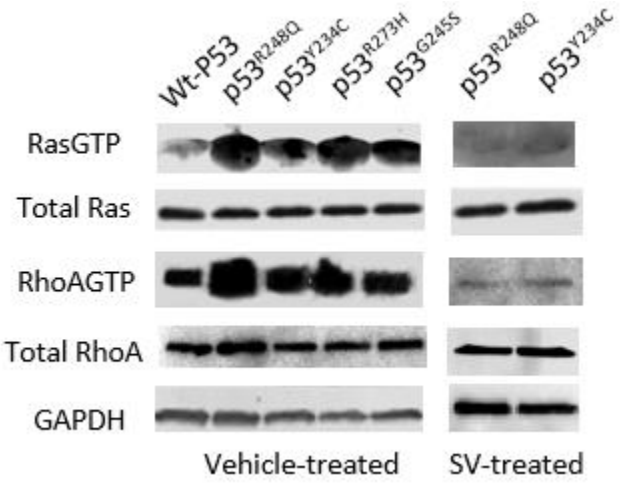


Figure 17. Ras and RhoA activation in mutant p53 MCF10As. Immunoblot analysis of RasGTP, RhoAGTP, total Ras, and total RhoA expression in mp53 and wtp53.MCF10A before SV treatment and $p53^{R248Q}$ and $p53^{Y234C}$ after SV treatment at 10 µM.

This observation was consistent with the reported gain of function of mutant p53 that elevates Ras activation through binding to BTG2 (Solomon et al., 2012). Similarly, RhoA is synergistically activated by mp53 and active Ras. High expression of RhoA-GTP was observed, while total RhoA expression did not change with p53 mutation. To investigate the effect of SV treatment on the mp53-induced Ras-RhoA activation, we measured RasGTP, RhoAGTP, total Ras, and total RhoA expression after 5 µM simvastatin treatment for 48 hours. SV dramatically reduced both activated Ras and activated RhoA in mp53.MCF10A cells, disrupting the mp53/Ras/RhoA oncogenic collaboration. A schematic illustration of the cooperation of RasGTP and RhoGTP with

p53 mutation status is shown, with the sites of action of prenylation inhibitors noted (**Figure 18**).

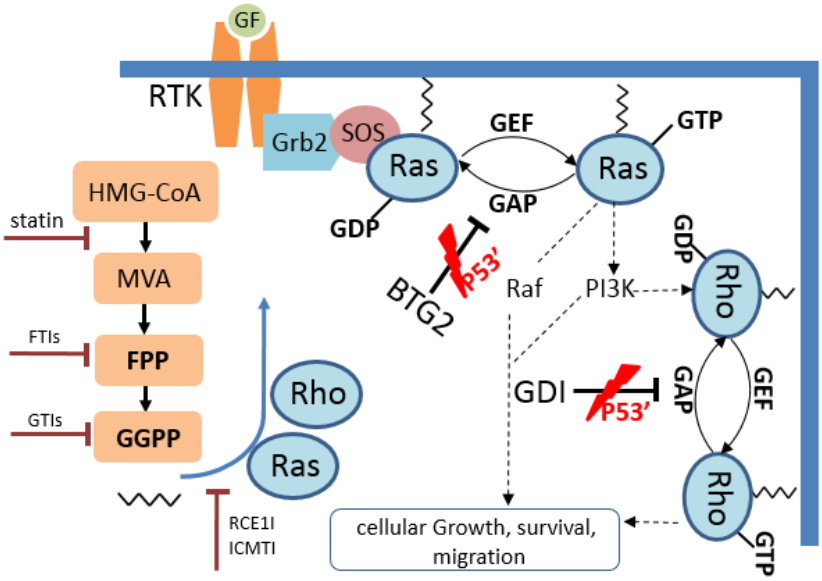


Figure 18. Schematic diagram of Ras activation.

Based on this model, we predicted that mutations in p53 would increase Ras localization to the plasma membrane. Using confocal microscopy of wtp53 and mp53.MCF10A cell lines under serum starvation, the majority of Ras was localized to the plasma membrane. After SV treatment (5 μM for 48 hrs), a cytosolic expression pattern of Ras is observed, in particular in the mp53.MCF10A cell lines (**Figure 19**).

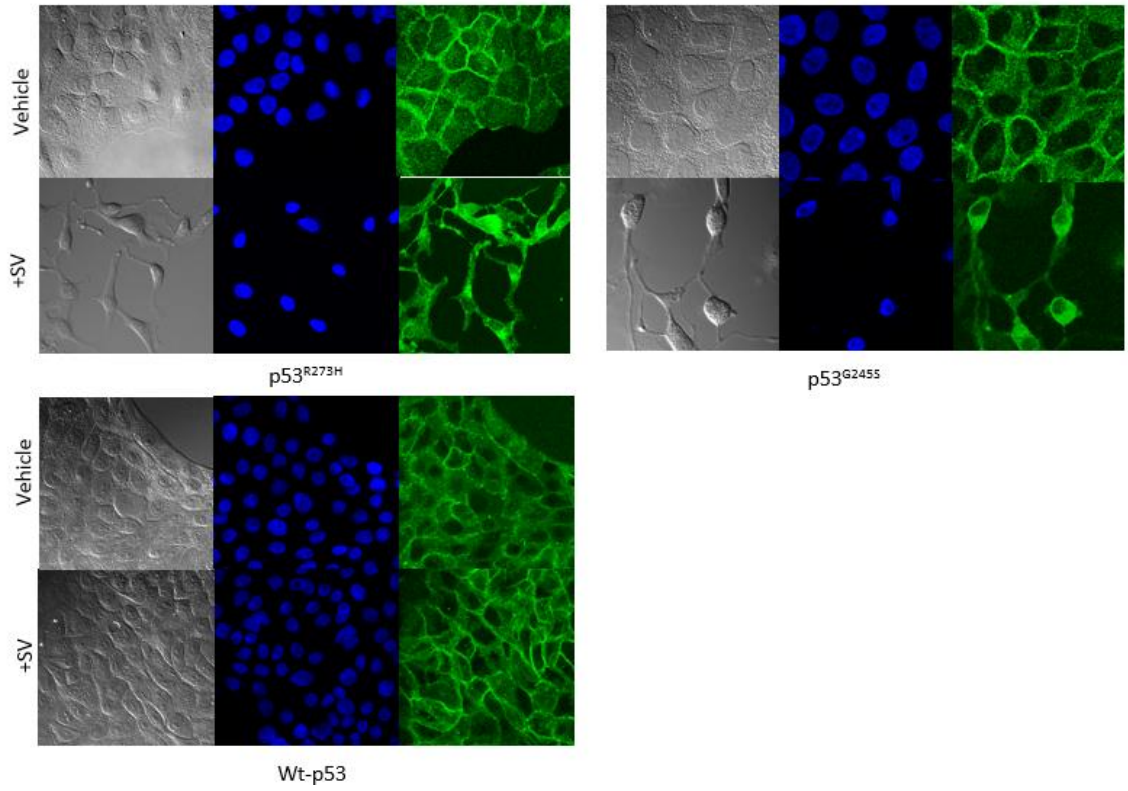


Figure 19. Ras translocation with SV treatment. Immunofluorescence images of Ras in transduced MCF10A cells, before and after treatment with 5 µM SV treatment for 24 hrs. Grey: phase contrast, Blue: DAPI, Green: Ras.

2.4.4. p53 mutation drives a Ras expression signature that correlates with simvastatin sensitivity

Based on the evidence that p53 mutation promotes Ras activation and upregulates small GTPases, we sought to define a signature to identify cancers with these characteristics. We hypothesized that cancer cells harboring the signature would be more susceptible to prenylation inhibition. We used the RNA-Seq data of mp53 and wtp53.MCF10A before and after SV treatment to test our hypothesis. First, we grouped 17 breast cancer cell lines

into three groups based on TP53 status (wild-type; deletion, insertion, or nonsense mutation; and missense mutation). A box-plot of each group with the corresponding SV-GI_{50} values derived from Broad Institute Cancer Cell line Encyclopedia (CCLE) is shown in **Figure 20**. While overall p53 mutation increases SV sensitivity ($p<0.05$), missense mutation status alone was not predictive of SV response (WT vs FS: not significant; WT vs MIS: significant; FS vs MIS: not significant). Therefore, we derived a TP53-Ras regulated gene signature from 47 genes in the enriched Ras-related pathways of the two most sensitive cell lines ($p53^{R273H}$ and $p53^{G245S}$.MCF10A). The baseline expression of these 47 genes are shown in a hierarchical clustered heatmap for mutant and wtp53.MCF10A cell lines (**Figure 21-A**). 18 genes (including ERBB2, SOS2 and MAPK3 and the GTPase activator DLC1) positively correlate with SV sensitivity, and 29 genes (including E2F1 and ARHGDIB) negatively correlate with SV sensitivity. As explained in the method, we used a Random Forest to determine the 16 genes that were significantly associated with SV sensitivity (**Figure 21-B**). The final mP53-Ras (MPR) gene signature for SV response consists of RNA expression of 16 genes and mutation status of TP53.

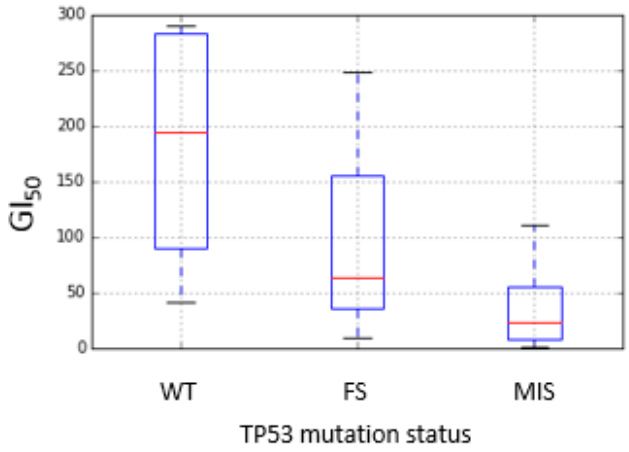


Figure 20. p53 mutation is not a good predictor of GI_{50}. Box-plot of 17 breast cancer cell lines based on TP53 genotype, wild-type (WT), FS (Deletion, insertion or nonsense), and missense (MIS).

2.4.5. Prediction of Prenylation inhibition response in breast cancer cell lines

We applied our Ras gene signature to the gene expression data of 17 breast cancer cell lines to test our SV prediction signature. **Figure 22** demonstrates that 5 cell lines out of 6 were correctly assigned 'sensitive' and 10 out of 11 were correctly assigned 'resistant' to SV. We next assessed whether PI sensitivity in our mp53.MCF10A cells correlates with the existing well-known breast cancer cell lines with the same p53 mutation.

In **Figure 23**, our data confirms that there is a clear separation of killing curves between resistant cells (T47D, MCF7) and sensitive cells (MDA-MB-231, MBA-MB-468, SKBR3 and HCC70). We noticed that all the mutant p53 cell lines (except T47D) had high sensitivity to prenylation inhibition in comparison with MCF-7 which has wild-type p53. Similar to our observation with mp53.MCF10As, MDA-468 (R273H mutation) was strikingly sensitive to SV and HCC70 (R248Q mutation) was less sensitive.

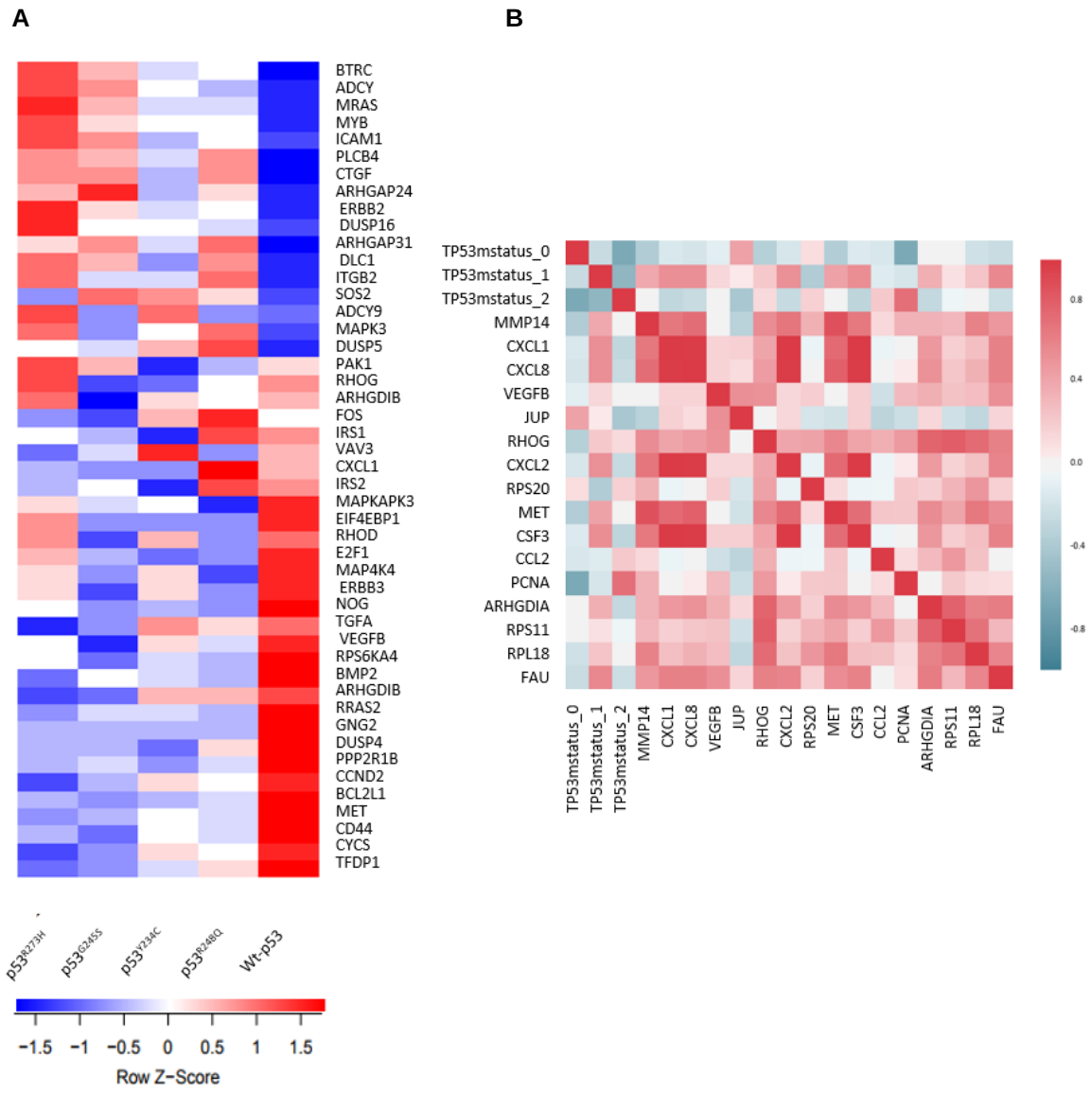


Figure 21. Ras-related gene signature of SV sensitivity. A) Supervised hierarchical clustering Log2 expression of 47 Ras-related genes for mp53.MCF10As and wtp53.MCF10A. B) Pearson correlation coefficient-based heatmap representation of genes with significant correlation with SV sensitivity. SV: simvastatin.

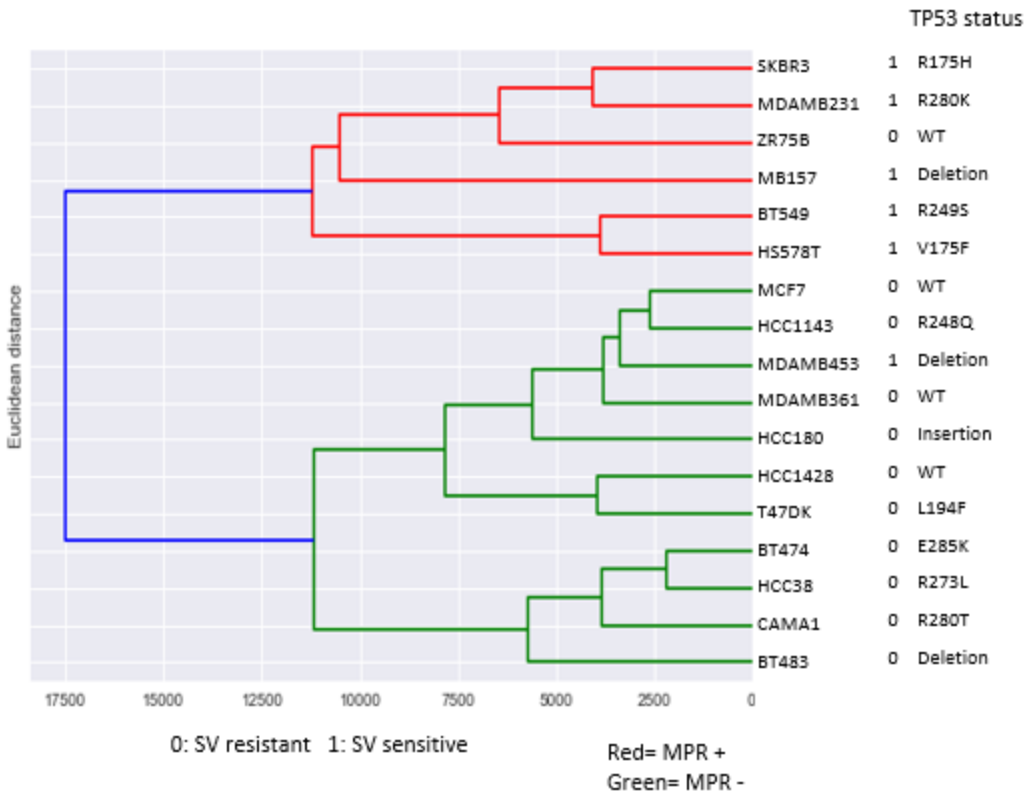


Figure 22. Prediction of simvastatin response in breast cancer cell lines.
Classification of 17 breast cancer cell lines using the MPR gene signature. NCI-60 GI_{50} value used to classify. GI_{50} of 20 µM is considered to be the cut off. $GI_{50} \leq 20$ µM =sensitive. $GI_{50} > 20$ µM=Resistant. Prediction accuracy is 89%.

It is important to consider other characteristics of these breast cancer cell lines (summarized in Fig.5C) to realize why T47D as a mutant p53 cell line is not very dependent on prenylation. As it is reported by Eckert.et al, RasGTP expression of T47D is as low as a wild-type p53 cell line such as MCF-7 (Eckert et al., 2004).

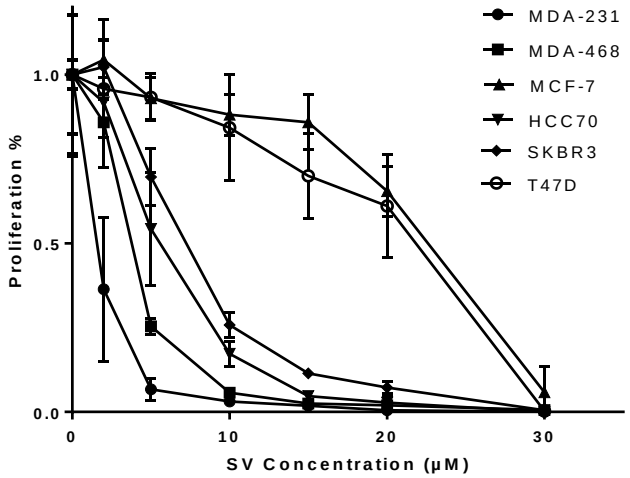


Figure 23. Breast cancer cell line sensitivity to simvastatin. Sensitivity of MDA-MB-231, MDA-MB-468, MCF-7, HCC70, SKBR3 and T47D to SV is confirmed by proliferation inhibition assay. Proliferation is reported as alive treated cells percentage of total alive vehicle treated cells at 0, 2.5, 5, 10, 15, 20 and 30 µM concentration after 48 hrs.

Next, we decided to apply our signature to predict response to all the prenylation inhibitors from the NCI-60 drug screening database. NCI-60 has GI50 values for simvastatin, fluvastatin, lovastatin, mevastatin, pitavastatin, atorvastatin, and zoledronate for five breast cancer cell lines (MDA-MB-231, HS578T, BT549, T47D, MCF-7). Our signature successfully predicts the response to prenylation inhibition for all the five cell lines (**Figure 24**).

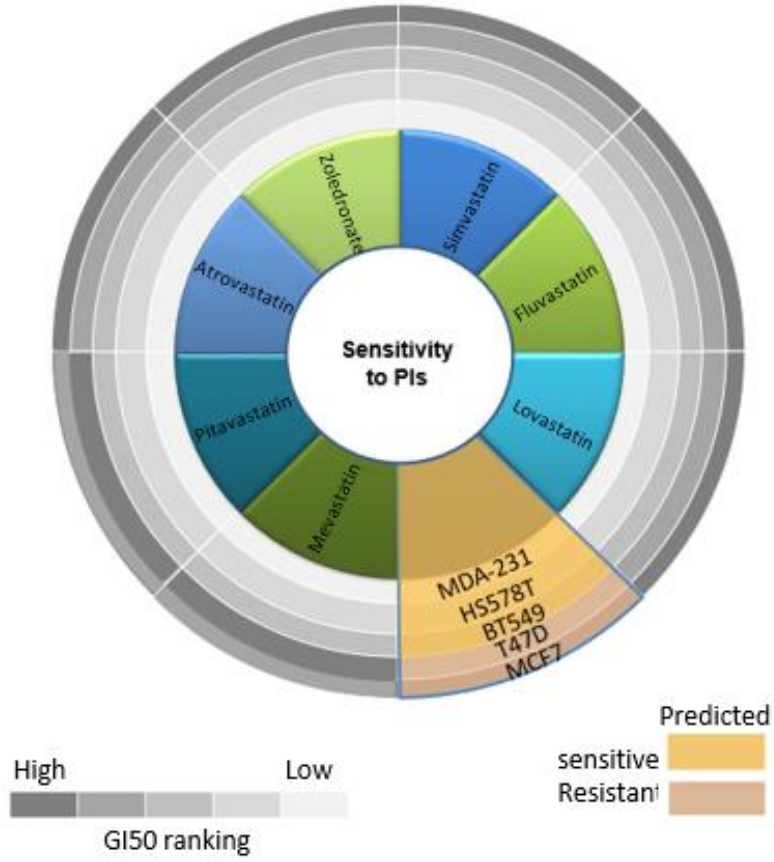


Figure 24. Prediction of prenylation inhibitors to breast cancer cell lines. MPR signature is applied to predict drug response to different prenylation inhibitors (PIs) in the mentioned breast cancer cell lines from NCI-60 database.

2.4.6. Ras signature is used to predict simvastatin response in breast cancer patients

Having identified a mp53-Ras regulated (MPR) gene signature to predict PI's anticancer response in breast cancer cell lines, we next examined this signature using a dataset from a pre-operative statin trial of breast cancer (Bjarnadottir et al., 2013). Gene expression from 25 paired pre- and post-atorvastatin tumor samples is used for classifying

into two groups of potential responders and non-responders by our MPR signature. Response to statin is assessed by the gene expression of proliferation marker Ki67 post- vs pre-statin, noted as the defined end point in this trial (Bjarnadottir et al., 2013). In our model, statin users were predicted to be 9 responders and 16 non-responders with no significant differences in expression of MKI67 (gene coding Ki67). Statin treatment significantly altered 1412 genes in responder group and 2670 genes in non-responders with 660 genes common in two groups (Fig.6A).

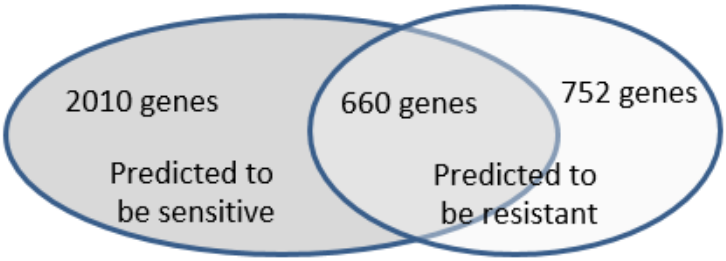


Figure 2-25. Differentially expressed genes post statin in two group pf MPR+ and MPR- patients. A) Classification of 25 newly diagnosed breast cancer patients into 9 responders and 16 non-responders using our prediction signature. TP53 status is not known and excluded from the signature. Paired pre-post treated differential gene expression analysis shows 1412 genes in responders and 2670 genes in non-responders are significantly altered and 660 genes are common between the two groups ($P<0.05$).

Gene ontology analysis of differential gene expression analysis of two groups present different patterns of gene enrichment between responders and non-responders (**Figure** 2-25). Expectedly, common enriched pathways between responders and non-responders are related to lipid lowering effect of statin; SREBP and other cholesterol biosynthesis transcription factors gene expression, cytokines and other immune

regulatory modulations, integrin interactions and NF-kappa B transcription pathway **Figure 26**. 24 and 27-hydroxycholesterol bile acid synthesis are also among the common pathways that are changed post-statin in both groups.

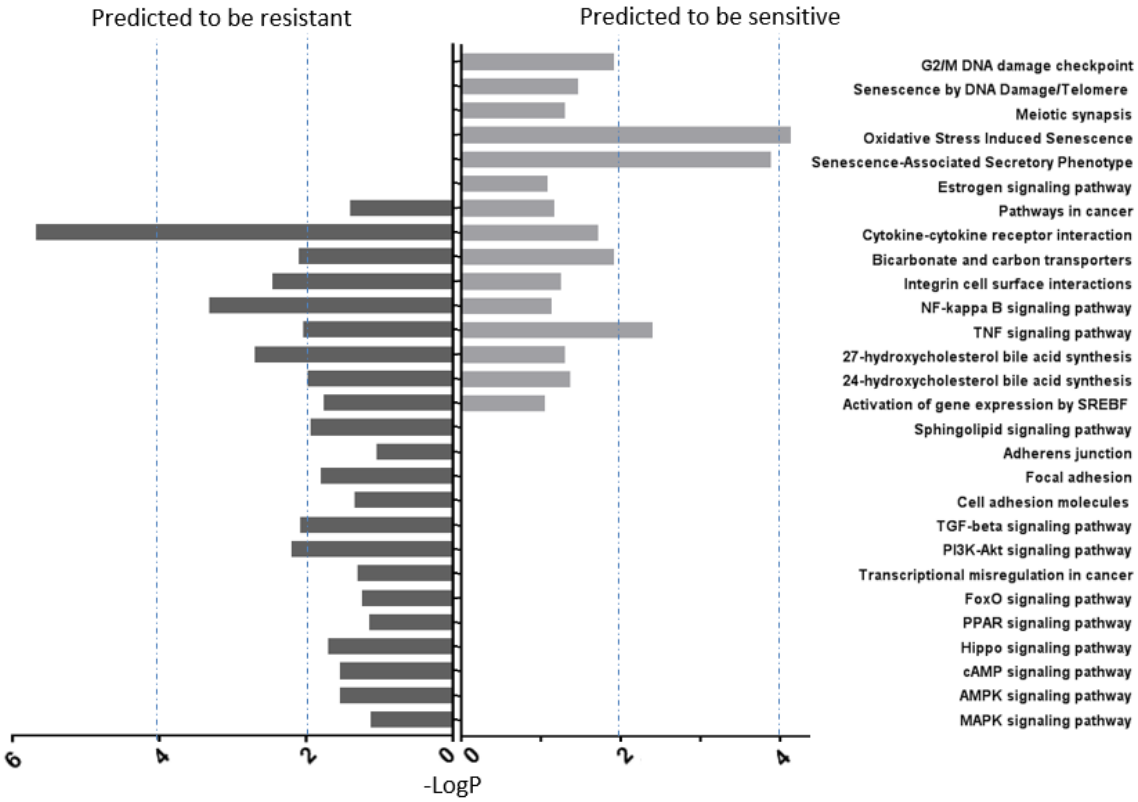


Figure 26. MPR signature is applied to predict response in patients treated with atorvastatin presurgically. Gene ontology analysis shows different pattern of enriched pathways among predicted to be responders and non-responders.

The major difference between the two groups is the highly enriched cell arrest and stress-induced pathways in responders that dominates all other cell events. On the other side, we observe regular growth and energy metabolism -related signaling events that are

targeted by statin, hence FoxO signaling is showing up as we have encountered it for our cell lines' post-statin pathway analysis **Figure 26**.

2.5. DISCUSSION

Current lack of biomarker studies of the anticancer efficacy of any of the PIs raised the challenge of selecting patients prospectively for clinical trials. Most cancer biomarkers are selected based on the statistically significant differences in an unselected population without adequate link to the molecular basis and tumor type. Here, we used pre-clinical studies to select our marker candidates for statin response. We used the Ras/Rho signaling associated genes whose expression was highly correlated with SV response in mp53.MCF10A cells to define a mp53-Ras regulated (MPR) gene signature. This signature was validated in breast cancer cell lines, both in response to statins and zoledronate. Using expression data from a breast cancer neoadjuvant trial of atorvastatin (n=25), we predicted 9 MPR+ patient. After two weeks of statin treatment, gene expression of these two groups represented major differences in drug response using gene ontology analysis. Tumors from patients predicted to be statin responders showed increased oxidative stress and DNA damage. Our Ras gene signature includes 16 genes and TP53 mutation status as wild type, missense, and other mutations.

Recent findings on the sensitivity of mp53 cells to the mevalonate pathway inhibition provides a unique opportunity to tackle over 40 percent of tumors in breast cancer. Although p53 sensitivity to statin has been explained by upregulation of sterol biosynthesis genes, the addback of cholesterol is not sufficient to rescue the effect. Our data is consistent with a large body of pre-clinical studies on statins but in the context of

p53 mutation gain of function. Based on the gene ontology results (**Appendix A**), SV treatment upregulates genes in sterol biosynthesis and fatty acid synthesis; alters membrane composition by changing lipid saturation; and deregulates interactions between integrins, epidermal growth factor and cytokine receptors. Hippo signaling, adhesion and migration signaling pathways are highly impaired presumably due to direct dependence on GTPases. SV induces mTOR and AMP-activating protein (AMPK), a central sensor of cellular energy metabolism. In addition to oxidative stress, impaired MAPK and PI3K signaling, and importantly inhibition of histone deacetylase activity results in FoxO3a-dependent apoptotic pathway signaling. Our biochemical data confirms that mutant p53 cancer cells are more dependent on Ras and RhoA for their transforming activity and survival. Add-back experiments demonstrates that either farnesylpyrophosphate or geranylgeranylpyrophosphate was enough to reverse the statin proliferation inhibition effect. This clarifies that prenylation deprivation is the main reason for successful inhibition of mp53-tumor growth by SV.

Dominant-negative effect of mp53 over wild-type p53 is complex and depends on the context off interaction with transcription factors and other proteins directly. We used MCF10A cells to minimize the effect of existing oncogenic collaborators to be able to understand the strategy of mutant p53 cells to thrive and transform. It is important to recognize that tumor heterogeneity is a huge barrier for the clinical implication of a target study, and we generated a mp53-regulated Ras signature to overcome this. Our data suggests that the mevalonate pathway blockade can be even more effective in cancers with oncogenic GTPase signaling such as prostate cancer. Although Ras mutation is infrequent in breast cancer, there is over 90% mutation frequency for some other cancer types (e.g., pancreatic, colon). There is an urgent need to characterize all the proteins that

require prenylation for their normal function and their role in cancer. FTIs and GTIs can be more potent if prenylation requirement of the tumor target is recognized and applied in clinical trial design. No doubt, our predictive gene signature could improve using large clinical datasets with genome, transcriptome, and clinical information which does not exist yet.

Over two decades of efforts in developing PIs specially FTIs to target the Ras genes, the most common oncogenic activating mutations, did not provide any survival benefit for the patients. Nonetheless, the biological role of prenylation is gaining more attention due to its crucial contribution in RasGTPase and RhoGTPase malignant transforming activities. Today, we have a better understanding that KRAS and HRAS can use either farnesylation or geranylgeranylation as their lipid modification and this can be the reason for KRAS tumor resistance to FTIs (M. Wang & Casey, 2016). Identification of proteins critical for a certain tumor that are exclusively either farnesylated or geranylated can give PIs a clinically meaningful improvement. For instance, the FTI antitumor effect does not rely on Ras activation status in prostate cancer cells and other downstream prenylated proteins such as RALA and RALB could be of importance (Lim et al., 2005) . However, targeting HMG-CoA reductase, upstream of prenylation, can limit both farnesylation and geranylgeranylation with the added benefit of inhibiting mevalonate kinase. Mevalonate kinase is reported to be associated with mp53 misfolding (W. Freed-Pastor & Prives, 2016; Parrales et al., 2016). We conclude that Inhibiting the mevalonate pathway will target mp53- Ras induced -RhoA axis effectively by mp53 degradation, changing the cellular Ras distribution and inhibiting Rho signaling.

CHAPTER 3

GENE THERAPY USING CRISPR-CAS9 SYSTEM

3.1. INTRODUCTION AND BACKGROUND

The CRISPR/Cas9 gene-editing tool has raised hopes for developing personalized treatments for complex diseases such as genetic disorders and cancer, which are currently in clinical trials (Cyranoski, 2016; Reardon, 2016). This excitement comes after a history of optimism and disappointment about the potential of gene therapy engendered by impressive success stories and serious adverse events (Cavazzana-Calvo et al., 2000; Cyranoski, 2016; Gaspar et al., 2004; Hacein-Bey-Abina et al., 2002; Howe et al., 2008; Manno et al., 2006; Marshall, 1999; Reardon, 2016). The expression of Cas9 in mice has been recently shown to evoke both cellular and humoral immune responses (Chew et al., 2016; J. Wang et al., 2013), which raises concerns regarding its safety and efficacy as a gene therapeutic. Lessons learned from the host immune reactions to the numerous exogenous gene delivery systems under investigation (Mays & Wilson, 2011; Mingozzi et al., 2013; Yin et al., 2014) suggest that this immunogenicity is potentially disruptive.

Both B-cell and T-cell host responses specific to either the transgene or the viral components of the adenoviral (Ahi, Bangari, & Mittal, 2011; Aldhamen & Amalfitano, 2016) and adeno-associated viral (AAV) (Ahi et al., 2011; Aldhamen & Amalfitano, 2016; Mays & Wilson, 2011; Mingozzi et al., 2013) vectors have been detected, despite known low immunogenicity of AAV. The potential consequences of this immune response include neutralization of the gene product; destruction of the cells expressing it leading to loss of therapeutic activity or tissue destruction; memory effect that prevents re-administration;

and violent innate inflammatory response (Brunetti-Pierri & Ng, 2009; Halbert, Standaert, Wilson, & Miller, 1998; H. Jiang et al., 2006; Kay, 2011; Nathwani et al., 2011). Another crucial concern facing the translation of gene manipulation techniques to humans is the more drastic immune response observed in humans and large-animal models compared with mice (Gao et al., 2009; Manno et al., 2006). The transgene expression, although sustained in animal models, is short-lived in humans (Manno et al., 2006), likely as a consequence of the immune response (Mingozzi et al., 2007).

Due to natural exposure, pre-existing immunity directed against the vector and less commonly the transgene is a common challenge in gene therapy. In the case of AAV, specific neutralizing antibodies and T cells are frequently detected in healthy donors (Boutin et al., 2010; Mingozzi et al., 2007; Thwaite, Pages, Chillon, & Bosch, 2015) and in contrast to mice, specific $CD8^+$ T cells were shown to expand following gene delivery (Mingozzi et al., 2007). There has been recent progress in developing strategies to overcome this problem (Bartel, Schaffer, & Buning, 2011; Martino et al., 2013; Mingozzi et al., 2013). Of the various Cas9 orthologs from different bacterial species studied (Esvelt et al., 2013; Hirano et al., 2016; Ran et al., 2015; Zetsche et al., 2015), the *Streptococcus pyogenes* Cas9 (SpCas9) is the best characterized. Being a bacterial protein, SpCas9 is likely to trigger cellular and humoral immune reaction in humans, as was demonstrated in naïve mice (Chew et al., 2016; J. Wang et al., 2013). More alarmingly, the ubiquity of *S. pyogenes* with 700 million infections annually (Carapetis, Steer, Mulholland, & Weber, 2005), suggests that pre-existing immunity to SpCas9 in healthy individuals is a reasonable concern.

Cas9-specific T-cell activation and proliferation were confirmed in an expanded CD45+ cell population following *in vivo* expression of Cas9 delivered by an AAV vector or

DNA electroporation in mice (Chew et al., 2016). This highlights the need to characterize the immunogenicity of Cas9 in humans as this gene-editing technology is moving to the clinic. Here, we sought to characterize the pre-existing immune response to SpCas9 in healthy individuals and to identify the immunodominant T-cell epitopes with the aim of modulating Cas9 immunogenicity.

3.2. MATERIALS AND METHODS

3.2.1. Detection of Cas9-Specific Serum Antibodies in Healthy Controls

Healthy control sera (n = 183) used in this study, previously described (Anderson et al., 2015) [38], are a subset of a molecular epidemiology study of head and neck cancer at the MD Anderson Cancer Center, collected between January 2006 and September 2008. *S. pyogenes* lysate was prepared by sonication of bacterial pellets from overnight cultures of *S. pyogenes* ATCC 19615 in the presence of 1 pill of cOmplete Protease Inhibitor (Sigma-Aldrich) after 3 cycles of freezing and thawing. Serum antibody detection was performed using ELISA. 96-well plates were coated with of 20 µg/mL recombinant *S. pyogenes* Cas9 nuclease (New England Biolabs, Ipswich, MA) or *S. pyogenes* lysate. Sera were diluted 1:50 in 10% *E. coli* lysate prepared in 5% milk-PBST (0.2% tween) (D. Wang et al., 2015), incubated with shaking for 2 h at room temperature, and added to the specified wells in duplicate. Horseradish peroxidase (HRP) anti-human IgG Abs (Jackson ImmunoResearch Laboratories, West Grove, PA) were added at 1:10,000, and detected using Supersignal ELISA Femto Chemiluminescent substrate (Thermo Fisher Scientific, Waltham, MA). Luminescence was detected as relative light units (RLU) on a Glomax 96

Microplate Luminometer (Promega, Madison, WI) at 425 nm. To establish cut-off values, an RLU ratio > (the mean +3 standard deviations) of 125 randomly chosen control samples was designated positive.

3.2.2. **Cas9 candidate T cell epitope prediction**

We used our previously described prediction strategies (Chowell et al., 2015; Krishna & Anderson, 2016) to predict candidate Cas9 T cell epitopes. Briefly, we predicted HLA-class I restricted 9-mer and 10-mer candidate epitopes derived from the Cas9 protein (Uniprot - Q99ZW2) for HLA A*02:01. The protein reference sequence was entered into 5 different prediction algorithms; 3 MHC-binding : IEDB-consensus binding (Moutaftsi et al., 2006) [41], NetMHCpan binding (Hoof et al., 2009), Syfpeithi (Rammensee, Bachmann, Emmerich, Bachor, & Stevanović, 1999) and 2 antigen-processing algorithms: IEDB-consensus processing, ANN processing (Tenzer et al., 2005) [44]. The individual scores from each of the prediction algorithms were then normalized within the pool of predicted peptides after exclusion of poor binders as previously detailed (Chowell et al., 2015; Krishna & Anderson, 2016), and the average normalized binding scores were used to re-rank the candidate peptides. The top 38 candidate peptides (Table 1) were selected for experimental testing.

3.2.3. Ex vivo stimulation and epitope mapping of Cas9 by ELISpot

All peripheral blood mononuclear cells (PBMCs) were obtained from healthy donors using informed consent under IRB# MOD00006783. PBMCs were isolated from

fresh heparinized blood by Ficoll–Hypaque (GE Healthcare, UK) density gradient centrifugation and stimulated as previously described [40]. Briefly, predicted Cas9 peptides (> 80% purity) were synthesized by Proimmune, UK. Each peptide was reconstituted at 1mg/mL in sterile PBS and pools were created by mixing 3-4 candidate peptides. Sterile multiscreen ELISpot plates, (Merck Millipore, Billerica, MA, USA) were coated overnight with 5µg/well of anti-IFNγ capture antibody (clone D1K, Mabtech, USA) diluted in sterile PBS. Frozen PBMCs were thawed rapidly and recombinant human IL-2 (20U/mL) was added. They were then stimulated in triplicates with 10µg/mL Cas9 peptide pools (or individual peptides for deconvolution), pre-mixed CEF pool as a positive control (ProImmune, UK), or DMSO as a negative control in the anti-IFNγ-coated ELISpot plates, (Merck Millipore, Billerica, MA, USA) and incubated in a 37°C, 5% CO_2 incubator for 48 hours. Plates were washed three times for 5 min each with ELISpot buffer (PBS + 0.5% FBS) and incubated with 1µg/mL anti-IFNγ secondary detection antibody (clone 7-B6-1, Mabtech, USA) for 2 hours at room temperature, washed and incubated with 1µg/mL Streptavidin ALP conjugate for 1 hour at room temperature. The wells were washed again with ELISpot buffer and spots were developed by incubating for 8-10 min with detection buffer (33µL NBT, 16.5µL BCIP, in 100mM Tris-HCl pH 9, 1mM $MgCl_2$, 150mM NaCl). Plates were left to dry for 2 days and spots were read using the AID ELISpot reader (Autoimmun Diagnostika GmbH, Germany). The average number of spot forming units for each triplicate was calculated for each test peptide or peptide pool and subtracted from the background signal.

3.2.4. Autologous APC generation from healthy donor PBMCs

Autologous CD40L-activated B-cell APCs were generated from healthy donors by incubating whole PBMCs with irradiated (32 Gy) K562-cell line expressing human CD40L (KCD40L) at a ratio of 4:1 (800,000 PBMCs to 200,000 irradiated KCD40Ls) in each well. The cells were maintained in B-cell media (BCM) consisting of IMDM (Gibco, USA), 10% heat-inactivated human serum (Gemini Bio Products, CA, USA), and Antibiotic-Antimycotic (Anti-Anti, Gibco, USA). BCM was supplemented with 10 ng/mL recombinant human IL-4 (R&D Systems, MN, USA), 2µg/mL Cyclosporin A (Sigma-Aldrich, CA, USA), and insulin transferrin supplement (ITES, Lonza, MD, USA). APCs were re-stimulated with fresh irradiated KCD40Ls on days 5 and 10, after washing with PBS and expanding into a whole 24-well plate. After two weeks, APC purity was assessed by CD19+ CD86+ expressing cells using flow cytometry, and were used for T-cell stimulation after >90% purity. APCs were either restimulated up to 4 weeks or cryopreserved for re-expansion as necessary.

3.2.5. T-cell stimulation by autologous APCs

Antigen-specific T-cells were generated by stimulating healthy donor B-cell APCs by either peptide pulsing of specific Cas9 epitopes, or by transfecting with the mammalian expression plasmid pCDNA3.2 (Invitrogen, CA, USA) encoding the whole Cas9 protein. Peptide pulsing of APCs was done under BCM 5% human serum, with recombinant IL-4. Transfection of APCs was done with primary P3 buffer in a Lonza 4D Nucleofector and program EO117 (Lonza, MD, USA) and incubated in BCM-10% human serum and IL-4.

Twenty-four hours later, on day 1, APCs were washed and incubated with thawed whole PBMCs at a ratio of 1:2 (200,000 APCs : 400,000 PBMCs) in a 24-well plate in BCM supplemented with 20U/mL recombinant human IL-2 (R&D Systems, MN, USA) and 5ng/mL IL-7 (R&D Systems, MN, USA). On day 5, partial media exchange was performed by replacing half the well with fresh B-cell media and IL-2. On day 10, fresh APCs were either peptide pulsed or transfected as described above in a new 24-well plate. On day 11, expanded T-cells were restimulated with peptide-pulsed, transfected APCs similar to day 1. T-cells were used for cytolytic assays or immunophenotyped after day 20.

3.2.6. Flow cytometry staining for T-cell

Cells were washed once in MACs buffer (containing PBS, 1% BSA, 0.5mM EDTA), centrifuged at 550g for 5 min and re-suspended in 200µL MACS buffer. Cells were stained in 100µL of staining buffer containing anti-CD137, conjugated with phycoerythrin (PE, clone 4B4-1; BD Biosciences, USA), anti-CD8-PC5 (clone B9.11; Beckman Coulter 1:100), anti-CD4 (clone SK3; BioLegend, 1:200), anti-CD14 (clone 63D3; BioLegend, 1:200), and anti-CD19 (clone HIB19; BioLegend,1:200), all conjugated to Fluorescein isothiocyanate (FITC) for exclusion gates, for 30 min on ice. Samples were covered and incubated for 30 min on ice, washed twice in PBS, and resuspended in 1mL PBS prior to analysis.

3.2.7. Pentamer staining for T-cell immunophenotyping

The following HLA-A*02:01 PE-conjugated Cas9 pentamers were obtained from ProImmune. T-cells were washed twice in MACS buffer with 5% human serum and

centrifuged at 550g for 5 min each time. They were then re-suspended in 100µL staining buffer (MACS buffer, with 5% human serum and 1mM Dasatanib (ThermoFisher Scientific, MA, USA). Each of the pentamers was added to resuspended T-cells stimulated with the respective peptide or APCs at a concentration of 1:100. Samples were incubated at room temperature for 30 min in the dark, then washed twice in MACS buffer. Cells were stained in 100µL MACS buffer with anti-CD8-PC5, anti-CD4-FITC, anti-CD14-FITC, and anti-CD19-FITC for exclusion gates, for 30 min on ice. Samples were then washed twice with PBS and analyzed by flow cytometry. For flow cytometric analysis, all samples were acquired with Attune flow cytometer (ThermoFisher Scientific, MA, USA) and analyzed using the Attune software. Gates for expression of different markers and pentamers were determined based on flow minus one (FMO) samples for each color after doublet discrimination. Percentages from each of the gated population were used for the analysis.

3.3. RESULTS

3.3.1. Detection of Cas9-Specific Serum Antibodies in Healthy Controls

We first investigated whether healthy donors, in particular those with previous exposure to *Streptococcus pyogenes*, have detectable IgG Abs to *Streptococcus pyogenes* Cas9 (SpCas9). Of 143 healthy control sera screened, 49.0% had detectable Abs against *S. pyogenes* lysate using ELISA. This positive subset along with 12 of the sera negative for *S. pyogenes* lysate that had the highest RLU value were screened for Abs against recombinant Cas9. We detected Cas9-specific Abs in at least 21.0% (n=30) of all sera screened (**Figure 27**).

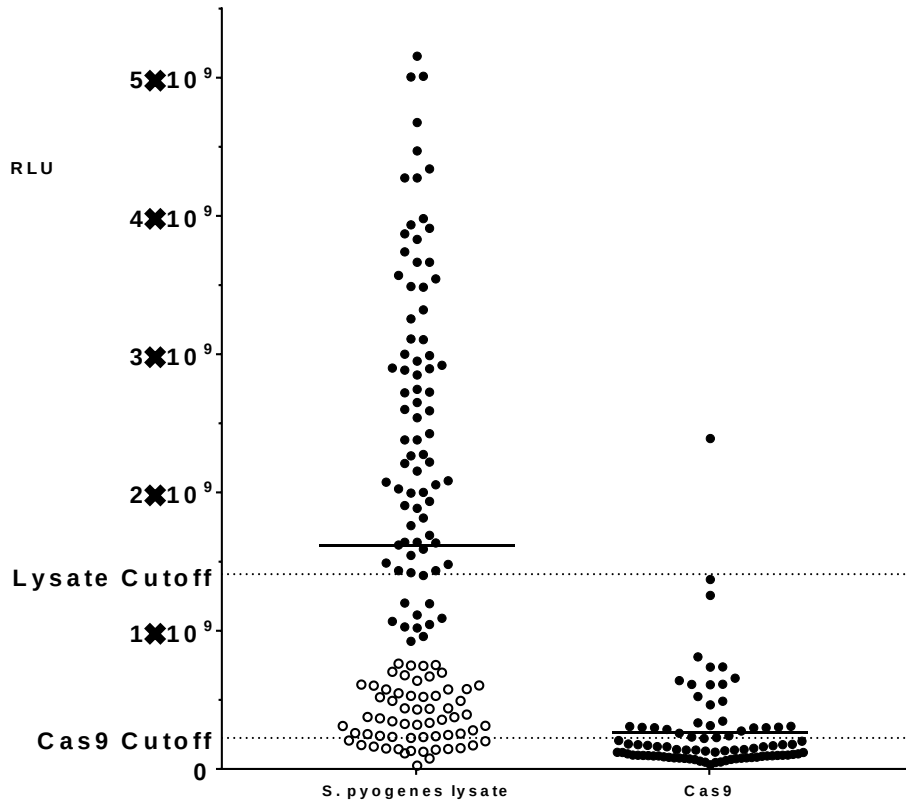


Figure 27. Serum antibody detection against *S. pyogenes* and Cas9. Specific serum Abs were detected against *S. pyogenes* lysate in 49.0% (above the dotted line) of 143 healthy controls (left). The subset shown in black circles was screened for Abs against recombinant Cas9 protein (right), of which 36.6% (21.0% of total samples screened) were positive.

3.3.2. In silico prediction of Cas9 immunogenic T cell epitopes

Probability and a peptide immunogenicity probability, we prioritized Cas9 peptides with predicted high binding and high immunogenicity (Chowell et al., 2015) (

Table 3).

In brief, IEDB consensus MHC-binding prediction algorithm (http://www.iedb.org/) was applied to obtain a list of high binding Cas9 peptides for HLA-A*02:01, each of which was assigned a normalized binding score (S_b). Next, an immunogenicity score (S_i) was calculated for each peptide based on its amino acid hydrophobicity. According to this prediction model,

Table 3. Binding and processing scores for Cas9 epitopes. the Cas9 HLA-A*02:01 epitopes predicted using IEDB and Syfpathi prediction software. The immunodominant epitopes are highlighted in dark gray. Other predicted immunogenic peptides confirmed via ELISpot assay are highlighted in light gray.

Aminoacid Position	Epitope Sequence	Code	IEDB bind	NetMHC bind	Syfpeithi bind	IEDB prot	ANN prot
1041-1050	YLNAVVGTAL	98	1.25	21.5	24	0.27	0.02
1334-1343	ILADANLDKV	81	1.25	11.37	31	-0.06	-0.49
289-297	GLFGNLIAL	84	0.6	10.12	29	1.15	1.04
293-301	NLIALSLGL	94	1.7	61.18	25	0.15	0.22
668-676	ILEDIVLTL	85	1.5	53.29	29	0.28	0.56
667-676	DILEDIVLTL	96	4.6	3105.79	28	-1.53	-1.02
468-476	HLGELHAIL	99	4.4	276.73	25	-0.75	-0.81
353-361	ILLSDILRV	83	0.3	6.51	29	0.67	0.7
1139-1148	VLSMPQVNIV	93	3.65	178.87	26	-1.05	-1.43
1399-1408	TLIHQSITGL	88	1.95	57.8	27	0.12	-0.06
1250-1259	KLPKYSLFEL	87	1.2	10.93	27	0.9	0.5
565-573	SLLYEYFTV	92	0.4	4.56	25	0.67	0.55
1280-1289	ALPSKYVNFL	91	4.3	111.14	27	0.05	-0.26
1049-1057	ALIKKYPKL	86	2.6	154.09	28	-0.27	0
274-282	RLENLIAQL	95	4.2	242.87	26	-0.46	-0.46
1290-1298	YLASHYEKL	90	1.2	10.3	26	0.9	0.84
795-803	KVVDELVKV	40	2.8	44.75	24	-0.06	-0.26
772-780	SLHEHIANL	82	1.4	9.14	30	0.93	0.82
1318-1326	YLDEIIEQI	89	0.3	4.8	26	0.62	0.6
604-613	LLFKTNRKV	97	3	381.3	25	-1.52	-1.25
772-781	SLHEHIANLA	13	4.7	60.17	19	-0.98	-1.74
1247-1256	LIIKLPKYSL	3	8.5	966.31	25	-0.97	-1.04
1094-1103	NIMNFFKTEI	12	2.65	314.8	19	-1.03	-0.9
1362-1371	IIHLFTLTNL	2	4.25	1083.6	24	-1.04	-0.78
714-723	RLSRKLINGI	17	3.5	278.03	24	-0.82	-1.05

1095-1103	IMNFFKTEI	7	3.2	131.4	21	-0.69	-0.87
868-877	YLQNGRDMYV	1	0.25	13.01	22	-0.18	-0.07
1265-1273	RMLASAGEL	4	3.2	333.2	22	-0.64	-0.51
1073-1082	KMIAKSEQEI	5	3.1	64.01	21	-0.36	-0.9
846-854	SQILKEHPV	19	2.8	191.23	16	-1.4	-1.36
1234-1243	FLEAKGYKEV	6	3.25	105.27	21	-1.08	-1.42
213-222	HMIKFRGHFL	9	4.75	324.13	21	-0.59	-0.73
194-203	KLVDSTDKA	11	3.4	274.05	20	-1.48	-1.17
525-534	TITPWNFEEV	8	4.45	124.55	21	-0.84	-1.21
247-256	QLFEENPINA	15	1.65	67.94	17	-0.71	-0.79
571-580	FTVYNELTKV	10	2.55	169.93	20	-1.12	-1.15
526-534	ITPWNFEEV	14	6.4	351.14	18	-1.25	-1.65
1023-1031	FQFYKVREI	18	2.7	135.61	16	-0.66	-0.39

Table 4. Predicted Cas9 immunogenic T cell epitopes. the Cas9 HLA-A*02:01 epitopes predicted using our prediction model and ranked according to their $S_i.S_b$ score. The immunodominant epitopes are highlighted in dark gray. Other predicted immunogenic peptides confirmed via ELISpot assay are highlighted in light gray.

Aminoacid Position	Epitope Sequence	Binding score	Sum proc	ANN Hydro	$S_b.S_i$	Rank
1041-1050	YLNAVVGTAL	0.068	0.027	0.975	0.002	1
1334-1343	ILADANLDKV	0.003	0.054	0.447	0.002	2
289-297	GLFGNLIAL	0.02	0.214	0.9	0.002	3
293-301	NLIALSLGL	0.061	0.036	0.903	0.006	4
668-676	ILEDIVLTL	0.023	0.082	0.71	0.007	5
667-676	DILEDIVLTL	0.063	0.248	0.888	0.007	6
468-476	HLGELHAIL	0.071	0.152	0.876	0.009	7
353-361	ILLSDILRV	0.019	0.134	0.404	0.011	8
1139-1148	VLSMPQVNIV	0.059	0.243	0.758	0.014	9
1399-1408	TLIHQSITGL	0.043	0.017	0.632	0.016	10
1250-1259	KLPKYSLFEL	0.04	0.136	0.579	0.017	11
565-573	SLLYEYFTV	0.056	0.119	0.678	0.018	12
1280-1289	ALPSKYVNFL	0.051	0.03	0.594	0.021	13
1049-1057	ALIKKYPKL	0.037	0.025	0.407	0.022	14
274-282	RLENLIAQL	0.061	0.089	0.581	0.026	15
1290-1298	YLASHYEKL	0.05	0.17	0.446	0.027	16
795-803	KVVDELVKV	0.074	0.031	0.505	0.036	17
772-780	SLHEHIANL	0.013	0.171	0.38	0.008	18
1318-1326	YLDEIIEQI	0.046	0.119	0.399	0.028	19
604-613	LLFKTNRKV	0.067	0.27	0.368	0.043	20
772-781	SLHEHIANLA	0.126	0.268	0.89	0.014	21

1247-1256	LIIKLPKYSL	0.09	0.197	0.841	0.014	22
1094-1103	NIMNFFKTEI	0.121	0.188	0.857	0.017	23
1362-1371	IIHLFTLTNL	0.085	0.177	0.787	0.018	24
714-723	RLSRKLINGI	0.078	0.183	0.746	0.02	25
1095-1103	IMNFFKTEI	0.103	0.153	0.724	0.028	26
868-877	YLQNGRDMYV	0.083	0.023	0.627	0.031	27
1265-1273	RMLASAGEL	0.095	0.112	0.65	0.033	28
1073-1082	KMIAKSEQEI	0.103	0.124	0.671	0.034	29
846-854	SQILKEHPV	0.149	0.27	0.766	0.035	30
1234-1243	FLEAKGYKEV	0.103	0.245	0.651	0.036	31
213-222	HMIKFRGHFL	0.11	0.129	0.628	0.041	32
194-203	KLVDSTDKA	0.114	0.259	0.52	0.055	33
525-534	TITPWNFEEV	0.107	0.201	0.429	0.061	34
247-256	QLFEENPINA	0.135	0.146	0.469	0.072	35
571-580	FTVYNELTKV	0.111	0.222	0.216	0.087	36
526-534	ITPWNFEEV	0.143	0.285	0.229	0.11	37
1023-1031	FQFYKVREI	0.148	0.102	0.229	0.114	38

peptides with low S_b (high binders) and high S_i (more hydrophobic) are expected to be more immunogenic (

Table 4**, Figure 28**).

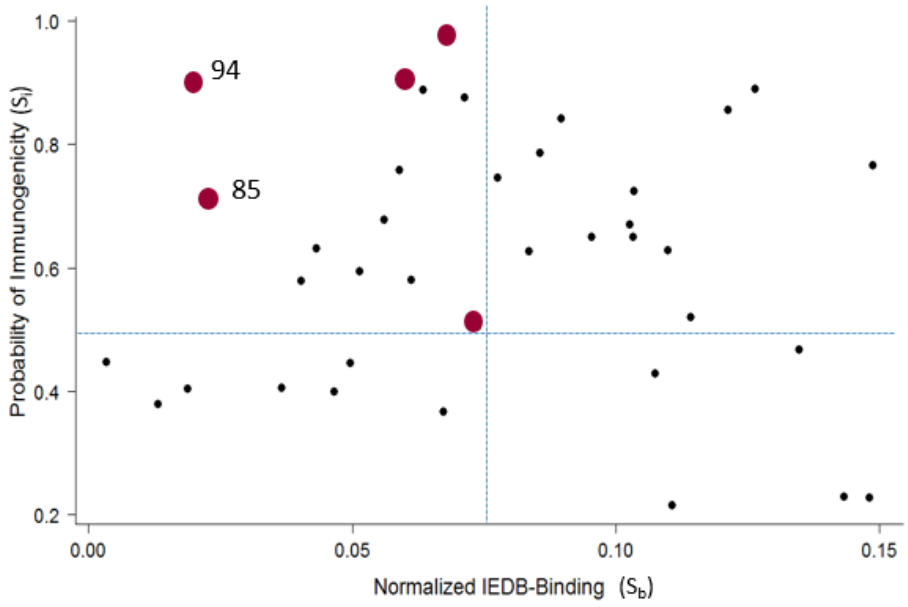


Figure 28. Improved epitope prediction model with applying immunogenicity score. Red dots represent epitopes that were shown immunogenic by ELISpot. S_b is normalized binding score, S_i is immunogenicity score.

3.3.3. Identification of two Cas9 immunodominant T cell epitopes

We sought to determine whether healthy donor peripheral blood mononuclear cells (PBMCs) displayed T cell reactivity against predicted Cas9 MHC class I epitopes. We synthesized the top 38 peptides and grouped them into 10 pools (each containing 3 or 4 peptides) for screening memory T cell response in healthy individuals using ELISpot. We tested the reactivity of 12 healthy donor peripheral

blood T cells to each peptide pool and found consistently high reactivity to pools 3 and/or 5 in 83% of the donors tested (**Figure 29**).

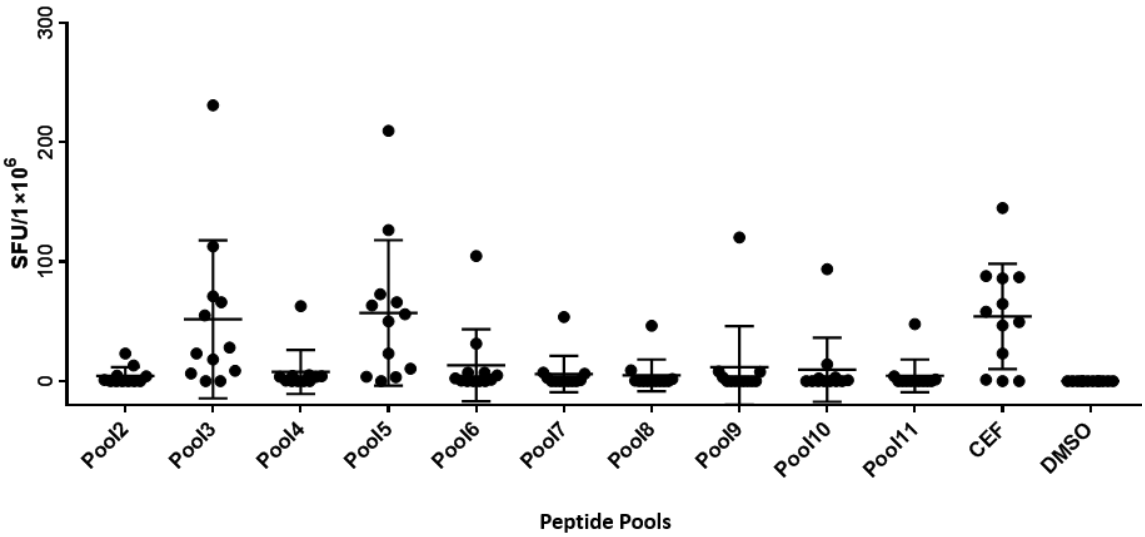


Figure 29. IFNγ ELISpot assay acreening for T cell reactivity. Twelve healthy idividuals were tested for 38 predicted epitopes grouped in 10 pools, CEF (positive control), and DMSO (negative control).

These 38 predicted epitopes cover about 30% of the Cas9 protein and their reactivity and position within the protein are shown in **Figure 30**. Upon deconvolution of pools 3 and 5 (7 peptides in total), the dominant immunogenic peptides were found to be 85 and 94, although reactivity to other peptides was also occasionally detected in some of the donors. The identified immunogenic epitopes are shown as red dots on the epitope prediction plot and the immunodominant epitopes (94 and 85) are labeled (Figure **37**). As predicted, these peptides are more immunogenic as shown by their low S_b and high S_i scores.

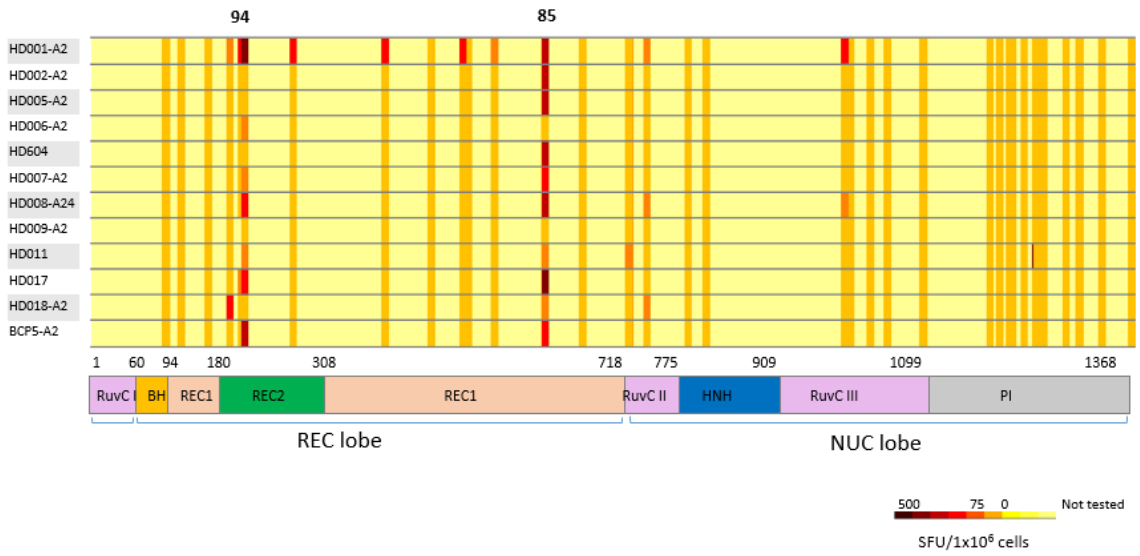


Figure 30. Reactivity of healthy donor T cells with the HLA types shown to epitopes across the different domains of the Cas9 protein.

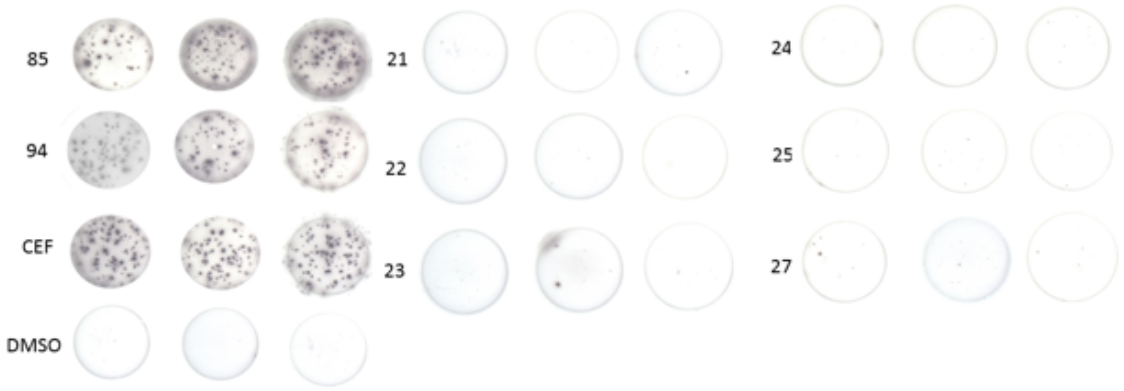
3.3.4. Modified Cas9 with mutated epitope(s) is less immunogenic while retaining its function

We hypothesized that mutation of the anchor residues of the identified immunogenic epitopes (94 and 85, **Figure 30**) will abolish the specific T cell immune response detected in positive donors. We created 3 modified cas9 constructs by mutating the second residue of peptide 94 (L294G; cas9-10), peptide 85 (L669G; cas9-01), or both (cas9-11) and tested their immunogenicity and function in comparison with wild-type cas9 (cas9-00). We also tested the reactivity of healthy donor PB T cells to modified peptides 94 and 85 with mutations in residues 2, 9, or both (**Figure 31**) using ELISpot.

We also tested the reactivity of healthy donor peripheral blood T cells to WT epitopes 94 and 85 or their modified versions with mutations in residues 2, 9, or both

(**Figure 32**) by using an IFN-γ ELISpot assay. We detected high epitope-specific T cell reactivity that was abolished or reduced with the mutant peptides 94 (**Figure 32A**) and 85 (**Figure 32B**).

Figure 31 shows the triplicate ELISpot wells for each peptide, the positive control (CEF), and the negative control (DMSO).



Peptide Code	Peptide Sequence	Peptide Code	Peptide Sequence
85	ILEDIVLTL	94	NLIALSLGL
21	IGEDIVLTL	24	NGIALSLGL
22	ILEDIVLTG	25	NLIALSLGG
23	IGEDIVLTG	27	NGIALSLGG

Figure 31. ELISpot assay for screening healthy donors' PBMCs to Cas9 epitopes. ELISpot assay comparing the T cell response to epitope 85 and 94 to their mutated peptides. Mutation to glycine has been introduced to amino acid position second or nine or both in peptide 85 and 94. CEF is used as a positive control. DMSO is used as the negative control.

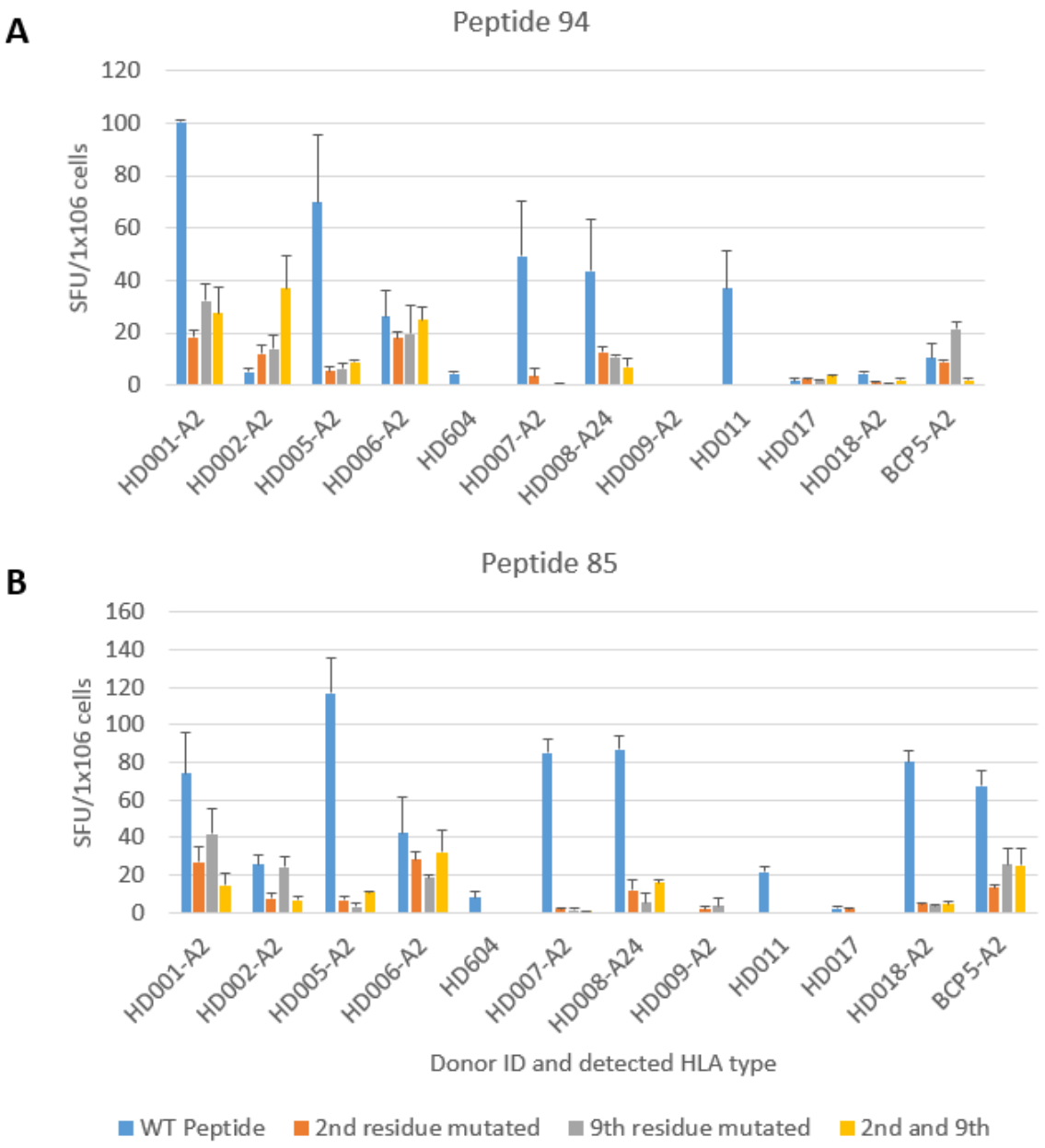


Figure 32. Decreasing T cell response to epitope 85 and 94 by mutating the epitope. Twelve health donors were tested for T cell response reduction upon mutation at te second or nine residue or both. Donor's HLA type is specified for the ones that are HLA-typed.

Mutated Cas9 proteins successfully recognized and bound their target DNA leading to enhanced target gene expression (**Figure 33A**). HEK293 cells were transfected with a plasmid encoding Infrared Fluorescent Protein (IRFP; an exogenous gene driven by a synthetic CRIPSR-activated promoter), with or without plasmids encoding MS2-P65-HSF1 (an activation mediator that activates the transcription of the target gene), WT (cas9-00) or mutated cas9 gene (cas9-01, -10, or -11), and 14nt gRNA targeting IRFP. Mutated Cas9 proteins also successfully recognized and bound to their target DNA leading to enhanced endogenous (chromosomal) target gene expression. HEK293 cells were transfected with plasmids encoding MS2-P65-HSF1 (an activation mediator that activates the transcription of the target gene) and 14-nt gRNA targeting the promoter regions of a gene encoding structural protein (TTN, Figure 33A), or a long noncoding RNA (MIAT, Figure 33B) with or without a plasmid encoding WT (cas9-00) or mutated cas9 gene (cas9-01, -10, or -11).

Mutated Cas9 proteins also successfully recognized and bound their target DNA leading to repression of target gene expression (**Figure 33B**). HEK293 cells were transfected with a plasmid encoding Yellow Fluorescent Protein (YFP; an exogenous gene driven by a synthetic constitutive promoter comprised of two mini CMVs and two CRISPR biding sites), with or without plasmids encoding WT (cas9-00) or mutated cas9 gene (cas9-01, -10, or -11), and 20nt gRNA targeting YFP. The expression of IRFP and YFP was measured by flow cytometry. Mutated Cas9 protein (Cas9-11) successfully recognized and bound its target DNA leading to the introduction of indels (**Figure 33C)** HEK293 cells were transfected with plasmids encoding WT (cas9-00) or mutated (cas9-11) cas9 gene, and 20-nt gRNA targeting a gene encoding structural proteins (EMX1). The amount of Cas9-induced indels in the targeted region was measured. Genomic DNA

from the heterogeneous population of Cas9-targeted cells is amplified by PCR to determine the indel percentage in EMX1 loci, amplicons are then sequenced. Cas9-mediated cleavage efficiency (percentage indel) is calculated on the basis of the fraction of cleaved DNA, as determined by sequencing.

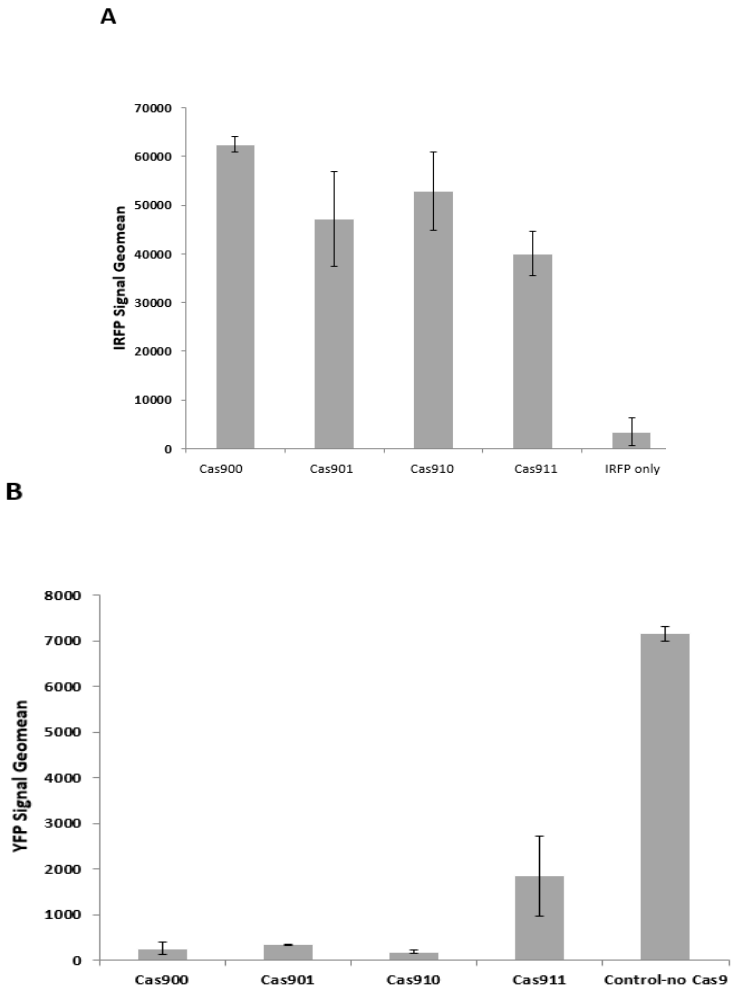


Figure 33. Comparable functionality of mutated Cas9 and wild-type Cas9. A) Measuring activation by IRFP signal intensity. B) Measuring repression of target DNA by YFP signal intensity.

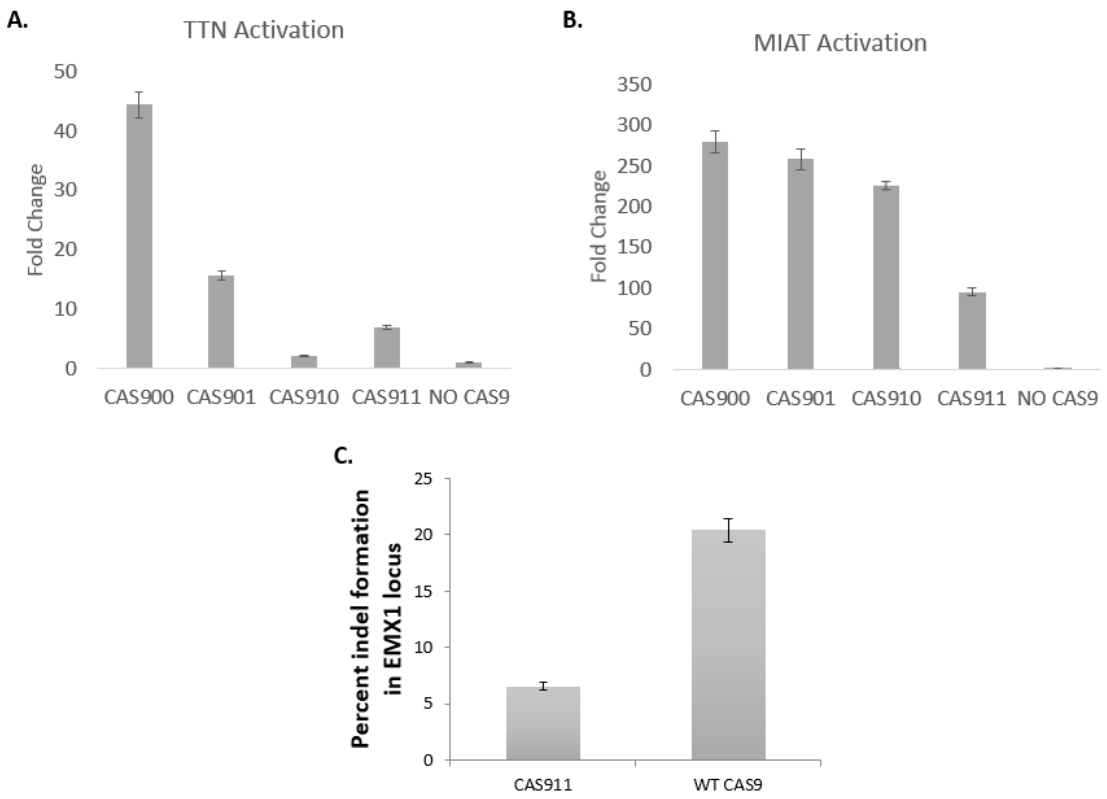


Figure 34. Mutated Cas9 proteins recognize and bind to their target DNAs, leading to enhanced endogenous target gene expression or introduction of indels. Activation and cutting of endogenous genes in HEK293T cells: (A and B) RNA expression of cells transfected with (i) indicated Cas9 proteins, (ii) MS2-P65-HSF1, and (iii) 14-nt gRNA targeting TTN (A) and MIAT (B). (C) Indel formation percentage of HEK293T cells transfected with the indicated Cas9 proteins and 20-nt gRNA targeting EMX1. Data indicate mean +SD. (n = 3 independent transfections).

3.3.5. Detection and Reduction of Epitope specific CD8 Response

Antigen-specific T cells were expanded from peptide-spiked autologous APCs after 18 days in two rounds of stimulation and analyzed for peptide 94 or 85-specific CD8

response. To achieve this goal, we measured CD137 as an early marker of T cell activation, detected 48 hours after the second round of stimulation (Wolfl et al., 2007). When peripheral blood (PB) T cells were stimulated with APCs spiked with peptide 94, the percentage of CD8+ CD137+ T cells was 4.37% (**Figure 35A**), while it decreased to 2.74% (**Figure 35B**) when peptide 24 (mutated peptide 94) was used.

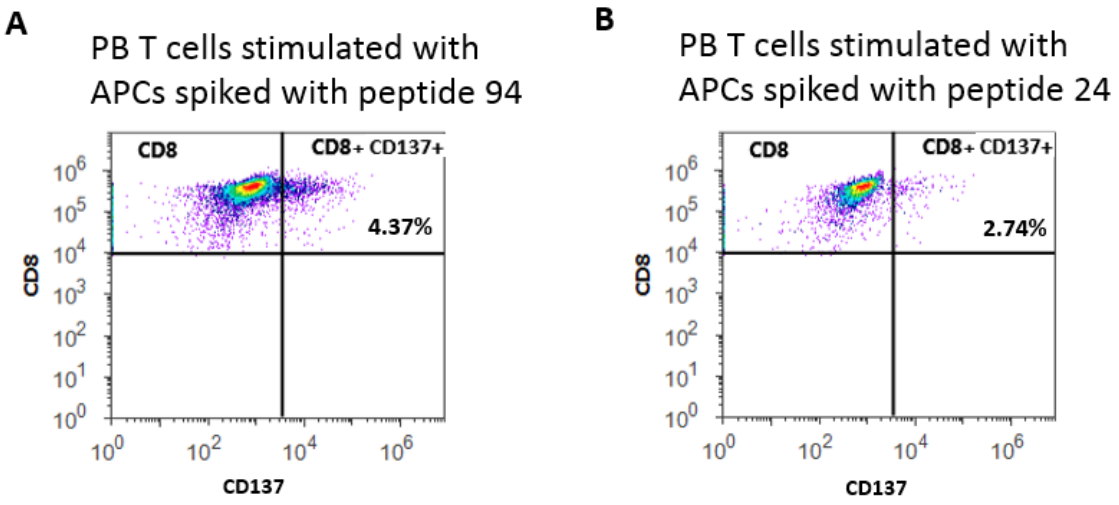


Figure 35. T cell activation with Cas9 epitope and mutated epitope. A) CD8+CD137 positive population is demonstrated after exposure to peptide 94. B) CD137 positive population is demonstrated after exposure to mutated peptide 94 (peptide 24).

We quantified the T cell response against epitope 85 by staining with a specific MHC-pentamer. The percentage of CD8+ pentamer+ T cell population was 3.09% (**Figure 36A**) when PB T cells were stimulated with APCs spiked with peptide 85 and it dropped to 0.3% (**Figure 36B**) when the mutated peptide (peptide 21) was used.

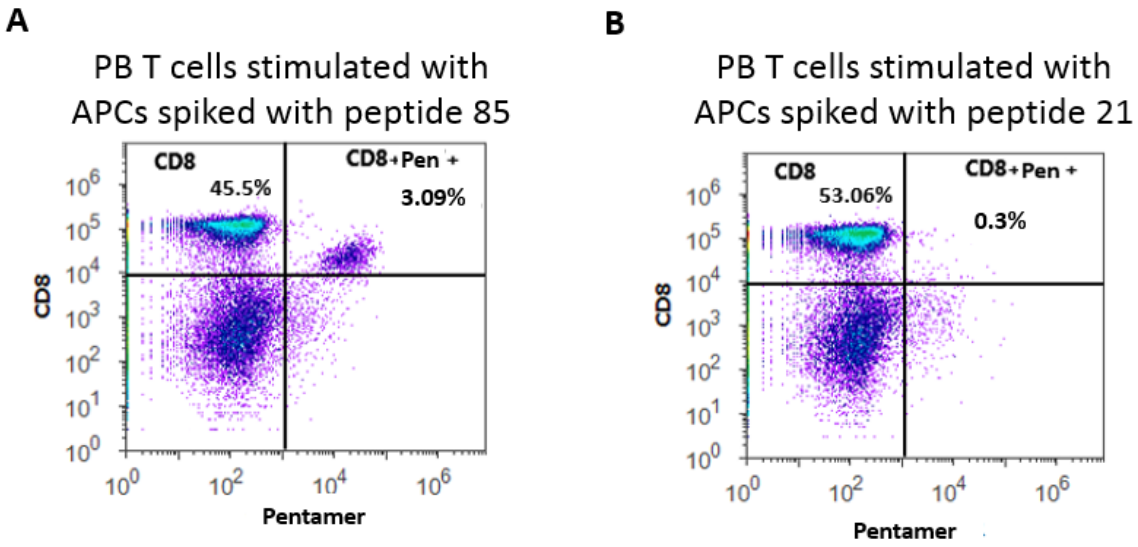


Figure 36. Epitope specific CD8 T cell response to epitope 85. CD8+Pet+ represents the epitope specific T cell response. Peptide 21 is the mutated form of peptide 85 and used as a control.

3.4. DISCUSSION

The CRISPR-Cas9 system is being applied for a vast variety of research purposes and exciting pre-clinical results are leading its way towards clinical use. Targeted genetic modification is a powerful tool that can be applied for the treatment or prevention of diseases involving somatic mutations. Examples are current human cancer clinical trials including lung, prostate, and renal cell cancers. Genetic engineering with CRISPR-Cas9 has successfully targeted convertase/subtilisin/kexin type 9 (PCSK9) to deregulate cholesterol metabolism in mouse hepatocytes (Ding et al., 2014). Another application involves improvement of muscle function in live animals by introducing dystrophin gene in the case of dystrophin deficiency (Long et al., 2016). Target discovery of p53 reactivating drugs using CRISPR-Cas9 is one of the many research applications of this gene editing system (Wanzel et al., 2015).

Clinical challenges and ethical questions have been intensely discussed as the CRISPR-Cas9 field is growing fast (Cox, Platt, & Zhang, 2015). Non-specific Cas9 nuclease cleavage has been reported to be more frequent in humans in comparison to other models (Hwang et al., 2013; L. Yang et al., 2015). Recent work suggests that the HDR-NHEJ ratio, a measure of efficacy, can be improved through three factors - DNA repair machinery, better delivery methods, and timing (Maeder & Gersbach, 2016). The delivery method has always been a challenge in gene therapy for several reasons. These include low transfection efficiency in primary cells, random plasmid insertion and integration, the cytotoxicity associated with the use of DNA, and bacterial DNA sequences present in plasmid backbones (Maeder & Gersbach, 2016; H. Wang, La Russa, & Qi,

2016). Adeno-associated virus (AAV)-based vectors are favored for use in somatic gene therapy as they are not pathogenic and are capable of targeting non-dividing cells. However, the packaging limit is problematic, given the large coding sequence of SpCas9 and the sgRNA. Unlike the mild immune response induced by adenoviral vectors that has been extensively studied, the immunogenicity of the bacterial Cas9 protein is unknown in humans. Success in clinical translation of targeted gene therapy is highly limited by the efficacy and undesired immune response.

In this project, pre-existing T cell and B cell responses to Cas9 is assessed in humans for the first time. A healthy population is screened for Cas9-specific serum antibody and CD8+ T cell responses. At least 21% of the healthy individuals screened had antibodies to Cas9 and strikingly 10 out of 12 donors had common reactivity to two epitopes of Cas9, 85 and 94. Here, we did not find any association between the T cell and B cell response to Cas9 (data not shown).

Cas9 B cell epitopes have been mapped in mice (Chew et al., 2016), while T cell epitope mapping is yet to be done. However, the Identified epitopes are not expected to be shared with humans, few overlapping epitopes has been observed between animal model and human antigens (Mazor et al., 2015). Ideally, if the T cell and B cell epitopes share sequences, mutating the epitope can result in a major reduction of the immune recognition. Yet disrupting the T cell epitopes of LMB-T20 (a recombinant immunotoxin), when there was pre-existing immune response, prevented B cell activation. (Mazor et al., 2015). Furthermore, Mazor *et al*. demonstrated that de-immunization of SS1P (a recombinant immunotoxin), by removing the dominant T cell epitopes prevented serum antibody production. In this study, we focused on pre-existing immune response and further studies are needed for post-treatment T cell response induction. The question of

whether persistent expression of a transgene increases the tolerance or unleashes cytokine secretion needs to be examined.

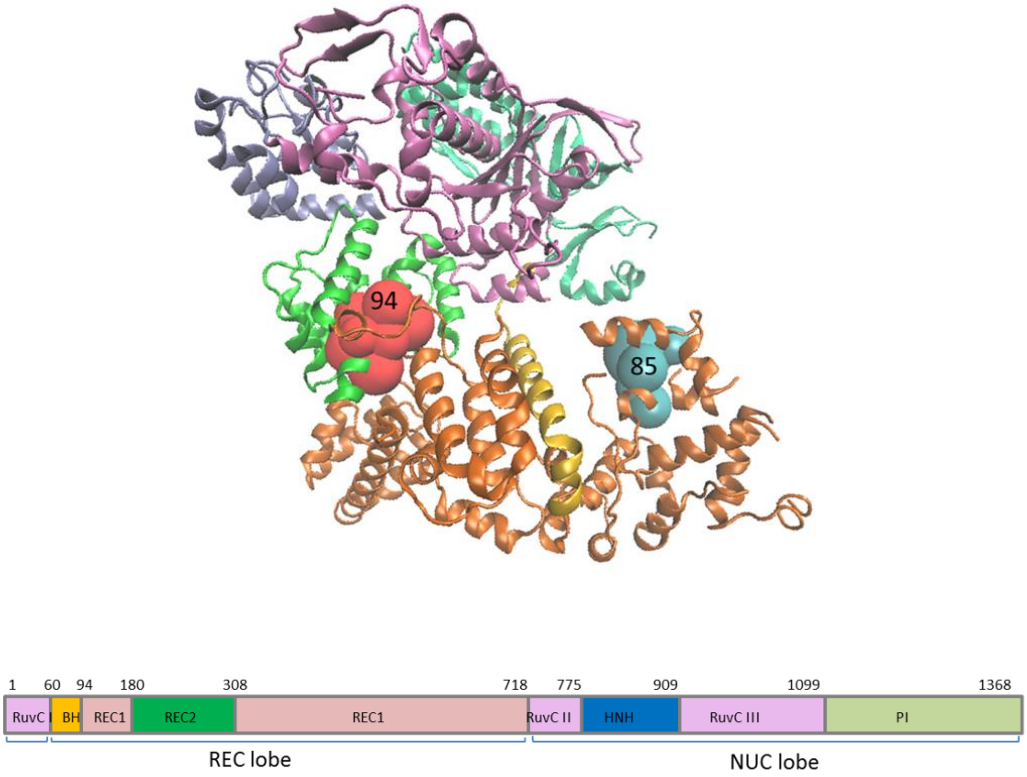


Figure 37. SpCas9 protein domains and epitope 85 and 94 locations on the protein.

Here, we designed a method that requires the least changes in the protein sequence to evade T cell recognition without disrupting the protein function. First, we limited the changes to the immunodominant epitopes as identified by our prediction model and validated by ELISpot. Second, we limited the mutation to the second residue of these epitopes, being one of two anchor residues necessary for binding to the MHC groove (Chowell et al., 2015). After mutation, the peptides were not recognized by T cells (**Figure** 31) and their binding scores (S_b) significantly increased. Fortunately, the identified

epitopes were not located in functionally critical positions of Cas9 (**Figure 37**) and the mutated protein preserved its function (**Figure 33**). For further validation of CD8 epitope-specific response, T cells were stained with MHC pentamer and peptide 85-specific CD8+ T cells were quantified (**Figure 36**).

Conventional methods of testing synthetic peptides to identify immunogenic epitopes are helpful for proof of principle but require an antigen presenting model for CD8 response. Antigen presenting cells (APCs) are a good model as we can directly control the transfection load of the exogenous gene. T cells will be stimulated with autologous APCs transfected with Cas9 mRNA and T cell activation will be measured using specific markers. Unfortunately, these experiments were not done in the time frame of this thesis.

Future studies will include the comparison of the antigenicity of APCs presenting Cas9 epitopes with APCs expressing mutated Cas9. The Cas9 sequence is made up of 1368 amino acids, with about 100 predicted HLA-A*02:01 high binding epitopes. It is probable that removing two epitopes will significantly decrease the T cell recognition but not completely abolish it. Another limitation to the project is the diversity of MHCs, the most polymorphic gene variants, in individuals. HLA-A*02:01 is the most common MHC type in Caucasians but a comprehensive immunogenicity evaluation should take all the HLAs into account if feasible.

REFERENCES

Ahi, Y. S., Bangari, D. S., & Mittal, S. K. (2011). Adenoviral Vector Immunity: Its Implications and circumvention strategies. *Current Gene Therapy*, *11*(4), 307–320. Retrieved from http://www.ncbi.nlm.nih.gov/pmc/articles/PMC4009923/

Aldhamen, Y. A., & Amalfitano, A. (2016). 16 - Methods to Mitigate Immune Responses to Adenoviral Vectors A2 - Curiel, David T. In *Adenoviral Vectors for Gene Therapy (Second Edition)* (pp. 391–422). San Diego: Academic Press. http://doi.org/https://doi.org/10.1016/B978-0-12-800276-6.00016-4

Anderson, K. S., Dahlstrom, K. R., Cheng, J. N., Alam, R., Li, G., Wei, Q., … Sturgis, E. M. (2015). HPV16 antibodies as risk factors for oropharyngeal cancer and their association with tumor HPV and smoking status. *Oral Oncol*, *51*(7), 662–667. http://doi.org/10.1016/j.oraloncology.2015.04.011

Assaily, W., Rubinger, D. A., Wheaton, K., Lin, Y., Ma, W., Xuan, W., … Benchimol, S. (2011). ROS-mediated p53 induction of Lpin1 regulates fatty acid oxidation in response to nutritional stress. *Molecular Cell*, *44*(3), 491–501. http://doi.org/10.1016/j.molcel.2011.08.038

Bartel, M., Schaffer, D., & Buning, H. (2011). Enhancing the Clinical Potential of AAV Vectors by Capsid Engineering to Evade Pre-Existing Immunity. *Front Microbiol*, *2*, 204. http://doi.org/10.3389/fmicb.2011.00204

Bergo, M. O., Gavino, B. J., Hong, C., Beigneux, A. P., McMahon, M., Casey, P. J., & Young, S. G. (2004). Inactivation of Icmt inhibits transformation by oncogenic K-Ras and B-Raf. *Journal of Clinical Investigation*, *113*(4), 539–550. http://doi.org/10.1172/JCI200418829

Bergo, M. O., Leung, G. K., Ambroziak, P., Otto, J. C., Casey, P. J., & Young, S. G. (2000). Targeted inactivation of the isoprenyleysteine carboxyl methyltransferase gene causes mislocalization of K-Ras in mammalian cells. *Journal of Biological Chemistry*, *275*(23), 17605–17610. http://doi.org/10.1074/jbc.C000079200

Berndt, N., Hamilton, A. D., & Sebti, S. M. (2011). Targeting protein prenylation for cancer therapy. *Nature Reviews. Cancer*, *11*(11), 775–91. http://doi.org/10.1038/nrc3151

Bieging, K. T., Mello, S. S., & Attardi, L. D. (2014). Unravelling mechanisms of p53-mediated tumour suppression. *Nature Reviews Cancer*, *14*(5), 359–370. http://doi.org/10.1038/nrc3711

Bisso, A., Collavin, L., & Del Sal, G. (2011). P73 As a Pharmaceutical Target for Cancer Therapy. *Current Pharmaceutical Design*, *17*(6), 578–90. http://doi.org/10.2174/138161211795222667

Bjarnadottir, O., Romero, Q., Bendahl, P. O., Jirström, K., Rydén, L., Loman, N., … Borgquist, S. (2013). Targeting HMG-CoA reductase with statins in a window-of-opportunity breast cancer trial. *Breast Cancer Research and Treatment*, *138*(2), 499–

508. http://doi.org/10.1007/s10549-013-2473-6

Borgquist, S., Giobbie-Hurder, A., Ahern, T. P., Garber, J. E., Colleoni, M., Láng, I., … Thürlimann, B. (2017). Cholesterol, Cholesterol-Lowering Medication Use, and Breast Cancer Outcome in the BIG 1-98 Study. *Journal of Clinical Oncology*, JCO.2016.70.311. http://doi.org/10.1200/JCO.2016.70.3116

Boutin, S., Monteilhet, V., Veron, P., Leborgne, C., Benveniste, O., Montus, M. F., & Masurier, C. (2010). Prevalence of serum IgG and neutralizing factors against adeno-associated virus (AAV) types 1, 2, 5, 6, 8, and 9 in the healthy population: implications for gene therapy using AAV vectors. *Hum Gene Ther*, *21*(6), 704–712. http://doi.org/10.1089/hum.2009.182

Brewer, T. M., Masuda, H., Liu, D. D., Shen, Y., Liu, P., Iwamoto, T., … Ueno, N. T. (2013). Statin use in primary inflammatory breast cancer: a cohort study. *British Journal of Cancer*, *109*, 318–24. http://doi.org/10.1038/bjc.2013.342

Brunetti-Pierri, N., & Ng, P. (2009). Progress towards liver and lung-directed gene therapy with helper-dependent adenoviral vectors. *Curr Gene Ther*, *9*(5), 329–340. Retrieved from http://www.ncbi.nlm.nih.gov/pubmed/19860648

Bykov, V. J. N., Issaeva, N., Shilov, A., Hultcrantz, M., Pugacheva, E., Chumakov, P., … Selivanova, G. (2002). Restoration of the tumor suppressor function to mutant p53 by a low-molecular-weight compound. *Nat Med*, *8*(3), 282–288. http://doi.org/10.1038/nm0302-282

Carapetis, J. R., Steer, A. C., Mulholland, E. K., & Weber, M. (2005). The global burden of group A streptococcal diseases. *Lancet Infect Dis*, *5*(11), 685–694. http://doi.org/10.1016/S1473-3099(05)70267-X

Cavazzana-Calvo, M., Hacein-Bey, S., de Saint Basile, G., Gross, F., Yvon, E., Nusbaum, P., … Fischer, A. (2000). Gene therapy of human severe combined immunodeficiency (SCID)-X1 disease. *Science*, *288*(5466), 669–672. Retrieved from http://www.ncbi.nlm.nih.gov/pubmed/10784449

Chen, Y., Sprung, R., Tang, Y., Ball, H., Sangras, B., Kim, S. C., … Zhao, Y. (2007). Lysine Propionylation and Butyrylation Are Novel Post-translational Modifications in Histones. *Molecular & Cellular Proteomics*, *6*(5), 812–819. http://doi.org/10.1074/mcp.M700021-MCP200

Chew, W. L., Tabebordbar, M., Cheng, J. K., Mali, P., Wu, E. Y., Ng, A. H., … Church, G. M. (2016). A multifunctional AAV-CRISPR-Cas9 and its host response. *Nat Methods*, *13*(10), 868–874. http://doi.org/10.1038/nmeth.3993

Chowdhury, S. K. R., Gemin, A., & Singh, G. (2005). High activity of mitochondrial glycerophosphate dehydrogenase and glycerophosphate-dependent ROS production in prostate cancer cell lines. *Biochemical and Biophysical Research Communications*, *333*(4), 1139–1145. http://doi.org/10.1016/j.bbrc.2005.06.017

Chowell, D., Krishna, S., Becker, P. D., Cocita, C., Shu, J., Tan, X., … Anderson, K. S.

(2015). TCR contact residue hydrophobicity is a hallmark of immunogenic CD8+ T cell epitopes. *Proc Natl Acad Sci U S A*, *112*(14), E1754-62. http://doi.org/10.1073/pnas.1500973112

Clayman, G. L., El-Naggar, A. K., Roth, J. A., Zhang, W. W., Goepfert, H., Taylor, D. L., & Liu, T. J. (1995). In Vivo Molecular Therapy with p53 Adenovirus for Microscopic Residual Head and Neck Squamous Carcinoma. *Cancer Research*, *55*(1), 1–6.

Clendening, J. W., Pandyra, A., Boutros, P. C., Ghamrasni, S. E., Khosravi, F., Trentin, G. A., … Penn, L. Z. (2010). Dysregulation of the mevalonate pathway promotes transformation. *Proceedings of the National Academy of Sciences*, *107*(34), 15051–15056. http://doi.org/10.1073/pnas.0910258107

Coleman, M. L., Marshall, C. J., & Olson, M. F. (2004). RAS and RHO GTPases in G1-phase cell-cycle regulation. *Nature Reviews. Molecular Cell Biology*, *5*(5), 355–366. http://doi.org/10.1038/nrm1365

Comerford, S. A., Huang, Z., Du, X., Wang, Y., Cai, L., Witkiewicz, A. K., … Tu, B. P. (2014). Acetate dependence of tumors. *Cell*, *159*(7), 1591–1602. http://doi.org/10.1016/j.cell.2014.11.020

Commisso, C., Davidson, S. M., Soydaner-Azeloglu, R. G., Parker, S. J., Kamphorst, J. J., Hackett, S., … Bar-Sagi, D. (2013). Macropinocytosis of protein is an amino acid supply route in Ras-transformed cells. *Nature*, *497*(7451), 633–637. http://doi.org/10.1038/nature12138

Conrad, M., & Sato, H. (2012). The oxidative stress-inducible cystine/glutamate antiporter, system x c -: Cystine supplier and beyond. In *Amino Acids* (Vol. 42, pp. 231–246). http://doi.org/10.1007/s00726-011-0867-5

Cox, D. B. T., Platt, R. J., & Zhang, F. (2015). Therapeutic genome editing: prospects and challenges. *Nature Medicine*, *21*(2), 121–131. http://doi.org/10.1038/nm.3793

Coxon, J. P., Oades, G. M., Kirby, R. S., & Colston, K. W. (2004). Zoledronic acid induces apoptosis and inhibits adhesion to mineralized matrix in prostate cancer cells via inhibition of protein prenylation. *BJU Int*, *94*(1), 164–170. http://doi.org/10.1111/j.1464-4096.2004.04831.x

Cyranoski, D. (2016). Chinese scientists to pioneer first human CRISPR trial. *Nature*, *535*(7613), 476–477. http://doi.org/10.1038/nature.2016.20302

Ding, Q., Strong, A., Patel, K. M., Ng, S. L., Gosis, B. S., Regan, S. N., … Musunuru, K. (2014). Permanent alteration of PCSK9 with in vivo CRISPR-Cas9 genome editing. *Circulation Research*, *115*(5), 488–492. http://doi.org/10.1161/CIRCRESAHA.115.304351

Drake, M. T., Clarke, B. L., & Khosla, S. (2008). Bisphosphonates: mechanism of action and role in clinical practice. *Mayo Clinic Proceedings*, *83*(9), 1032–45. http://doi.org/10.4065/83.9.1032

Eckert, L. B., Repasky, G. A., Ulkü, A. S., McFall, A., Zhou, H., Sartor, C. I., & Der, C. J. (2004). Involvement of Ras activation in human breast cancer cell signaling, invasion, and anoikis. *Cancer Research*, *64*(13), 4585–92. http://doi.org/10.1158/0008-5472.CAN-04-0396

Esvelt, K. M., Mali, P., Braff, J. L., Moosburner, M., Yaung, S. J., & Church, G. M. (2013). Orthogonal Cas9 proteins for RNA-guided gene regulation and editing. *Nat Methods*, *10*(11), 1116–1121. http://doi.org/10.1038/nmeth.2681

Freed-Pastor, W. A., Mizuno, H., Zhao, X., Langerød, A., Moon, S. H., Rodriguez-Barrueco, R., … Prives, C. (2012). Mutant p53 disrupts mammary tissue architecture via the mevalonate pathway. *Cell*, *148*(1–2), 244–258. http://doi.org/10.1016/j.cell.2011.12.017

Freed-Pastor, W. A., & Prives, C. (2012). Mutant p53: One name, many proteins. *Genes and Development*, *26*(12), 1268–1286. http://doi.org/10.1101/gad.190678.112

Freed-Pastor, W., & Prives, C. (2016). Targeting mutant p53 through the mevalonate pathway. *Nature Cell Biology*, *18*(11), 1122–1124. http://doi.org/10.1038/ncb3435

Fritsch, R., Krijger, I. De, Fritsch, K., George, R., Reason, B., Kumar, M. S., … Downward, J. (2013). RAS and RHO Families of GTPases Directly Regulate Distinct Phosphoinositide 3-Kinase Isoforms. *Cell*, *153*(5), 1050–1063. http://doi.org/10.1016/j.cell.2013.04.031

Gao, G., Wang, Q., Calcedo, R., Mays, L., Bell, P., Wang, L., … Wilson, J. M. (2009). Adeno-associated virus-mediated gene transfer to nonhuman primate liver can elicit destructive transgene-specific T cell responses. *Hum Gene Ther*, *20*(9), 930–942. http://doi.org/10.1089/hum.2009.060

Gaspar, H. B., Parsley, K. L., Howe, S., King, D., Gilmour, K. C., Sinclair, J., … Thrasher, A. J. (2004). Gene therapy of X-linked severe combined immunodeficiency by use of a pseudotyped gammaretroviral vector. *Lancet*, *364*(9452), 2181–2187. http://doi.org/10.1016/S0140-6736(04)17590-9

Grasberger, B. L., Lu, T., Schubert, C., Parks, D. J., Carver, T. E., Koblish, H. K., … Bone, R. F. (2005). Discovery and cocrystal structure of benzodiazepinedione HDM2 antagonists that activate p53 in cells. *Journal of Medicinal Chemistry*, *48*(4), 909–912. http://doi.org/10.1021/jm049137g

Grassian, A. R., Coloff, J. L., & Brugge, J. S. (2011). Extracellular matrix regulation of metabolism and implications for tumorigenesis. *Cold Spring Harbor Symposia on Quantitative Biology*, *76*, 313–324. http://doi.org/10.1101/sqb.2011.76.010967

Hacein-Bey-Abina, S., Le Deist, F., Carlier, F., Bouneaud, C., Hue, C., De Villartay, J. P., … Cavazzana-Calvo, M. (2002). Sustained correction of X-linked severe combined immunodeficiency by ex vivo gene therapy. *N Engl J Med*, *346*(16), 1185–1193. http://doi.org/10.1056/NEJMoa012616

Halbert, C. L., Standaert, T. A., Wilson, C. B., & Miller, A. D. (1998). Successful

readministration of adeno-associated virus vectors to the mouse lung requires transient immunosuppression during the initial exposure. *J Virol*, *72*(12), 9795–9805. Retrieved from http://www.ncbi.nlm.nih.gov/pubmed/9811715

Hanahan, D., & Weinberg, R. A. (2000). The hallmarks of cancer. *Cell*, *100*(1), 57–70. http://doi.org/10.1007/s00262-010-0968-0

Hao, Y., Samuels, Y., Li, Q., Krokowski, D., Guan, B.-J., Wang, C., … Wang, Z. (2016). Oncogenic PIK3CA mutations reprogram glutamine metabolism in colorectal cancer. *Nature Communications*, *7*, 11971. http://doi.org/10.1038/ncomms11971

Heffernan-Stroud, L. A., & Obeid, L. M. (2011). P53 and regulation of bioactive sphingolipids. *Advances in Enzyme Regulation*. http://doi.org/10.1016/j.advenzreg.2010.10.003

Hirano, H., Gootenberg, J. S., Horii, T., Abudayyeh, O. O., Kimura, M., Hsu, P. D., … Nureki, O. (2016). Structure and Engineering of Francisella novicida Cas9. *Cell*, *164*(5), 950–961. http://doi.org/10.1016/j.cell.2016.01.039

Hoof, I., Peters, B., Sidney, J., Pedersen, L. E., Sette, A., Lund, O., … Nielsen, M. (2009). NetMHCpan, a method for MHC class I binding prediction beyond humans. *Immunogenetics*, *61*(1), 1.

Howe, S. J., Mansour, M. R., Schwarzwaelder, K., Bartholomae, C., Hubank, M., Kempski, H., … Thrasher, A. J. (2008). Insertional mutagenesis combined with acquired somatic mutations causes leukemogenesis following gene therapy of SCID-X1 patients. *J Clin Invest*, *118*(9), 3143–3150. http://doi.org/10.1172/JCI35798

Hwang, W. Y., Fu, Y., Reyon, D., Maeder, M. L., Tsai, S. Q., Sander, J. D., … Joung, J. K. (2013). Efficient genome editing in zebrafish using a CRISPR-Cas system. *Nature Biotechnology*, *31*(3), 227–229. http://doi.org/10.1038/nbt.2501

Ide, T., Brown-Endres, L., Chu, K., Ongusaha, P. P., Ohtsuka, T., El-Deiry, W. S., … Lee, S. W. (2009). GAMT, a p53-Inducible Modulator of Apoptosis, Is Critical for the Adaptive Response to Nutrient Stress. *Molecular Cell*, *36*(3), 379–392. http://doi.org/10.1016/j.molcel.2009.09.031

Issaeva, N., Bozko, P., Enge, M., Protopopova, M., Verhoef, L. G. G. C., Masucci, M., … Selivanova, G. (2004). Small molecule RITA binds to p53, blocks p53–HDM-2 interaction and activates p53 function in tumors. *Nature Medicine*, *10*(12), 1321–1328. http://doi.org/10.1038/nm1146

Jiang, H., Couto, L. B., Patarroyo-White, S., Liu, T., Nagy, D., Vargas, J. A., … Pierce, G. F. (2006). Effects of transient immunosuppression on adenoassociated, virus-mediated, liver-directed gene transfer in rhesus macaques and implications for human gene therapy. *Blood*, *108*(10), 3321–3328. http://doi.org/10.1182/blood-2006-04-017913

Jiang, P., Du, W., Wang, X., Mancuso, A., Gao, X., Wu, M., & Yang, X. (2011). p53 regulates biosynthesis through direct inactivation of glucose-6-phosphate

dehydrogenase. *Nature Cell Biology*, *13*(3), 310–316. http://doi.org/10.1038/ncb2172

Jones, R. G., & Thompson, C. B. (2009). Tumor suppressors and cell metabolism: A recipe for cancer growth. *Genes and Development*. http://doi.org/10.1101/gad.1756509

Jost, C. a, Marin, M. C., & Kaelin, W. G. (1997). P73 Is a Simian [Correction of Human] P53-Related Protein That Can Induce Apoptosis. *Nature*, *389*(6647), 191–4. http://doi.org/10.1038/38298

Katchman, B. A., Barderas, R., Alam, R., Chowell, D., Field, M. S., Esserman, L. J., … Anderson, K. S. (2016). Proteomic mapping of p53 immunogenicity in pancreatic, ovarian, and breast cancers. *Proteomics - Clinical Applications*, *10*(7), 720–731. http://doi.org/10.1002/prca.201500096

Kay, M. A. (2011). State-of-the-art gene-based therapies: the road ahead. *Nat Rev Genet*, *12*(5), 316–328. http://doi.org/10.1038/nrg2971

Kazi, A., Carie, A., Blaskovich, M. a, Bucher, C., Thai, V., Moulder, S., … Sebti, S. M. (2009). Blockade of protein geranylgeranylation inhibits Cdk2-dependent p27Kip1 phosphorylation on Thr187 and accumulates p27Kip1 in the nucleus: implications for breast cancer therapy. *Molecular and Cellular Biology*, *29*(8), 2254–2263. http://doi.org/10.1128/MCB.01029-08

Khoo, K. H., Hoe, K. K., Verma, C. S., & Lane, D. P. (2014). Drugging the p53 pathway: understanding the route to clinical efficacy. *Nature Reviews. Drug Discovery*, *13*(3), 217–36. http://doi.org/10.1038/nrd4236

Khosravi-far, R., Solski, P. A., Clark, G. J., Kinch, M. S., Der, C. J., Carolina, N., … Carolina, N. (1995). Activation of Rac1 , RhoA , and Mitogen-Activated Protein Kinases Is Required for Ras Transformation, *15*(11), 6443–6453.

Kim, E., Ambroziak, P., Otto, J. C., Taylor, B., Ashby, M., Shannon, K., … Young, S. G. (1999). Disruption of the mouse Rce1 gene results in defective Ras processing and mislocalization of Ras within cells. *Journal of Biological Chemistry*, *274*(13), 8383–8390. http://doi.org/10.1074/jbc.274.13.8383

Koppenol, W. H., Bounds, P. L., & Dang, C. V. (2011). Otto Warburg's contributions to current concepts of cancer metabolism. *Nature Reviews Cancer*, *11*(5), 325–337. http://doi.org/10.1038/nrc3038

Krishna, S., & Anderson, K. S. (2016). T-Cell Epitope Discovery for Therapeutic Cancer Vaccines. *Vaccine Design: Methods and Protocols: Volume 1: Vaccines for Human Diseases*, 779–796.

Lawson, C. D., Fan, C., Mitin, N., Baker, N. M., George, S. D., Graham, D. M., … Rossman, K. L. (2016). Rho GTPase transcriptome analysis reveals oncogenic roles for rho GTPase-activating proteins in basal-like breast cancers. *Cancer Research*, *76*(13), 3826–3837. http://doi.org/10.1158/0008-5472.CAN-15-2923

Lee, J. V., Carrer, A., Shah, S., Snyder, N. W., Wei, S., Venneti, S., … Wellen, K. E.

(2014). Akt-dependent metabolic reprogramming regulates tumor cell Histone acetylation. *Cell Metabolism*, *20*(2), 306–319. http://doi.org/10.1016/j.cmet.2014.06.004

Levine, A. J., & Puzio-Kuter, A. M. (2010). The Control of the Metabolic Switch in Cancers by Oncogenes and Tumor Suppressor Genes. *Science*, *330*(6009), 1340–1344. http://doi.org/10.1126/science.1193494

Li, D., Marchenko, N. D., Schulz, R., Fischer, V., Velasco-Hernandez, T., Talos, F., & Moll, U. M. (2011). Functional Inactivation of Endogenous MDM2 and CHIP by HSP90 Causes Aberrant Stabilization of Mutant p53 in Human Cancer Cells. *Molecular Cancer Research*, *9*(5), 577–588. http://doi.org/10.1158/1541-7786.MCR-10-0534

Lieberman, B. P., Ploessl, K., Wang, L., Qu, W., Zha, Z., Wise, D. R., … Kung, H. F. (2011). PET Imaging of Glutaminolysis in Tumors by 18F-(2S,4R)4-Fluoroglutamine. *Journal of Nuclear Medicine*, *52*(12), 1947–1955. http://doi.org/10.2967/jnumed.111.093815

Lim, K. H., Baines, A. T., Fiordalisi, J. J., Shipitsin, M., Feig, L. A., Cox, A. D., … Counter, C. M. (2005). Activation of RalA is critical for Ras-induced tumorigenesis of human cells. *Cancer Cell*, *7*(6), 533–545. http://doi.org/10.1016/j.ccr.2005.04.030

Lindsten, T., Golden, J. a, Zong, W.-X., Minarcik, J., Harris, M. H., & Thompson, C. B. (2003). The proapoptotic activities of Bax and Bak limit the size of the neural stem cell pool. *The Journal of Neuroscience : The Official Journal of the Society for Neuroscience*, *23*(35), 11112–9. http://doi.org/23/35/11112 [pii]

Long, C., Amoasii, L., Mireault, A. A., McAnally, J. R., Li, H., Sanchez-Ortiz, E., … Olson, E. N. (2016). Postnatal genome editing partially restores dystrophin expression in a mouse model of muscular dystrophy. *Science*, *351*(6271), 400–403. http://doi.org/10.1126/science.aad5725

Luo, J., Emanuele, M. J., Li, D., Creighton, C. J., Schlabach, M. R., Westbrook, T. F., … Elledge, S. J. (2009). A Genome-wide RNAi Screen Identifies Multiple Synthetic Lethal Interactions with the Ras Oncogene. *Cell*, *137*(5), 835–848. http://doi.org/10.1016/j.cell.2009.05.006

Ma, P., Magut, M., Chen, X., & Chen, C. (2002). p53 Is Necessary for the Apoptotic Response Mediated by a Transient Increase of Ras Activity p53 Is Necessary for the Apoptotic Response Mediated by a Transient Increase of Ras Activity. *Molecular and Cellular Biology*, *22*(9), 2928–2938. http://doi.org/10.1128/MCB.22.9.2928

Maeder, M. L., & Gersbach, C. A. (2016). Genome-editing Technologies for Gene and Cell Therapy. *Molecular Therapy*, *24*(3), 430–446. http://doi.org/10.1038/mt.2016.10

Manno, C. S., Pierce, G. F., Arruda, V. R., Glader, B., Ragni, M., Rasko, J. J., … Kay, M. A. (2006). Successful transduction of liver in hemophilia by AAV-Factor IX and limitations imposed by the host immune response. *Nat Med*, *12*(3), 342–347. http://doi.org/10.1038/nm1358

Marshall, E. (1999). Gene Therapy Death Prompts Review of Adenovirus Vector. *Science*, *286*(5448), 2244–2245. http://doi.org/10.1126/science.286.5448.2244

Martino, A. T., Basner-Tschakarjan, E., Markusic, D. M., Finn, J. D., Hinderer, C., Zhou, S., … Herzog, R. W. (2013). Engineered AAV vector minimizes in vivo targeting of transduced hepatocytes by capsid-specific CD8+ T cells. *Blood*, *121*(12), 2224–2233. http://doi.org/10.1182/blood-2012-10-460733

Mays, L. E., & Wilson, J. M. (2011). The complex and evolving story of T cell activation to AAV vector-encoded transgene products. *Mol Ther*, *19*(1), 16–27. http://doi.org/10.1038/mt.2010.250

Mazor, R., Crown, D., Addissie, S., Jang, Y., Kaplan, G., & Pastan, I. (2015). Elimination of murine and human T-cell epitopes in recombinant immunotoxin eliminates neutralizing and anti-drug antibodies in vivo. *Cellular and Molecular Immunology*, (July), 1–11. http://doi.org/10.1038/cmi.2015.91

Mendes-Pereira, A. M., Martin, S. A., Brough, R., McCarthy, A., Taylor, J. R., Kim, J. S., … Ashworth, A. (2009). Synthetic lethal targeting of PTEN mutant cells with PARP inhibitors. *EMBO Molecular Medicine*, *1*(6–7), 315–322. http://doi.org/10.1002/emmm.200900041

Mingozzi, F., Anguela, X. M., Pavani, G., Chen, Y., Davidson, R. J., Hui, D. J., … High, K. A. (2013). Overcoming preexisting humoral immunity to AAV using capsid decoys. *Sci Transl Med*, *5*(194), 194ra92. http://doi.org/10.1126/scitranslmed.3005795

Mingozzi, F., Maus, M. V, Hui, D. J., Sabatino, D. E., Murphy, S. L., Rasko, J. E., … High, K. A. (2007). CD8(+) T-cell responses to adeno-associated virus capsid in humans. *Nat Med*, *13*(4), 419–422. http://doi.org/10.1038/nm1549

Mohammed, I., Hampton, S. E., Ashall, L., Hildebrandt, E. R., Kutlik, R. A., Manandhar, S. P., … Dore, T. M. (2016). 8-Hydroxyquinoline-based inhibitors of the Rce1 protease disrupt Ras membrane localization in human cells. *Bioorganic and Medicinal Chemistry*, *24*(2), 160–178. http://doi.org/10.1016/j.bmc.2015.11.043

Moutaftsi, M., Peters, B., Pasquetto, V., Tscharke, D. C., Sidney, J., Bui, H.-H., … Sette, A. (2006). A consensus epitope prediction approach identifies the breadth of murine TCD8+-cell responses to vaccinia virus. *Nature Biotechnology*, *24*(7), 817.

Muller, P. A. J., & Vousden, K. H. (2014). Mutant p53 in cancer: New functions and therapeutic opportunities. *Cancer Cell*, *25*(3), 304–317. http://doi.org/10.1016/j.ccr.2014.01.021

Muller, P. a J., & Vousden, K. H. (2013). P53 Mutations in Cancer. *Nature Cell Biology*, *15*(1), 2–8. http://doi.org/10.1038/ncb2641

Nathwani, A. C., Tuddenham, E. G., Rangarajan, S., Rosales, C., McIntosh, J., Linch, D. C., … Davidoff, A. M. (2011). Adenovirus-associated virus vector-mediated gene transfer in hemophilia B. *N Engl J Med*, *365*(25), 2357–2365. http://doi.org/10.1056/NEJMoa1108046

Nielsen, S. F., Nordestgaard, B. G., & Bojesen, S. E. (2012). Statin use and reduced cancer-related mortality. *The New England Journal of Medicine*, *367*, 1792–802. http://doi.org/10.1056/NEJMoa1201735

Nomura, D. K., Long, J. Z., Niessen, S., Hoover, H. S., Ng, S. W., & Cravatt, B. F. (2010). Monoacylglycerol Lipase Regulates a Fatty Acid Network that Promotes Cancer Pathogenesis. *Cell*, *140*(1), 49–61. http://doi.org/10.1016/j.cell.2009.11.027

Oldham, W. M., Clish, C. B., Yang, Y., & Loscalzo, J. (2015). Hypoxia-Mediated Increases in l-2-hydroxyglutarate Coordinate the Metabolic Response to Reductive Stress. *Cell Metabolism*, *22*(2), 291–303. http://doi.org/10.1016/j.cmet.2015.06.021

Parrales, A., & Iwakuma, T. (2015). Targeting Oncogenic Mutant p53 for Cancer Therapy. *Frontiers in Oncology*, *5*(288), 1–13. http://doi.org/10.3389/fonc.2015.00288

Parrales, A., Ranjan, A., Iyer, S. V., Padhye, S., Weir, S. J., Roy, A., & Iwakuma, T. (2016). DNAJA1 controls the fate of misfolded mutant p53 through the mevalonate pathway. *Nature Cell Biology*, *18*(11), 1233–1243. http://doi.org/10.1038/ncb3427

Pavlova, N. N., & Thompson, C. B. (2016). The Emerging Hallmarks of Cancer Metabolism. *Cell Metabolism*. http://doi.org/10.1016/j.cmet.2015.12.006

Peterson, Y. K., Kelly, P., Weinbaum, C. A., & Casey, P. J. (2006). A novel protein geranylgeranyltransferase-I inhibitor with high potency, selectivity, and cellular activity. *Journal of Biological Chemistry*, *281*(18), 12445–12450. http://doi.org/10.1074/jbc.M600168200

Postdiagnosis Statin Use and Mortality in Danish Patients With Prostate Cancer. (n.d.).

Rammensee, H.-G., Bachmann, J., Emmerich, N. P. N., Bachor, O. A., & Stevanović, S. (1999). SYFPEITHI: database for MHC ligands and peptide motifs. *Immunogenetics*, *50*(3–4), 213–219.

Ran, F. A., Cong, L., Yan, W. X., Scott, D. A., Gootenberg, J. S., Kriz, A. J., … Zhang, F. (2015). In vivo genome editing using Staphylococcus aureus Cas9. *Nature*, *520*(7546), 186–191. http://doi.org/10.1038/nature14299

Reardon, S. (2016). First CRISPR clinical trial gets green light from US panel. *Nature*, *531*.

Rysman, E., Brusselmans, K., Scheys, K., Timmermans, L., Derua, R., Munck, S., … Swinnen, J. V. (2010). De novo lipogenesis protects cancer cells from free radicals and chemotherapeutics by promoting membrane lipid saturation. *Cancer Research*, *70*(20), 8117–8126. http://doi.org/10.1158/0008-5472.CAN-09-3871

Sahai, E., & Marshall, C. J. (2002). Rho–Gtpases and Cancer. *Nature Reviews Cancer*, *2*(2), 133–142. http://doi.org/10.1038/nrc725

Scholl, C., Fröhling, S., Dunn, I. F., Schinzel, A. C., Barbie, D. A., Kim, S. Y., … Gilliland, D. G. (2009). Synthetic Lethal Interaction between Oncogenic KRAS Dependency

and STK33 Suppression in Human Cancer Cells. *Cell*, *137*(5), 821–834. http://doi.org/10.1016/j.cell.2009.03.017

Sen, N., Satija, Y. K., & Das, S. (2011). PGC-1??, a Key Modulator of p53, Promotes Cell Survival upon Metabolic Stress. *Molecular Cell*, *44*(4), 621–634. http://doi.org/10.1016/j.molcel.2011.08.044

Solomon, H., Buganim, Y., Kogan-sakin, I., Pomeraniec, L., Assia, Y., Madar, S., … Rotter, V. (2012). Various p53 mutant proteins differently regulate the Ras circuit to induce a cancer-related gene signature, 3144–3152. http://doi.org/10.1242/jcs.099663

Sorrentino, G., Ruggeri, N., Specchia, V., Cordenonsi, M., Mano, M., Dupont, S., … Del Sal, G. (2014). Metabolic control of YAP and TAZ by the mevalonate pathway. *Nature Cell Biology*, *16*(4), 357–366. http://doi.org/10.1038/ncb2936

Sun, J., Ohkanda, J., Coppola, D., Yin, H., Kothare, M., Busciglio, B., & Hamilton, A. D. (2003). Geranylgeranyltransferase I Inhibitor GGTI-2154 Induces Breast Carcinoma Apoptosis and Tumor Regression in H-Ras Transgenic Mice Geranylgeranyltransferase I Inhibitor GGTI-2154 Induces Breast Carcinoma Apoptosis and Tumor Regression in H-Ras Transgenic Mi, (13), 8922–8929.

Sun, J., Ohkanda, J., Coppola, D., Yin, H., Kothare, M., Busciglio, B., … Sebti, S. M. (2003). Geranylgeranyltransferase I Inhibitor GGTI-2154 Induces Breast Carcinoma Apoptosis and Tumor Regression in H-Ras Transgenic Mice. *Cancer Research*, *63*(24), 8922–8929.

Sun, J., Qian, Y., Chen, Z., Marfurt, J., Hamilton, A. D., & Sebti, S. M. (1999). The geranylgeranyltransferase I inhibitor GGTI-298 induces hypophosphorylation of retinoblastoma and partner switching of cyclin- dependent kinase inhibitors: A potential mechanism for GGTI-298 antitumor activity. *Journal of Biological Chemistry*, *274*(11), 6930–6934. http://doi.org/10.1074/jbc.274.11.6930

Tenzer, S., Peters, B., Bulik, S., Schoor, O., Lemmel, C., Schatz, M. M., … Holzhütter, H.-G. (2005). Modeling the MHC class I pathway by combining predictions of proteasomal cleavage, TAP transport and MHC class I binding. *Cellular and Molecular Life Sciences*, *62*(9), 1025–1037.

Thompson, C. B. (2011). Rethinking the regulation of cellular metabolism. *Cold Spring Harbor Symposia on Quantitative Biology*, *76*, 23–29. http://doi.org/10.1101/sqb.2012.76.010496

Thurnher, M., Nussbaumer, O., & Gruenbacher, G. (2012). Novel aspects of mevalonate pathway inhibitors as antitumor agents. *Clinical Cancer Research*, *18*(13), 3524–3531. http://doi.org/10.1158/1078-0432.CCR-12-0489

Thwaite, R., Pages, G., Chillon, M., & Bosch, A. (2015). AAVrh.10 immunogenicity in mice and humans. Relevance of antibody cross-reactivity in human gene therapy. *Gene Ther*, *22*(2), 196–201. http://doi.org/10.1038/gt.2014.103

Tsimberidou, A. M., Chandhasin, C., & Kurzrock, R. (2010). Farnesyltransferase inhibitors: where are we now? *Expert Opinion on Investigational Drugs*, *19*(12), 1569–1580. http://doi.org/10.1517/13543784.2010.535516

Vassilev, L. T. (2004). In Vivo Activation of the p53 Pathway by Small-Molecule Antagonists of MDM2. *Science*, *303*(5659), 844–848. http://doi.org/10.1126/science.1092472

Vogt, A., Sun, J., Qian, Y., Hamilton, A. D., & Sebti, S. M. (1997). The geranylgeranyltransferase-I inhibitor GGTI-298 arrests human tumor cells in G0/G1 and induces p21(WAF1/CIP1/SD11) in a p53-independent manner. *Journal of Biological Chemistry*, *272*(43), 27224–27229. http://doi.org/10.1074/jbc.272.43.27224

Vousden, K. H., & Ryan, K. M. (2009). p53 and metabolism. *Nature Reviews Cancer*, *9*(10), 691–700. http://doi.org/10.1038/nrc2715

Wade, M., Li, Y.-C., & Wahl, G. M. (2013). MDM2, MDMX and p53 in oncogenesis and cancer therapy. *Nature Reviews: Cancer*, *13*(2), 83–96. http://doi.org/10.1038/nrc3430

Walker, K., & Olson, M. F. (2005). Targeting Ras and Rho GTPases as opportunities for cancer therapeutics. *Current Opinion in Genetics and Development*, *15*(1), 62–68. http://doi.org/10.1016/j.gde.2004.11.001

Wang, D., Mou, H., Li, S., Li, Y., Hough, S., Tran, K., … Xue, W. (2015). Adenovirus-Mediated Somatic Genome Editing of Pten by CRISPR/Cas9 in Mouse Liver in Spite of Cas9-Specific Immune Responses. *Hum Gene Ther*, *26*(7), 432–442. http://doi.org/10.1089/hum.2015.087

Wang, H., La Russa, M., & Qi, L. S. (2016). CRISPR/Cas9 in Genome Editing and Beyond. *Annual Review of Biochemistry*, *85*(1), 227–264. http://doi.org/10.1146/annurev-biochem-060815-014607

Wang, J., Barker, K., Steel, J., Park, J., Saul, J., Festa, F., … Qiu, J. (2013). A versatile protein microarray platform enabling antibody profiling against denatured proteins. *Proteomics Clin Appl*, *7*(5–6), 378–383. http://doi.org/10.1002/prca.201200062

Wang, M., & Casey, P. J. (2016). Protein prenylation: unique fats make their mark on biology. *Nature Reviews Molecular Cell Biology*, *17*(2), 110–122. http://doi.org/10.1038/nrm.2015.11

Wanzel, M., Vischedyk, J. B., Gittler, M. P., Gremke, N., Seiz, J. R., Hefter, M., … Stiewe, T. (2015). CRISPR-Cas9–based target validation for p53-reactivating model compounds. *Nature Chemical Biology*, *12*(1), 22–28. http://doi.org/10.1038/nchembio.1965

Winter-Vann, A. M., & Casey, P. J. (2005). Post-prenylation-processing enzymes as new targets in oncogenesis. *Nature Reviews. Cancer*, *5*(5), 405–12. http://doi.org/10.1038/nrc1612

Wolfe, A. R., Debeb, B. G., Lacerda, L., Larson, R., Bambhroliya, A., Huang, X., … Woodward, W. A. (2015). Simvastatin prevents triple-negative breast cancer metastasis in pre-clinical models through regulation of FOXO3a. *Breast Cancer Research and Treatment*, *154*(3), 495–508. http://doi.org/10.1007/s10549-015-3645-3

Wolfl, M., Kuball, J., Ho, W. Y., Nguyen, H., Manley, T. J., Bleakley, M., & Greenberg, P. D. (2007). Activation-induced expression of CD137 permits detection, isolation, and expansion of the full repertoire of CD8+ T cells responding to antigen without requiring knowledge of epitope specificities. *Blood*, *110*(1), 201–210. http://doi.org/10.1182/blood-2006-11-056168

Xia, M., & Land, H. (2007). Tumor suppressor p53 restricts Ras stimulation of RhoA and cancer cell motility. *Nature Structural & Molecular Biology*, *14*(3), 215–223. http://doi.org/10.1038/nsmb1208

Xie, F., Li, P., Gong, J., Zhang, J., & Ma, J. (2015). The bisphosphonate zoledronic acid effectively targets lung cancer cells by inhibition of protein prenylation. *Biochemical and Biophysical Research Communications*, *467*(4), 664–669. http://doi.org/10.1016/j.bbrc.2015.10.089

Yahagi, N., Shimano, H., Matsuzaka, T., Najima, Y., Sekiya, M., Nakagawa, Y., … Yamada, N. (2003). p53 activation in adipocytes of obese mice. *Journal of Biological Chemistry*, *278*(28), 25395–25400. http://doi.org/10.1074/jbc.M302364200

Yang, C., Passaniti, A., Cirielli, C., Capogrossi, M. C., & Cirielli, C. (1995). Adenovirus-mediated Wild-Type p53 Expression Induces Apoptosis and Suppresses Tumorigenesis of Prostatic Tumor Cells. *Cancer Research*, *55*(19), 4210–4213.

Yang, H. W., Shin, M., Lee, S., Kim, J., Park, W. S., Cho, K., … Heo, W. Do. (2012). Article Cooperative Activation of PI3K by Ras and Rho Family Small GTPases, 281–290. http://doi.org/10.1016/j.molcel.2012.05.007

Yang, L., Guell, M., Niu, D., George, H., Lesha, E., Grishin, D., … Church, G. (2015). Genome-wide inactivation of porcine endogenous retroviruses (PERVs). *Science*, *350*(6264), 1101–1104. http://doi.org/10.1126/science.aad1191

Yin, H., Kanasty, R. L., Eltoukhy, A. A., Vegas, A. J., Dorkin, J. R., & Anderson, D. G. (2014). Non-viral vectors for gene-based therapy. *Nat Rev Genet*, *15*(8), 541–555. http://doi.org/10.1038/nrg3763

Yu, X., Narayanan, S., Vazquez, A., & Carpizo, D. R. (2014). Small molecule compounds targeting the p53 pathway: Are we finally making progress? *Apoptosis*, *19*(7), 1055–1068. http://doi.org/10.1007/s10495-014-0990-3

Zetsche, B., Gootenberg, J. S., Abudayyeh, O. O., Slaymaker, I. M., Makarova, K. S., Essletzbichler, P., … Zhang, F. (2015). Cpf1 is a single RNA-guided endonuclease of a class 2 CRISPR-Cas system. *Cell*, *163*(3), 759–771. http://doi.org/10.1016/j.cell.2015.09.038

Zhang, W. W., Fang, X., Mazur, W., French, B. A., Georges, R. N., & Roth, J. A. (1994). High-efficiency gene transfer and high-level expression of wild-type p53 in human lung cancer cells mediated by recombinant adenovirus. *Cancer Gene Therapy*, *1*(1), 5–13.

Zimonjic, D. B. ., Chan, L. N. ., Tripathi, V. ., Lu, J. ., Kwon, O. ., Popescu, N. C. ., … Tamanoi, F. . (2013). In vitro and in vivo effects of geranylgeranyltransferase I inhibitor P61A6 on non-small cell lung cancer cells. *BMC Cancer*, *13*. http://doi.org/10.1186/1471-2407-13-198

APPENDIX A

LIST OF ENRICHED PATHWAYS MUTANT P53 MCF10AS.

GENE ENRICHMENT ANALYSIS OF DIFFERENTIALLY EXPRESSED GENES IN MUTANT P53 MCF10AS VS. WT P53 MCF10A.

Category	Pathways enriched in R273H mp53 vs wtp53.MCF10A	P-Value	FE
REACTOME	R-HSA-2424491:DAP12 signaling	0.037	2.47
KEGG	hsa04144:Endocytosis	0.037	1.38
REACTOME	R-HSA-1566948:Elastic fiber formation	0.038	3.08
REACTOME	R-HSA-380270:Recruitment of mitotic centrosome proteins and complexes	0.038	1.78
REACTOME	R-HSA-512988:Interleukin-3, 5 and GM-CSF signaling	0.038	2.70
KEGG	hsa04120:Ubiquitin mediated proteolysis	0.042	1.55
REACTOME	R-HSA-383280:Nuclear Receptor transcription pathway	0.043	2.00
REACTOME	R-HSA-2995383:Initiation of Nuclear Envelope Reformation	0.044	3.56
KEGG	hsa04910:Insulin signaling pathway	0.045	1.54
REACTOME	R-HSA-166166:MyD88-independent TLR3/TLR4 cascade	0.046	4.63
REACTOME	R-HSA-5675221:Negative regulation of MAPK pathway	0.047	2.19
REACTOME	R-HSA-166016:Toll Like Receptor 4 (TLR4) Cascade	0.047	2.92
REACTOME	R-HSA-2565942:Regulation of PLK1 Activity at G2/M Transition	0.049	1.68
KEGG	hsa05166:HTLV-I infection	0.051	1.36
KEGG	hsa05222:Small cell lung cancer	0.053	1.70
REACTOME	R-HSA-909733:Interferon alpha/beta signaling	0.053	1.80
REACTOME	R-HSA-937041:IKK complex recruitment mediated by RIP1	0.054	2.49
REACTOME	R-HSA-193775:Synthesis of bile acids and bile salts via 24-hydroxycholesterol	0.056	3.31
REACTOME	R-HSA-5362517:Signaling by Retinoic Acid	0.057	2.78
KEGG	hsa04151:PI3K-Akt signaling pathway	0.059	1.29
REACTOME	R-HSA-5620912:Anchoring of the basal body to the plasma membrane	0.060	1.61
KEGG	hsa04512:ECM-receptor interaction	0.062	1.66
KEGG	hsa04914:Progesterone-mediated oocyte maturation	0.062	1.66
KEGG	hsa05230:Central carbon metabolism in cancer	0.062	1.81
KEGG	hsa04660:T cell receptor signaling pathway	0.063	1.59
REACTOME	R-HSA-3000170:Syndecan interactions	0.064	2.40

REACTOME	R-HSA-2993913:Clearance of Nuclear Envelope Membranes from Chromatin	0.064	4.11
REACTOME	R-HSA-425986:Sodium/Proton exchangers	0.064	4.11
REACTOME	R-HSA-549127:Organic cation transport	0.064	4.11
REACTOME	R-HSA-114608:Platelet degranulation	0.066	1.56
KEGG	hsa04540:Gap junction	0.067	1.65
KEGG	hsa05211:Renal cell carcinoma	0.068	1.78
REACTOME	R-HSA-2559580:Oxidative Stress Induced Senescence	0.068	1.50
KEGG	hsa04145:Phagosome	0.069	1.45
REACTOME	R-HSA-3772470:Negative regulation of TCF-dependent signaling by WNT ligand antagonists	0.070	3.08
KEGG	hsa04150:mTOR signaling pathway	0.072	1.83
KEGG	hsa05203:Viral carcinogenesis	0.075	1.37
REACTOME	R-HSA-216083:Integrin cell surface interactions	0.076	1.61
REACTOME	R-HSA-445355:Smooth Muscle Contraction	0.077	2.12
REACTOME	R-HSA-975634:Retinoid metabolism and transport	0.077	1.98
REACTOME	R-HSA-912631:Regulation of signaling by CBL	0.081	2.52
KEGG	hsa00310:Lysine degradation	0.083	1.86
KEGG	hsa04915:Estrogen signaling pathway	0.084	1.56
REACTOME	R-HSA-1234158:Regulation of gene expression by Hypoxia-inducible Factor	0.084	3.70
REACTOME	R-HSA-5210891:Uptake and function of anthrax toxins	0.084	3.70
REACTOME	R-HSA-74749:Signal attenuation	0.084	3.70
REACTOME	R-HSA-1963642:PI3K events in ERBB2 signaling	0.086	2.89
REACTOME	R-HSA-2559584:Formation of Senescence-Associated Heterochromatin Foci (SAHF)	0.086	2.89
REACTOME	R-HSA-446652:Interleukin-1 signaling	0.087	2.06

Category	Pathways enriched in G245S mp53 vs wtp53.MCF10A	P-Value	FE
REACTOME	hsa909733:Interferon alpha/beta signaling	9.10E-12	3.96
REACTOME	hsa877300:Interferon gamma signaling	4.47E-06	2.63
KEGG	hsa05168:Herpes simplex infection	7.32E-06	2.10

REACTOME	hsa1236977:Endosomal/Vacuolar pathway	1.33E-04	5.71
KEGG	hsa04142:Lysosome	5.21E-04	2.07
KEGG	hsa05164:Influenza A	8.18E-04	1.83
KEGG	hsa04145:Phagosome	8.62E-04	1.89
KEGG	hsa05160:Hepatitis C	9.79E-04	1.96
KEGG	hsa05169:Epstein-Barr virus infection	0.0019	1.73
KEGG	hsa04012:ErbB signaling pathway	0.0030	2.11
KEGG	hsa05133:Pertussis	0.0036	2.19
REACTOME	hsa983231:Factors involved in megakaryocyte development and platelet production	0.0045	1.84
KEGG	hsa04620:Toll-like receptor signaling pathway	0.0055	1.91
KEGG	hsa01100:Metabolic pathways	0.0066	1.20
KEGG	hsa05161:Hepatitis B	0.0070	1.73
REACTOME	hsa983168:Antigen processing: Ubiquitination & Proteasome degradation	0.0076	1.47
KEGG	hsa05205:Proteoglycans in cancer	0.0078	1.59
KEGG	hsa05162:Measles	0.0091	1.74
KEGG	hsa04722:Neurotrophin signaling pathway	0.011	1.77
REACTOME	hsa112409:RAF-independent MAPK1/3 activation	0.012	3.96
REACTOME	R-HSA-212436:Generic Transcription Pathway	0.013	1.37
KEGG	hsa04630:Jak-STAT signaling pathway	0.013	1.66
REACTOME	hsa112411:MAPK1 (ERK2) activation	0.014	4.76
KEGG	hsa05212:Pancreatic cancer	0.014	2.08
KEGG	hsa05152:Tuberculosis	0.014	1.58
KEGG	hsa04064:NF-kappa B signaling pathway	0.016	1.89
REACTOME	hsa982772:Growth hormone receptor signaling	0.017	2.86
KEGG	hsa05145:Toxoplasmosis	0.018	1.72
REACTOME	hsa1989781:PPARA activates gene expression	0.020	1.67
KEGG	hsa04010:MAPK signaling pathway	0.020	1.44
REACTOME	hsa110056:MAPK3 (ERK1) activation	0.022	4.29
KEGG	hsa04668:TNF signaling pathway	0.023	1.73
REACTOME	hsa983170:Antigen Presentation: Folding, assembly and peptide loading of class I MHC	0.026	2.64
REACTOME	hsa912694:Regulation of IFNA signaling	0.026	2.64

KEGG	hsa04380:Osteoclast differentiation	0.027	1.62
KEGG	hsa05140:Leishmaniasis	0.029	1.90
REACTOME	R-HSA-5620916:VxPx cargo-targeting to cilium	0.029	2.86
REACTOME	R-HSA-1059683:Interleukin-6 signaling	0.031	3.90
REACTOME	R-HSA-2562578:TRIF-mediated programmed cell death	0.031	3.90
REACTOME	R-HSA-937072:TRAF6 mediated induction of TAK1 complex	0.040	3.03
KEGG	hsa04070:Phosphatidylinositol signaling system	0.043	1.67
REACTOME	R-HSA-5620924:Intraflagellar transport	0.044	1.91
KEGG	hsa04146:Peroxisome	0.044	1.74
REACTOME	R-HSA-2032785:YAP1- and WWTR1 (TAZ)-stimulated gene expression	0.045	2.37
REACTOME	R-HSA-1566948:Elastic fibre formation	0.050	2.86
KEGG	hsa04210:Apoptosis	0.051	1.87
REACTOME	R-HSA-5656169:Termination of translesion DNA synthesis	0.053	2.29
KEGG	hsa05219:Bladder cancer	0.056	2.12
REACTOME	R-HSA-166166:MyD88-independent TLR3/TLR4 cascade	0.056	4.29
KEGG	hsa04917:Prolactin signaling pathway	0.059	1.77
KEGG	hsa00562:Inositol phosphate metabolism	0.059	1.77
REACTOME	R-HSA-5620912:Anchoring of the basal body to the plasma membrane	0.060	1.57
KEGG	hsa05220:Chronic myeloid leukemia	0.064	1.74
REACTOME	R-HSA-168138:Toll Like Receptor 9 (TLR9) Cascade	0.069	6.43
REACTOME	R-HSA-204174:Regulation of pyruvate dehydrogenase (PDH) complex	0.071	3.06
REACTOME	R-HSA-1660516:Synthesis of PIPs at the early endosome membrane	0.071	3.06
REACTOME	R-HSA-194840:Rho GTPase cycle	0.071	1.48
KEGG	hsa00760:Nicotinate and nicotinamide metabolism	0.072	2.33
REACTOME	R-HSA-264876:Insulin processing	0.074	2.31
REACTOME	R-HSA-6788467:IL-6-type cytokine receptor ligand interactions	0.075	2.57
KEGG	hsa05203:Viral carcinogenesis	0.075	1.37
KEGG	hsa00480:Glutathione metabolism	0.076	1.89
REACTOME	R-HSA-1169408:ISG15 antiviral mechanism	0.077	1.64
REACTOME	R-HSA-549127:Organic cation transport	0.077	3.81
REACTOME	R-HSA-727802:Transport of nucleotide sugars	0.077	3.81
KEGG	hsa04144:Endocytosis	0.081	1.31
REACTOME	R-HSA-912526:Interleukin receptor SHC signaling	0.086	2.22
REACTOME	R-HSA-140534:Ligand-dependent caspase activation	0.088	2.86

REACTOME	R-HSA-4419969:Depolymerisation of the Nuclear Lamina	0.088	2.86
REACTOME	R-HSA-975577:N-Glycan antennae elongation	0.088	2.86
REACTOME	R-HSA-428540:Activation of Rac	0.088	2.86
REACTOME	R-HSA-1810476:RIP-mediated NFkB activation via ZBP1	0.089	2.45

Category	Pathways enriched in R248Q mp53 vs wtp53.MCF10A	P-Value	FE
KEGG	hsa05200:Pathways in cancer	2.85E-04	1.61
KEGG	hsa04151:PI3K-Akt signaling pathway	7.34E-04	1.61
KEGG	hsa04360:Axon guidance	8.21E-04	2.10
KEGG	hsa04380:Osteoclast differentiation	1.27E-03	2.04
KEGG	hsa05416:Viral myocarditis	1.31E-03	2.73
KEGG	hsa04510:Focal adhesion	1.42E-03	1.78
REACTOME	R-HSA-2129379:Molecules associated with elastic fibres	1.69E-03	3.17
REACTOME	R-HSA-383280:Nuclear Receptor transcription pathway	1.74E-03	2.79
KEGG	hsa04015:Rap1 signaling pathway	1.95E-03	1.75
KEGG	hsa05222:Small cell lung cancer	3.29E-03	2.22
KEGG	hsa05205:Proteoglycans in cancer	3.40E-03	1.72
KEGG	hsa05230:Central carbon metabolism in cancer	3.93E-03	2.43
KEGG	hsa05212:Pancreatic cancer	4.52E-03	2.39
KEGG	hsa04668:TNF signaling pathway	5.94E-03	1.99
REACTOME	R-HSA-114608:Platelet degranulation	7.84E-03	1.94
KEGG	hsa04210:Apoptosis	8.20E-03	2.33
REACTOME	R-HSA-3000170:Syndecan interactions	9.02E-03	3.24
KEGG	hsa05219:Bladder cancer	9.21E-03	2.71
KEGG	hsa04145:Phagosome	9.41E-03	1.74
KEGG	hsa05140:Leishmaniasis	9.72E-03	2.19
REACTOME	hsa2151201:Transcriptional activation of mitochondrial bio	1.03E-02	2.67
KEGG	hsa04142:Lysosome	1.11E-02	1.84
KEGG	hsa04010:MAPK signaling pathway	1.21E-02	1.52
KEGG	hsa00561:Glycerolipid metabolism	1.29E-02	2.30

KEGG	hsa04066:HIF-1 signaling pathway	1.33E-02	1.93
REACTOME	RHSA-446107:Type I hemidesmosome assembly	1.35E-02	4.97
REACTOME	R-HSA-3000178:ECM proteoglycans	1.74E-02	2.04
REACTOME	R-HSA-1236977:Endosomal/Vacuolar pathway	1.88E-02	4.56
KEGG	hsa01100:Metabolic pathways	1.90E-02	1.19
REACTOME	R-HSA-1566948:Elastic fibre formation	1.97E-02	3.64
KEGG	hsa05166:HTLV-I infection	2.10E-02	1.48
REACTOME	R-HSA-216083:Integrin cell surface interactions	2.32E-02	1.91
KEGG	hsa05215:Prostate cancer	2.44E-02	1.89
REACTOME	R-HSA-1971475:A GAG synthesis	2.68E-02	2.94
REACTOME	R-HSA-194840:Rho GTPase cycle	2.79E-02	1.70
KEGG	hsa04150:mTOR signaling pathway	3.22E-02	2.11
REACTOME	R-HSA-3928662:EPHB-mediated forward signaling	3.39E-02	2.34
KEGG	hsa04115:p53 signaling pathway	3.52E-02	1.99
KEGG	hsa05120:Epithelial cell signaling in Helicobacter pylori	3.52E-02	1.99
KEGG	hsa05231:Choline metabolism in cancer	3.53E-02	1.76
KEGG	hsa04350:TGF-beta signaling pathway	3.59E-02	1.85
KEGG	hsa02010:ABC transporters	3.99E-02	2.27
REACTOME	R-HSA-446652:Interleukin-1 signaling	4.15E-02	2.43
REACTOME	R-HSA-2214320:Anchoring fibril formation	4.17E-02	3.64
REACTOME	R-HSA-428543:Inactivation of Cdc42 and Rac	4.20E-02	4.86
REACTOME	R-HSA-2408550:Metabolism of ingested H2SeO4 and H2SeO3 into H2Se	4.41E-02	8.20
REACTOME	R-HSA-5365859:RA biosynthesis pathway	4.46E-02	2.98
REACTOME	R-HSA-1474228:Degradation of the extracellular matrix	4.56E-02	1.85
KEGG	hsa04512:ECM-receptor interaction	4.59E-02	1.79
KEGG	hsa05150:Staphylococcus aureus infection	4.95E-02	2.06
KEGG	hsa05134:Legionellosis	4.95E-02	2.06
KEGG	hsa05323:Rheumatoid arthritis	4.97E-02	1.77

KEGG	hsa00340:Histidine metabolism	4.98E-02	2.90
REACTOME	R-HSA-112043:PLC beta mediated events	5.17E-02	3.42
REACTOME	R-HSA-202733:Cell surface interactions at the vascular wall	5.41E-02	2.02
KEGG	hsa00512:Mucin type O-Glycan biosynthesis	5.45E-02	2.51
REACTOME	R-HSA-877300:Interferon gamma signaling	5.56E-02	1.74
KEGG	hsa00280:Valine, leucine and isoleucine degradation	5.59E-02	2.13
REACTOME	R-HSA-418889:Ligand-independent caspase activation	5.60E-02	4.37
KEGG	hsa04960:Aldosterone-regulated sodium reabsorption	5.61E-02	2.28
REACTOME	hsa352230:Amino acid transport across the plasma mem	5.83E-02	2.47
KEGG	hsa00450:Selenocompound metabolism	5.99E-02	3.27
KEGG	hsa00910:Nitrogen metabolism	5.99E-02	3.27
KEGG	hsa05221:Acute myeloid leukemia	6.02E-02	1.98
KEGG	hsa00520:Amino sugar and nucleotide sugar metabolism	6.21E-02	2.08
REACTOME	R-HSA-1369062:ABC transporters in lipid homeostasis	6.29E-02	3.22
KEGG	hsa00380:Tryptophan metabolism	6.30E-02	2.22
KEGG	hsa04071:Sphingolipid signaling pathway	7.01E-02	1.57
KEGG	hsa05332:Graft-versus-host disease	7.05E-02	2.36
REACTOME	R-HSA-71240:Tryptophan catabolism	7.19E-02	3.98
REACTOME	R-HSA-351906:Apoptotic cleavage of cell adhesion proteins	7.19E-02	3.98
REACTOME	R-HSA-200425:Import of palmitoyl-CoA into the mitochondri	7.19E-02	3.98
REACTOME	R-HSA-1266695:Interleukin-7 signaling	7.19E-02	3.98
REACTOME	R-HSA-210991:Basigin interactions	7.19E-02	2.62
REACTOME	R-HSA-4085001:Sialic acid metabolism	7.52E-02	2.32
REACTOME	R-HSA-983170:Antigen Presentation: Folding, assembly and peptide loading of class I MHC	8.27E-02	2.52
KEGG	hsa04514:Cell adhesion molecules (CAMs)	8.46E-02	1.49
KEGG	hsa00350:Tyrosine metabolism	8.90E-02	2.22

Category	Pathways enriched in Y234C mp53 vs wtp53.MCF10A	P-Value	FE
REACTOME	R-HSA-212436:Generic Transcription Pathway	0.00064	1.65
REACTOME	R-HSA-191273:Cholesterol biosynthesis	0.00069	4.92
REACTOME	R-HSA-2426168:Activation of gene expression by SREBF	0.0016	3.22
KEGG	hsa05166:HTLV-I infection	0.0020	1.73
REACTOME	hsa139915:Activation of PUMA and translocation to mitochondria	0.0023	7.69
REACTOME	hsa174417:Telomere C-strand (Lagging Strand) Synthesis	0.0047	9.84
KEGG	hsa03440:Homologous recombination	0.0052	3.60
KEGG	hsa04012:ErbB signaling pathway	0.0059	2.25
KEGG	hsa03430:Mismatch repair	0.0064	3.97
KEGG	hsa01100:Metabolic pathways	0.0065	1.24
KEGG	hsa05202:Transcriptional misregulation in cancer	0.0088	1.78
REACTOME	hsa174414:Processive synthesis on the C-strand of the telomere	0.0089	8.20
KEGG	hsa04666:Fc gamma R-mediated phagocytosis	0.011	2.17
REACTOME	hsa1368082:RORA activates gene expression	0.019	3.19
REACTOME	hsa69091:Polymerase switching	0.022	4.39
REACTOME	hsa174411:Polymerase switching on the C-strand of the telomere	0.022	4.39
KEGG	hsa05132:Salmonella infection	0.023	2.04
KEGG	hsa05212:Pancreatic cancer	0.025	2.21
REACTOME	hsa2032785:YAP1- and WWTR1 (TAZ)-stimulated gene expression	0.027	2.97
REACTOME	hsa1912408:Pre-NOTCH Transcription and Translation	0.027	2.97
KEGG	hsa05161:Hepatitis B	0.028	1.71
KEGG	hsa00564:Glycerophospholipid metabolism	0.028	1.92
REACTOME	hsa428540:Activation of Rac	0.029	4.10
KEGG	hsa05120:Epithelial cell signaling in Helicobacter pylori infection	0.030	2.14
KEGG	hsa04668:TNF signaling pathway	0.031	1.84
REACTOME	hsa2559585:Oncogene Induced Senescence	0.031	2.87

KEGG	hsa05205:Proteoglycans in cancer	0.031	1.56
KEGG	hsa04810:Regulation of actin cytoskeleton	0.032	1.54
REACTOME	hsa111448:Activation of NOXA and translocation to mitochondria	0.035	9.22
KEGG	hsa00910:Nitrogen metabolism	0.036	3.83
KEGG	hsa03410:Base excision repair	0.037	2.77
REACTOME	hsa5656169:Termination of translesion DNA synthesis	0.041	2.69
REACTOME	hsa69183:Processive synthesis on the lagging strand	0.042	4.92
REACTOME	hsa174437:Removal of the Flap Intermediate	0.042	4.92
REACTOME	hsa-74749:Signal attenuation	0.042	4.92
REACTOME	hsa400253:Circadian Clock	0.042	2.26
KEGG	hsa05231:Choline metabolism in cancer	0.044	1.81
KEGG	hsa04210:Apoptosis	0.045	2.10
KEGG	hsa04152:AMPK signaling pathway	0.045	1.71
REACTOME	hsa5696397:Gap-filling DNA repair synthesis and ligation in GG-NER	0.047	2.95
REACTOME	hsa383280:Nuclear Receptor transcription pathway	0.052	2.17
REACTOME	hsa2586552:Signaling by Leptin	0.054	4.47
REACTOME	R-HSA-74713: IRS activation	0.056	7.38
KEGG	hsa04621:NOD-like receptor signaling pathway	0.056	2.13
KEGG	hsa04360:Axon guidance	0.060	1.64
REACTOME	hsa3928664:Ephrin signaling	0.063	3.24
REACTOME	hsa1475029: Reversible hydration of carbon dioxide	0.068	4.10
KEGG	hsa04115:p53 signaling pathway	0.068	1.95
KEGG	hsa04390:Hippo signaling pathway	0.069	1.55
KEGG	hsa04932:Non-alcoholic fatty liver disease (NAFLD)	0.069	1.55
REACTOME	hsa1989781:PPARA activates gene expression	0.073	1.63
REACTOME	R-HSA-3560783:Defective B4GALT7 causes EDS	0.074	3.07
REACTOME	R-HSA-189483: Heme degradation	0.079	6.15
KEGG	hsa04010:MAPK signaling pathway	0.080	1.38
KEGG	hsa00900:Terpenoid backbone biosynthesis	0.083	2.96
REACTOME	hsa1483213:Synthesis of PE	0.083	3.78
REACTOME	hsa112409:RAF-independent MAPK1/3 activation	0.083	3.78
REACTOME	hsa5675221:Negative regulation of MAPK pathway	0.084	2.27

REACTOME	hsa5651801:PCNA-Dependent Long Patch Base E Repair	0.085	2.93
REACTOME	hsa5621575:CD209 (DC-SIGN) signaling	0.085	2.93
KEGG	hsa00562:Inositol phosphate metabolism	0.091	1.84
KEGG	hsa04014:Ras signaling pathway	0.096	1.38